THE
PHYSICAL REVIEW
A Journal of Experimental and Theoretical Physics
VOL. 46, NO. 1 JULY 1, 1934 SECOND SERIES

Energy and Stability Related to Composition of Atomic Nuclei

E. D. EASTMAN, *Department of Chemistry, University of California, Berkeley*

(Received May 2, 1934)

Examination of the postulates of Heisenberg concerning the energy of binding of neutrons and protons to atomic nuclei shows that factors not included in the primary considerations are of appreciable effect in determining nuclear composition and stability, and result in deviations of a periodic character from the requirements of the theory. Nevertheless, the formulation of binding energies as linear functions of the neutron-proton ratio of the nucleus is adequate as a rough approximation over a large range of elements, as is also the proportionality assumed between the radius and the cube root of the mass number. For evaluation of the various constants, it is assumed that the boundary of stability in emission of beta-particles should be centrally placed with respect to existing nuclear species. Reasons supporting this placement, and the manner of adjustment of the alpha-boundary, for which the distribution of nuclei alone is not an adequate guide, are outlined. The application in various fields of nuclear physics and chemistry of the constants thus determined is discussed and illustrated. The nuclear radii resulting in these calculations agree excellently with those found by other methods. An equation for the energy of formation of nuclei from neutrons and protons is obtained and found to hold, within experimental error, for all elements above $_{24}$Cr for which data are available for comparison. Calculated energies of spontaneously emitted alpha- and beta-particles and energies of capture of various particles by light nuclei, are in rough agreement with known values. Energies in nuclear collision processes are calculated with fair average agreement with experimental values, and the indications of the theory regarding critical energies and nuclear composition in such reactions discussed. Specific characteristics are not faithfully predicted in the various nuclear changes above, but the average accuracy of calculated energies is superior, for all but the light elements, to that obtainable from present values of atomic masses. In addition, these calculations are possible in cases where the masses are not yet measured. Spontaneous emission of protons from any existing nuclei is indicated to be impossible. A chart is given showing in what region of nuclear composition this and other similar changes might occur. The alpha-disintegration is considered to be possible in elements as low as $_{51}$Sb. The possibility of beta-changes, or their reverse, in certain isobaric pairs among the "non-radioactive" elements is pointed out. The "end" of the periodic system and the limiting spread in mass numbers of isotopes as influenced by the various types of nuclear instability are also discussed.

HEISENBERG, in recent papers,[1] discusses the properties of atomic nuclei assumed to consist entirely of neutrons and protons. Among other results, he obtains approximations to the forms of the stability-composition relations in alpha- and beta-disintegrations. This phase of his analysis is based upon assumptions concerning the interaction of single neutrons and protons with nuclei of various compositions, which may be cast in algebraic form as follows:

$$\bar{E}_N = K_1 + K_2 N/Z, \quad (1)$$

$$\bar{E}_P = k_1 + k_2 N/Z. \quad (2)$$

$\bar{E}_N$ and $\bar{E}_P$, to be referred to as the binding energy of the neutron and the proton, designate the difference in energy between the highest point of the potential-distance curve (compare Fig. 3) and the lowest level of the particle when

[1] Heisenberg, I, Zeits. f. Physik **77**, 1 (1932); II, ibid. **78**, 156 (1932); III, ibid. **80**, 587 (1933).

combined in a nucleus synthesizable from N neutrons and Z protons.[2] The "radius" of the nucleus, designated by R_0 and defined later, is assumed to be given by

$$R_0 = r_0 M^{1/3}, \tag{3}$$

where r_0 is a constant.

Making these approximations, and the assumption that energy is conserved (statistically at least) in all processes considered, Heisenberg shows that the condition for zero energy in a beta-disintegration is

$$N/Z = C_1 + C_2 Z/M^{1/3}. \tag{4}$$

Similarly, the limiting condition for stability with respect to alpha-emission is

$$N/Z = c_1 + c_2 Z/M^{1/3}. \tag{5}$$

If E_N° and E_α° represent the energy evolved in the formation from protons and electrons of a neutron and an alpha-particle, respectively, and e is the charge of the electron, the constants in (4) and (5) have the values

$$C_1 = (K_1 - k_1 + E_N^\circ)/(k_2 - K_2),$$

$$C_2 = e^2/r_0(k_2 - K_2),$$

$$c_1 = (E_\alpha^\circ/2 - E_N^\circ - k_1 - K_1)/(k_2 + K_2)$$

and

$$c_2 = e^2/r_0(k_2 + K_2).$$

Assuming that the upper limit of N/Z in existing nuclear species is fixed by (4) and the lower limit by (5), Heisenberg plots these extreme values against Z. Curves of the form of Eqs. (4) and (5) with the constants C and c empirically chosen delineate roughly the field within which the known nuclei lie, and to that extent support the theory.

Further support of the original assumptions, including a check of the magnitudes of the constants, is none the less desirable. Conversely, if the assumptions can be verified, and the stability curves correctly placed, the determination of the magnitudes of the constants in (1), (2) and (3) becomes itself of value. A detailed examination of the subject has therefore been made with the objectives of testing the assumptions, fixing the constants, and applying the theory to various problems of nuclear physics and chemistry.

[2] Departure is here made from Heisenberg's notation partly for mnemonic reasons and partly in order to obtain the final equations in terms of quantities which are independent of any theory as to the nature of the nucleus. Thus, the number of protons in the present theory is the atomic number, usually represented by Z. Similarly if M is allowed to represent the mass number of a nuclear species, N is $M-Z$. In Heisenberg's notation $N=n_1$, $Z=n_2$ and $M=n$.

A Test of the Basic Assumptions

If Eqs. (1), (2) and (3) are valid approximations, and if the energy, E, evolved in the formation of any nucleus from neutrons and protons is a function of N and Z alone (that is, constitutional or structural factors are absent or negligible), the following equations should also be approximately true:

$$(\partial E/\partial N)_Z = \bar{E}_N = K_1 + K_2 N/Z, \tag{6}$$

$$(\partial^2 E/\partial Z \partial N) = -K_2 N/Z^2, \tag{7}$$

$$(\partial E/\partial Z)_N = \bar{E}_P - Ze^2/r_0 M^{1/3} = k_1 + k_2 N/Z - Ze^2/r_0 M^{1/3}, \tag{8}$$

$$(\partial^2 E/\partial N \partial Z) = k_2/Z + Ze^2/3r_0 M^{4/3}. \tag{9}$$

Equating the second derivatives in (7) and (9) gives a relation which may be cast in the form

$$N/Z = -k_2/K_2 - Z^2 e^2/3K_2 r_0 M^{4/3}. \tag{10}$$

Setting the constant term $-k_2/K_2 = D_1$, and $-e^2/3K_2 r_0 = D_2$, this becomes

$$N/Z = D_1 + D_2 Z^2/M^{4/3}, \tag{10a}$$

which is the equation of a straight line if N/Z and $Z^2/M^{4/3}$ are taken as the variables. The extent to which Eq. (10) or (10a) is satisfied, and the original assumptions substantiated, may therefore be simply tested by plotting these quantities for existing atomic species against each other.

The features which are of particular interest in plots of this kind are brought out most clearly by using values of N and $M^{4/3}$ obtained from the chemical atomic weight, A, of each element. This provides a sort of average of the variables to be plotted which gives most weight to the isotopes of greatest abundance, allows each element to be represented by a single point, and permits the inclusion of the elements whose isotopic composition is as yet unknown. This plot is shown in Fig. 1.

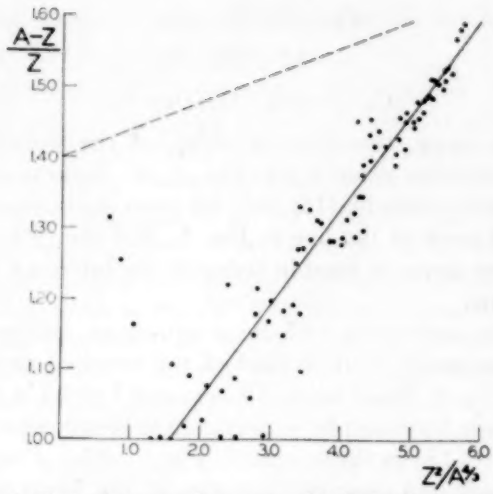

FIG. 1. Test of assumptions averaging isotopic masses by use of chemical atomic weights.

The points in Fig. 1 show deviations from the straight line representing their general trend which are roughly but distinctly periodic in character. This behavior is not surprising, since the probable existence of more or less sharply marked "periods" in the system of nuclei is already known. It was first pointed out by Harkins, and is clearly shown in his recent plots[3] of isotopic number[4] against atomic number. It is most obvious among the lighter elements, and, in the present plot at least, is not distinguishable in the elements of atomic number greater than about 60.

The existence of this periodicity indicates that some factor not included in Heisenberg's simple assumptions is operative to a significant extent in determining nuclear composition. Some sort of exclusion principle might explain the periodicity, or it may result from the effects of spin, leading to structures of the kind proposed by Latimer.[5] Where it is necessary to consider these effects they will be referred to loosely as "structural factors." It will be considered here that they are superimposed upon the more general interchange forces, and are of secondary importance, so far as energy effects are concerned, in large nuclei.

It can, therefore, by no means be claimed that the points in this diagram are best represented by a straight line. Nevertheless, insofar as rough numerical approximation is concerned, a linear function is adequate. In Fig. 1, for example, with the exception of a few of the light elements, deviations from the line are seldom more than 10 percent in N/Z. If the individual isotopes be considered the spread in N/Z is often much greater. This may be seen in Fig. 2, which is sufficiently similar to the diagram in question to illustrate this point. Restriction to atomic numbers greater than about 10 largely eliminates the worst of these discrepancies. Within this range, the larger deviations from the representative line seldom exceed about 15 percent in N/Z among the lower atomic numbers and decrease to half this value in the heavy elements. In elements of odd atomic number the deviations are smaller. A great majority of the points for all the more abundant species fall fairly close to the line. These facts are interpreted to mean that although the form of the equations cannot be closely correct, in a purely numerical sense no serious inaccuracy is represented in the assumptions of (1), (2) and (3). Additional tests, introducing the magnitudes of the constants, are therefore in order.

Numerical Evaluation of Constants

From the relations between the constants of (4) and (5) it is found that

$$K_1=(C_1/C_2-c_1/c_2)e^2/2r_0+E_a^\circ/4-E_N^\circ, \quad (11)$$

$$K_2=(1/c_2-1/C_2)e^2/2r_0, \quad (12)$$

$$k_1=-(C_1/C_2+c_1/c_2)e^2/2r_0+E_a^\circ/4, \quad (13)$$

$$k_2=(1/c_2+1/C_2)e^2/2r_0. \quad (14)$$

As a preliminary to the determination of the constants C and c in these equations, and from them the constants K and k, it may be pointed out that Eqs. (4) and (5) are linear in N/Z and $Z/M^{1/3}$. Making use of this simplifying feature, N/Z is plotted in Fig. 2 against $Z/M^{1/3}$ for the isotopes of all elements that have been analyzed by the mass-spectrograph, and for the radio-elements. Where more than one isotope is known

[3] Harkins, Phys. Rev. **37**, 1180 (1931).
[4] The isotopic number invented by Harkins represents in terms of the present theory simply the excess, $N-Z$, of neutrons over protons in the nucleus.
[5] Latimer, J. Am. Chem. Soc. **53**, 981 (1931). See also Latimer and Libby, J. Chem. Phys. **1**, 133 (1933).

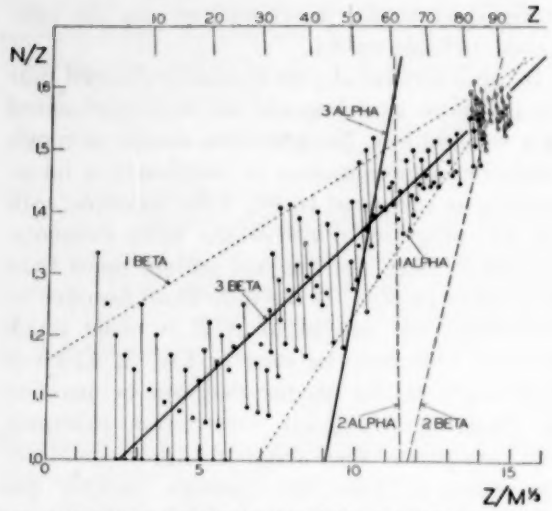

FIG. 2. Stability boundaries for alpha- and beta-processes.

for a given element, points connected by a line are shown for the heaviest and lightest species. For the radioactive elements all isotopes are shown. They are represented by open circles, with strokes pointing downward to designate emitters of beta-particles and upward for the alpha-emitters.[6]

The lines marked 1 beta and 1 alpha in the figure represent the condition adopted by Heisenberg for zero energy of emission of the beta- and alpha-particles. These curves, however, fail to meet the quantitative tests described later. Numerous variations of them, with the obvious faults corrected but still based on the idea that they should skirt, as far as possible, the edges of the field of points, were therefore tested. None of these proved successful in all respects. This was interpreted to mean that stability alone is not fully effective in determining the boundaries of this field. The existence of unstable species of very long life periods, and fluctuations from the mean positions, largely obscure the proper placement of the curves. Resort was made, therefore, to indirect criteria of correctness in placement.

Theoretical conditions affecting boundary curves

The constants in Eqs. (4), (5) and (10) are theoretically related as follows:

$$C_2 = 3D_2/(D_1+1), \tag{15}$$

$$c_2 = 3D_2/(D_1-1), \tag{16}$$

$$C_2/c_2 = (D_1-1)/(D_1+1). \tag{17}$$

The slope, therefore, of either of the stability boundaries desired for Fig. 2, is theoretically determinable by (15) and (16) from the intercept and slope of the line in Fig. 1. And the ratio of these slopes is fixed in terms of the intercept D_1 alone.

In conformity with these equations, attempts were made to place lines of the required slopes in Fig. 2. Those marked 2 beta and 2 alpha in the figure, for example, were chosen so that constants derived from them reproduce as to order of magnitude the observed energies of the beta- and alpha-disintegrations of the heavy elements. Although they meet successfully these requirements and several other tests that may be made, they fail in other respects. It seems impossible to accept such a placement, and no other based on strict application of (15) and (16) has been found satisfactory.

Were we dealing with a rigorous theory, the discrepancies above could only mean a failure of the basic postulates, or incorrectness in interpretation of the nature of one or the other of the radioactive processes. The beta-process is by no means above suspicion in this last respect, and its correct formulation must remain as an important possibility in removal of the disagreement. Since the theory is but roughly approximate in character, however, neither of these alternatives can be claimed. A part, but not the larger part, of the discrepancy is indeed due to the fact that D_1 and D_2 are of the nature of average values, not exactly applicable to points far from the mean positions in the diagrams. The principal difficulty, however, may lie in an extreme sensitivity, often found in similar connections of the conditions imposed by equating the second derivatives. Regardless of what causes the difficulty, it has proved sufficient in all quantitative tests discussed later to treat Eq. (10) as a rough numerical requirement only. In the final placement of the curves, next to be discussed, the demands of (10) are given some weight, since the later energy equations are otherwise rather meaningless, but the attempt at strict fulfillment is abandoned.

[6] It is assumed that the beta-activity of potassium and rubidium is due to isotopes 41 and 87, respectively, and the alpha-activity of samarium is attributed to Sm^{147}.

Final choice of stability boundaries for the beta- and alpha-changes

Among all the changes that nuclei may undergo, the emission of beta-particles is unique in one respect. Its reversal,[7] in such cases as are energetically favorable, apparently should require the assistance of no external agency to supply the particle. The *s* electrons of the extra-nuclear shells are directed toward the nucleus. Even though the de Broglie wave-lengths of these electrons at every point in their fall through the Coulomb field be much different from nuclear dimensions, making the probability of capture small for a single encounter, this may be compensated by the high frequency of approach. A calculation attributed[8] to Gamow, for instance, shows that the K electrons of nitrogen "penetrate" the nucleus about 10^{20} times per second. The infrequent occurrence of isobars of unit difference in atomic number may perhaps be taken as direct evidence that such reversals can in fact occur. For there is no reason to suppose that the processes of atomic evolution, either of decay or synthesis, will not often produce such isobaric pairs. If relatively rapid beta-changes are possible in both the forward and the reverse direction, only stable members of such pairs should persist. If, however, the reaction is of unusually long period in either direction, both the stable and unstable species should exist. Actually they are seldom found (compare a later section). We may therefore assume tentatively that the reaction of one of the external electrons with the nucleus is of sufficient probability to require consideration.

It then becomes clear that the line of zero energy of the beta-change should be centrally placed with respect to the existing nuclei. Its strict application would indeed require that the nuclei be restricted to a narrow field, with only one stable isotope of each element. This behavior is actually approached by the elements of odd atomic number, which seldom show more than one abundant isotope. If one recognizes the structural influences previously pointed out, or assumes a nearly flat minimum in the curve of nuclear energy as a function of the number of neutrons associated with a fixed number of protons,[9] the opportunity for a somewhat wider spread of the isotopes becomes apparent, particularly in elements of even atomic number. The more or less central location of the beta-stability curve remains, however, most probable.

The line marked 3 beta in Fig. 5 has therefore been chosen as representing approximately the boundary of beta-stability toward which the elements tend. With this boundary fixed, there are various limitations which apply to the alpha-boundary and which serve as criteria of the correctness of any position assumed for it, or for the two lines together. These criteria may be listed as follows: (1) the approximate equality of the two forms of the second derivative of the nuclear energy, Eqs. (7) and (9); (2) absence of consistent trend in the constant of integration of Eq. (19) below; (3) agreement of required value of r_0 with values obtained by other methods; (4) correctness as to order of magnitude of the energy effects in known alpha- and beta-disintegrations; (5) correctness in magnitude of energy effects in collision processes; (6) agreement of calculated binding energies of neutron and proton with those obtained from atomic masses in light elements.

Of the many combinations that have been tested by these criteria, the 3 beta—3 alpha pair of Fig. 2 is, on the whole, the most satisfactory. The constants of these curves are $C_1=0.885$, $C_2=0.0478$, $c_1=-1.600$, and $c_2=0.2863$. Appraisal of these values by criteria 2–6 may be made from results in following sections. Concerning the first criterion, it remains only to say that these constants determine the broken line in Fig. 1. Numerically, for average values of N/Z at $Z=90$, the second derivative according

[7] The reverse of the beta-ray change might be formulated as the ejection of a positron. Observation of an artificially induced process of this type is reported by Joliot and Curie, Nature **133**, 201 (1934). In net effect this would be equivalent to the capture of a beta-particle by the nucleus, which is assumed above to constitute the reverse process. Exact equivalence requires, of course, equality in the energy involved in the two processes. The available energy of the change may determine the process by which it occurs. Thus the ejection of the positron must evolve at least a million electron-volts, whereas the introduction of the electron apparently might occur even with a smaller energy change. When the energy is of the required magnitude, positron emission appears the more probable of the two reverse-beta mechanisms.

[8] cf. Chadwick, Constable and Pollard, Proc. Roy. Soc. **A130**, 480 (1931).

[9] Heisenberg, reference 1, II, p. 157, 158, explains the existence of isobars with Z even by curves of energy against N, M constant. The curve above is similar in form.

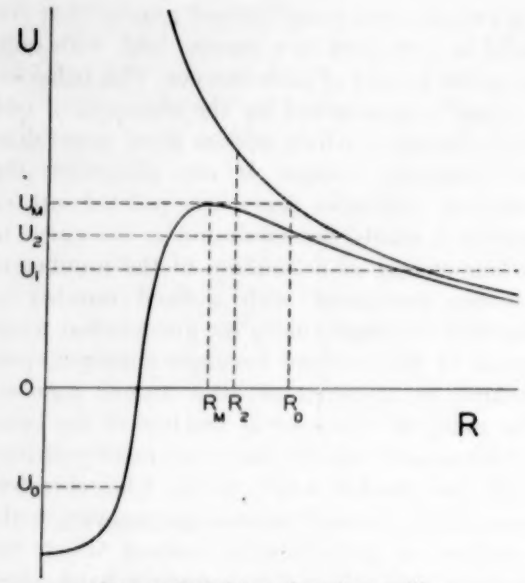

FIG. 3. Definition of nuclear radii.

to (7) is 3.01×10^{-7}, and by (9) 2.22×10^{-7}. At $Z=10$ the corresponding figures are 18.2×10^{-7} and 18.1×10^{-7}, with energy in ergs.

Magnitude of the proportionality constant r_0, and definition of nuclear radii

The constant r_0 of Eq. (3) is necessary in the solution of Eqs. (11–14). It has been treated in this work as an adjustable constant, chosen simultaneously with the constants C and c to secure the best apparent agreement according to the previously listed criteria. This amounts to a determination of this constant from the other data employed. The value found is 1.6×10^{-13} cm.

This value is in agreement with those obtained by other methods. Gamow,[10] from the quantum-mechanical relation between the energy changes and decay constants, calculated the "effective radius" of the nucleus of each of the principal alpha-ray emitters. From his values of R_0, r_0 is found to vary from about 1.28 to 1.40×10^{-13} for these elements. Rutherford, Chadwick and Ellis[11] conclude, from studies by Bieler and by Rutherford and Chadwick of the deviations from Coulomb's law in wide angle scattering of alpha-particles by the nuclei of aluminum and magnesium, that r_0 may be taken as about 1.2×10^{-13}. The definition of R_0 is not quite the same in the two last methods of estimation, and in neither of them is it identical with that implied in the present calculation. The relations between the various definitions are made clear in Fig. 3.

In this diagram, the lower curve is of the type usually adopted for the representation of the potential energy, U, of a system consisting of a nucleus and a positive particle as a function of the distance, R, between their centers. The curve is in this case drawn to scale, down to $U=0$, from the equation $U=2Ze^2/R-a/R^3$, with the constant a as determined by Bieler for the alpha-particle in the field of the aluminum nucleus. The upper curve is the corresponding Coulombic function. U_0 represents the lowest energy level, U_1 and U_2 excited levels. U_M is the maximum potential that the system can possess according to Bieler's treatment. R_M, 3.44×10^{-13} cm, is the radius resulting from the scattering experiments. R_0, the distance at which the purely Coulombic potential is equal to U_M, is the radius of the nucleus defined by the present calculations. (Based on Bieler's determination of U_M, it has the value 5.15×10^{-13} cm as compared with 4.8×10^{-13} determined, entirely independently of the theoretical relation between the two definitions by the present calculations.) R_2 results from the quantum-mechanical treatment as applied in Gamow's theory to the level U_2. As the degree of excitation varies, the radius thus calculated also changes. It approaches R_0 as a limit at high excitation,[12] and at lower levels may be equal to R_M, as it is for U_1, or be less than this value. The radius determined by the present calculations is, therefore, theoretically somewhat larger than the others, as was found, and allowing for this, agrees with them excellently.

The present method of determination involves a great variety of data and appears to yield a pretty reliable estimate of r_0. The definition of this constant in the present theory has also the advantage that its use in Coulomb's law gives

[10] Gamow, *Der Bau des Atomkerns und die Radioaktivität*, S. Hirzel, Leipsig, 1932, pp. 58–65.

[11] Rutherford, Chadwick and Ellis, *Radiations from Radioactive Substances*, The Macmillan Co., New York, 1930, p. 280.

[12] The discovery by Gamow that the effective radius in his calculations is greater for excited than for normal nuclei appears therefore to result in part from the nature of his approximations, and does not necessarily imply any change in R_M, for example.

directly the height of the potential barrier, which Bieler's theory does by use of an additional constant, and Gamow's does not do at all.

The mass of the neutron

To determine $E_N°$, the mass of the neutron must be known. Chadwick[13] obtained its atomic weight as 1.0067. Various other values have since been proposed. The best value is now uncertain and will no doubt remain subject to modification for some time in the future. For the purposes of the present work Chadwick's figure has been adopted. The corresponding value for the energy of formation is $E_N°=0.159\times10^{-5}$ erg per neutron. In many of the calculations of this paper the value chosen for $E_N°$ is without influence on the final result. Wherever this is not the case, comment is made.

Other auxiliary constants

The energy of formation of the helium nucleus from protons and electrons is taken as $E_a°=4.285\times10^{-5}$ erg per atom.

The electronic charge, 4.767×10^{-10} e.s.u., as given by Birge[14] is used here. Avogadro's number correspondingly is taken as 6.068×10^{23}.

Final values of constants of Eqs. (1) and (2), and the range of their validity

On substituting the values just discussed of the various constants appearing in Eqs. (11–14), it is found that, in ergs,

$$K_1=2.624\times10^{-5}, \qquad k_1=0.153\times10^{-5},$$
$$K_2=-1.237\times10^{-5}, \qquad k_2=1.733\times10^{-5}.$$

Of these constants, K_1 alone is dependent on the mass of the neutron.

The intention of Heisenberg was to restrict his theory to the heavy elements only. In this work, however, no very urgent reason for rigid restriction of this kind has appeared. In Figs. 1 and 2, for example, the fluctuations, periodic and otherwise, increase only gradually in magnitude from the heavy to the light elements. They become exceptionally large, however, below atomic number 10 and here, also, the packing fractions of different isotopes lie on divergent curves. Up to this value of Z, numerical approximations of the theory (such as the equality of Z and $Z-1$ or $Z-2$, and the equivalence of integrals with the corresponding summations) may also introduce appreciable errors. For these reasons the application of the above constants has been restricted to elements with $Z>10$.

[13] Chadwick, Proc. Roy. Soc., **A136**, 692 (1932).
[14] Birge, Phys. Rev. **42**, 736 (1932).

NUCLEAR ENERGIES

The energy of formation of any nucleus from neutrons and protons is approximately expressible in terms of N and Z and the constants above. This quantity will be represented by E and taken as $-\Delta E$ for the process of synthesis. From Eqs. (6) and (8),

$$dE=(K_1+K_2N/Z)dN + (k_1+k_2N/Z-e^2Z/r_0M^{1/3})dZ. \quad (18)$$

Integration of this equation, assuming N/Z to be maintained constant during the synthesis of the nucleus, yields

$$E=(K_1+k_2)N+K_2N^2/Z+k_1Z - 3e^2Z^2/5r_0M^{1/3}+I. \quad (19)$$

Here I is the constant of integration.

With values of E determined from the masses[15] of all nuclear species of $Z>10$ for which a measured value of the packing fraction has been published, adjustment of the constants was made to secure constancy in I and to meet simultaneously the criteria 4 and 5 above. The results are shown in Table I.

The degree of constancy of I may be seen in the last two columns. These include, respectively, the algebraic deviation of individual values of I from the mean, -9.6, of all, and the experimental uncertainty resulting from the error in the determinations of isotopic weight.[16]

[15] Now conveniently collected in Aston's recent book, *Mass Spectra and Isotopes*, Longman's, Green and Co., New York, 1933.

[16] The experimental uncertainties given in Table I are based on the author's estimates of error in the original papers, and are usually "limits." In some instances these have since been replaced by "probable errors" in Aston's tabulation. They are listed in the table opposite the isotope for which the primary determination of mass was made, and with which the other isotopes given were compared. In certain instances a numerical estimate of error was not originally given by Aston, the measurement being designated as "rough" or "provisional." In such cases, the experimental uncertainty is given in the last column of the table as greater than that estimated for neighboring elements. Aston has not published a definite packing faction for lead, but makes the statement that the atomic weights of the isotopes studied are integral with those of mercury to 1 or 2 parts in 10,000.

The mean deviation from the average I is 1.5, and the average experimental uncertainty is 2.8. Of the elements in the table from $_{24}Cr^{53}$ to $_{82}Pb^{208}$, there is none for which the deviation from the average I significantly exceeds the experimental uncertainty.

Eq. (19) is of some intrinsic interest as a fairly successful attempt at an energy equation. Over much of its range of application, nuclear energies or isotopic weights can be calculated with as much accuracy (within about 10 million electron-volts or 0.01 atomic weight unit on the average) as they have hitherto been measured. As more accurate experimental values for the heavy elements become available in the future, this will no doubt no longer be possible by so simple an equation. Moreover, energy relations in particular nuclear processes can usually be more satisfactorily treated by equations specifically applicable, of types discussed later. The principal interest of the general energy equation centers therefore, in the present connection, in its bearing upon the self-consistency and numerical reliability of the constants involved.

The values of the energies of formation in Table I are greatly affected by the mass adopted for the neutron. Fortunately, the integration constant, I, is independent of $E_N°$. The desired tests are therefore uninfluenced by uncertainties in it.

Energy of Emission or Capture of Particles by Nuclei

The change in energy that accompanies an emission or (with reversed signs) a capture of any particle of zero kinetic energy is conveniently formulated as $\Delta E=\bar{E}-V$, where V represents the Coulombic energy. For the neutron and proton, the binding energies are, of course, given by Eqs. (1) and (2). The binding energy of any composite particle is obtainable in terms of the simple ones. For the alpha-particle,

$$\bar{E}_a=2(K_1+k_1)-E_a°+2E_N° +2(K_2+k_2)N/Z. \quad (20)$$

Inserting numerical values of the constants,[17]

$$\bar{E}_a=1.587+0.992N/Z. \quad (20a)$$

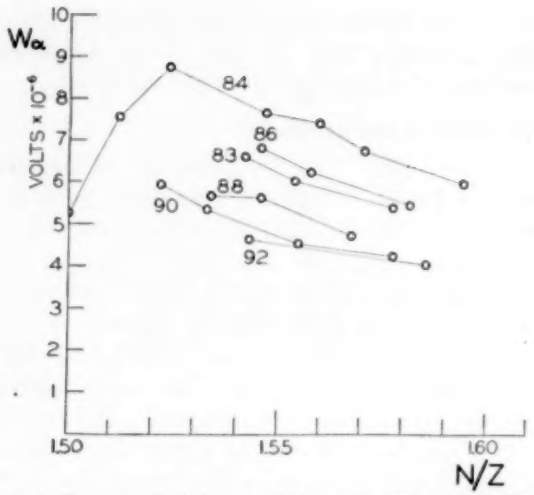

FIG. 4. Energy of alpha-particles as function of N/Z of parent atom in series of isotopes.

Similarly, for the deuton,

$$\bar{E}_D=K_1+k_1+E_N°-E_D°+(K_2+k_2)N/Z, \quad (21)$$

$$\bar{E}_D=2.652+0.496N/Z. \quad (21a)$$

Energy of emission of alpha-particles

If the kinetic energy of the emitted alpha-particle is denoted by W_a, we may write approximately, $W_a=V_a-\bar{E}_a$. This becomes

$$W_a=E_a°-2E_N°-2(K_1+k_1) -2(K_2+k_2)N/Z+2e^2Z/r_0M^{1/3} \quad (22)$$

or

$$W_a=-1.588-0.992N/Z+0.284Z/M^{1/3}. \quad (22a)$$

The general requirements of Eq. (22) in relation to the experimental facts are clearly brought out by the following considerations. The factor $M^{1/3}$ in the last term of (22) varies less than 2 percent among the isotopes of any radioactive element. For any constant value of Z, therefore, the energy of the emitted alpha-particle should, according to (22), be a nearly linear function of N/Z. This is tested graphically in Fig. 4. The points of this figure represent the observed energies of the particles plotted against N/Z. Those belonging to the isotopes of a single element are connected by lines marked with the

[17] In all numerical equations the resultant energies are in units of 10^{-6} erg per atom. In the tables and tests, comparisons are sometimes made in other units. Conversion factors are 10^{-6} erg $=6.28\times10^{6}$ electron-volts, and 10^{-6} erg per atom $=0.00675$ g per g atom, $O^{16}=16$.

TABLE I. *Energy of formation of nuclei from neutrons and protons.* (The unit[17] of energy in each of the last four columns is 10^{-6} erg.)

—Element— Z	Symbol	M	Energy of formation	I Eq. 19	$(I-I_{Av.})$	Exp't'l uncertainty
10	Ne	20	21.9	− 7.7	1.9	0.1
		22	24.2	− 8.8	0.8	
14	Si	28	32.6	− 7.8	1.8	0.4
15	P	31	35.7	− 9.0	0.6	0.7
17	Cl	35	40.0	−10.0	−0.4	0.7
		37	42.4	−10.9	−1.3	
18	A	36	42.1	− 8.4	1.2	0.6
		40	46.8	−10.4	−0.8	
24	Cr	52	64.1	− 8.0	1.6	2.2
28	Ni	58	70.6	− 7.3	2.3	(2.2?)
30	Zn	64	77.6	− 8.2	1.4	>2.5?
33	As	75	89.2	−10.6	−1.0	1.6
34	Se	78	91.7	−11.6	−2.0	>2.4
		80	93.5	−12.3	−2.7	2.4
35	Br	79	94.5	− 9.8	−0.2	1.8
		81	96.9	−10.0	−0.4	
36	Kr	78	94.1	− 7.9	1.7	2.4
		80	96.1	− 9.0	0.6	2.4
		82	97.9	−10.1	−0.5	1.8
		83	98.9	−10.3	−0.7	1.8
		84	99.8	−10.5	−0.9	1.9
		86	101.6	−10.9	−1.3	1.9
41	Cb	93	109.8	− 9.9	−0.3	>2.8?
42	Mo	98	111.9	−13.5	−3.9	>3.0?
		100	114.0	−13.7	−4.1	
50	Sn	112	131.2	− 7.4	2.2	
		114	133.3	− 8.0	1.6	
		115	134.5	− 8.0	1.6	
		116	135.7	− 8.2	1.4	
		117	136.6	− 8.3	1.3	
		118	137.7	− 8.5	1.1	
		119	138.9	− 8.3	1.3	
		120	140.1	− 8.1	1.5	3.6
		121	141.0	− 8.2	1.4	
		122	142.2	− 8.0	1.6	
		124	144.4	− 7.6	2.0	
52	Te	126	142.6	−11.5	−1.9	4.0
		128	144.6	−11.4	−1.8	
53	I	127	144.5	−10.5	−0.9	3.7
54	Xe	124	141.4	− 9.8	−0.2	
		126	143.5	−10.0	−0.4	
		128	145.6	−10.1	−0.5	
		129	146.6	−10.3	−0.7	
		130	147.8	−10.3	−0.7	
		131	148.8	−10.2	−0.6	
		132	150.0	− 9.7	−0.1	
		134	152.1	− 9.5	0.1	4.0
		136	154.3	− 8.8	0.8	
55	Cs	133	150.5	−10.2	−0.6	4.0
56	Ba	138	158.3	− 7.1	2.5	4.0
73	Ta	181	201.8	− 1.9	7.7	>5.5?
75	Re	187	200.2	− 8.4	1.2	5.5
76	Os	190	203.4	− 7.7	1.9	5.6
		192	205.4	− 6.8	2.8	
80	Hg	196	204.8	−10.6	−1.0	
		197	205.8	−10.6	−1.0	
		198	206.8	−10.6	−1.0	5.9
		199	207.7	−10.6	−1.0	
		200	208.7	−10.3	−0.7	
		201	209.7	−10.2	−0.6	
		202	210.7	−10.1	−0.5	
		203	211.7	− 9.7	−0.1	
		204	212.7	− 9.5	0.1	
81	Tl	203	204.9	−16.3	−6.7	5.9
		205	206.9	−16.0	−6.4	
82	Pb	206	215.0	− 8.8	0.8	(5.9?)
		207	216.0	− 8.8	0.8	
		208	217.0	− 8.5	1.1	
			Average	− 9.56	1.5	2.8

atomic number to which they correspond. With the exception of two points belonging to element 84, the required variation of energy with N/Z is roughly substantiated. The essentials of this relation were first discovered and discussed by Fajans[18] who pointed out a connection between atomic weight and stability.

A second requirement of Eq. (22) is, however, contradicted in Fig. 4. At constant values of N/Z the expectation is that the energy of the alpha-particle should be greater the larger the value of Z. This is not fulfilled, and presents an interesting problem. It is related, obviously, to the fact that in a series of successive alpha-disintegrations the energy of the particles, as a rule, progressively increases. This can be taken as an indication that structural effects, neglected in the simple theory, are of some importance here. It is possible that the removal of particles from a completed group would leave the remaining structure progressively less stable until the next sub-group is approached. If this is not the explanation, the behavior is still explicable on the basis of the failure of the tacit assumption that excited states are not involved. If the departure of an alpha-particle, for example, leaves the residual nucleus with an excitation which, because of some sort of forbidden transition, cannot be relieved by radiation, the particles from the residual nucleus will have greater energies than expected.

Whatever the cause of the difficulty, it is apparent that faithfulness to detail will not be

[18] Fajans, Le Radium **10**, 171 (1913); Naturwiss. **14**, 963 (1926); *the Baker Lectures*, Cornell University, McGraw Hill Book Co., N. Y. 1931.

TABLE II. *Energy of alpha-particles.* (The unit[17] of energy is 10^{-5} erg per particle.)

Element	Isotope	W_α (obs.)	W_α (calc.)	Difference
83 Ac C	211	1.058	0.842	0.216
Th C	212	0.962	0.824	0.138
Ra C	214	0.876	0.786	0.090
84 Ra F	210	0.840	0.936	−0.096
Ac C'	211	1.200	0.918	0.282
Th C'	212	1.402	0.898	0.504
Ra C'	214	1.228	0.866	0.362
Ac A	215	1.184	0.846	0.338
Th A	216	1.078	0.830	0.248
Ra A	218	0.956	0.794	0.162
86 An	219	1.092	0.930	0.162
Tn	220	1.000	0.912	0.088
Rn	222	0.870	0.874	−0.004
88 Ac X	223	0.900	1.010	−0.110
Th X	224	0.902	0.994	−0.092
Ra	226	0.755	0.960	−0.205
90 Ra Ac	227	0.942	1.090	−0.148
Ra Th	228	0.850	1.076	−0.226
Io	230	0.726	1.040	−0.314
Th	232	0.676	1.006	−0.330
91 Pa	231	0.797	1.098	−0.301
92 U II	234	0.740	1.122	−0.382
U I	238	0.648	1.042	−0.384
			Average	0.26

achieved by Eq. (22). Average behavior of the radioactive group as a whole must, however, be reflected in the equation if the constants are correctly chosen. Adjustment of them has been made with this in mind.

In Table II the observed and calculated energies are compared for the alpha-emitters appearing in Fig. 4. The average deviation of the calculated from the observed energies corresponds to 1.6×10^6 electron-volts, or about 0.0015 atomic weight unit. Although this is large compared to the error of direct measurement, it represents an accuracy about 20 times that of the average at present achieved above mass number 100 by the use of the mass-spectrograph. For calculations relating to nuclear species which, because of very long life period or very short range of particle, cannot be directly studied, a considerable increase in accuracy over the only other method of calculation available is therefore gained in this range. This, and the approximate substantiation of the constants employed, constitute the only value of (22), which obviously does not contain all of the factors requisite for close approximation.

TABLE III. *Energy of beta-ray changes.* (The unit[17] of energy is 10^6 electron-volts.)

Element	Isotope	Obs. energy of particles (Average)	Obs. energy of photons (Average per particle)	Total energy (Obs.)	Calculated energy
81 Th C''	208	0.70	—	—	0.52
82 Ra D	210	0.01	0.05	0.06	0.29
Th B	212	0.10	<0.21	<0.31	0.79
Ra B	214	0.23	0.20	0.43	1.3
83 Ra E	210	0.34	0.0	0.34	−0.43
Th C	212	0.7	—	—	0.05
Ra C	214	0.76	1.66	2.42	0.53
90 UX I	234	0.11	—	—	0.31
91 UX II	234	0.39	—	—	−0.40
19 K	41?	0.4	0.06	0.46	0.15
37 Rb	87?	0.15	—	0.15	1.2

Energy of beta-ray changes

Measurements of the mean energy of beta-particles are available for nine of the radio-elements.[19]. For five of these the mean energy, per disintegration, of the photons emitted may be inferred from data cited by Rutherford, Chadwick and Ellis.[20] These data are compared in Table III with energies calculated by the equation

$$W_\beta = k_1 - K_1 - E_N^\circ + (k_2 - K_2)N/Z - e^2Z/r_0M^{1/3}, \quad (23)$$

which, with the present constants, becomes

$$W_\beta = -2.630 + 2.970N/Z - 0.142Z/M^{1/3}. \quad (23a)$$

The energies calculated by (23) presumably represent the total energy of the change. For the cases shown in the table the average difference of the calculated from the observed total energies is less than a million volts. The agreement is, therefore, as good as in any other part of this work. The curve 3 beta was placed in Fig. 2 so as to fall between the lowest isotopes of the even and odd numbered beta emitters among the heavy radio-elements. This is reflected in Table

[19] See Gamow, reference 10, p. 67 for detailed references.
[20] Reference 11, pp. 401, 403, 501.

TABLE IV. *Decrease in mass on capture of particles by nuclei of light elements.* (The unit[17] is the gram per gram atom, $O^{16}=16$.)

Particle captured	Original and final nuclei	Observed decrease in mass	Calculated decrease in mass	Difference calc.-obs.	Exp't'l uncertainty
Proton	$Be^{9}-B^{10}$	0.0098	0.0138	0.0040	0.002
	$B^{11}-C^{12}$	.0152	.0129	−.0023	.003
	$C^{13}-N^{14}$	.0038	.0122	.0084	.006
	$N^{15}-O^{16}$	.0110	.0117	.0007	.003
	$O^{18}-F^{19}$	.0143	.0127	−.0016	.005
	$F^{19}-Ne^{20}$	.0110	.0108	−.0002	.003
			Average	.0029	.0037
Deuton	$Li^{7}-Be^{9}$	0.0127	0.0197	0.0070	.001
	$Be^{9}-B^{11}$	.0181	.0199	.0018	.002
	$B^{10}-C^{12}$	.0235	.0190	−.0045	.003
	$B^{11}-C^{13}$	.0206	.0198	−.0008	.004
	$C^{12}-N^{14}$	.0092	.0187	.0095	.004
	$C^{13}-N^{15}$	.0144	.0182	.0038	.006
	$N^{14}-O^{16}$	.0216	.0185	−.0031	.003
	$O^{18}-Ne^{20}$	.0234	.0192	−.0042	.004
			Average[21]	0.0041	.0037
Neutron	$Li^{6}-Li^{7}$	0.0066	0.0094	0.0028	0.001
	$B^{10}-B^{11}$	.0092	.0094	.0002	.003
	$C^{12}-C^{13}$	.0063	.0094	.0031	.004
	$N^{14}-N^{15}$	.0115	.0094	−.0021	.006
	$O^{16}-O^{18}$	−.0008	.0115	.0107	.003
	$Ne^{20}-Ne^{22}$	.0093	.0118	.0025	.002
			Average[21]	.0037	.0036
Alpha-Particle	$Li^{6}-B^{10}$	0.0032	0.0142	0.0110	0.002
	$Li^{7}-B^{11}$	.0058	.0166	.0108	.002
	$Be^{9}-C^{13}$	.0137	.0154	.0017	.004
	$B^{10}-N^{14}$	.0077	.0130	.0053	.004
	$B^{11}-N^{15}$	.0100	.0144	.0044	.004
	$C^{12}-O^{16}$	.0058	.0124	.0066	.001
	$N^{15}-F^{19}$	.0054	.0129	.0075	.005
	$O^{16}-Ne^{20}$	.0055	.0113	.0058	.001
	$O^{18}-Ne^{22}$	.0140	.0132	−.0008	.004
			Average[21]	0.0046	.0033

III by the fact that the calculated energies are usually too high for the even numbered and too low for the odd numbered elements. Better agreement would be obtained by treating these classes separately. This has been sacrificed throughout the present work for the sake of representing average behavior and general trends.

Energy evolved in capture of various particles by nuclei of light elements

A check of the constants derived here when applied to nuclei below the heaviest elements is to be desired. Unfortunately the only available data of sufficient experimental accuracy to permit reliable tests pertain to the elements below atomic number 10. In order to make sure that the proposed constants do not lead to absurd results even in this region, calculations have been made of the energy which would be liberated if a proton, a neutron, a deuton or an alpha-particle were captured by various light nuclei. The calculated energies are compared in Table IV with the decrease in mass corresponding to the change.

The calculated values will be referred to as ΔE and are based on the following equations:

$$\Delta E_P = -0.153 - 1.733N/Z + 0.142Z/M^{1/3}; \quad (24)$$

$$\Delta E_N = -2.624 + 1.237N/Z; \quad (25)$$

$$\Delta E_D = -2.652 - 0.496N/Z + 0.142Z/M^{1/3}; \quad (26)$$

$$\Delta E_\alpha = -1.587 - 0.992N/Z + 0.284Z/M^{1/3}. \quad (27)$$

In applying Eqs. (24)–(27) to the processes indicated in Table IV, the values of N and Z are taken to correspond to the nucleus to which the particle is added. The calculated values of ΔE_N are greatly affected by the mass adopted for the neutron, but the "observed" values are also affected in the same way. The difference between the observed and calculated results is therefore independent of the mass of the neutron.

The average difference of the calculated from the observed results in Table IV varies between about 2.7 and 4.3 million volts for the different processes while the average experimental uncertainty is of the order of 3.5 million volts.[21]

As applied to the very light elements in Table IV, the interest in Eqs. (24)–(27) centers entirely in the control afforded of the constants selected. In this region the basic curves adopted as standard seem to introduce definite, but not unduly large, trends away from the experimental values in the case of the alpha-particle. However, the trends and individual fluctuations should

[21] These differences are computed omitting the figures for lithium, on the basis of its extreme lightness, from the averages. The experimental uncertainty in the last column is based on an estimate of 0.003 unit for C^{13}, N^{15} and O^{18}, with the observers estimates employed for the remaining elements.

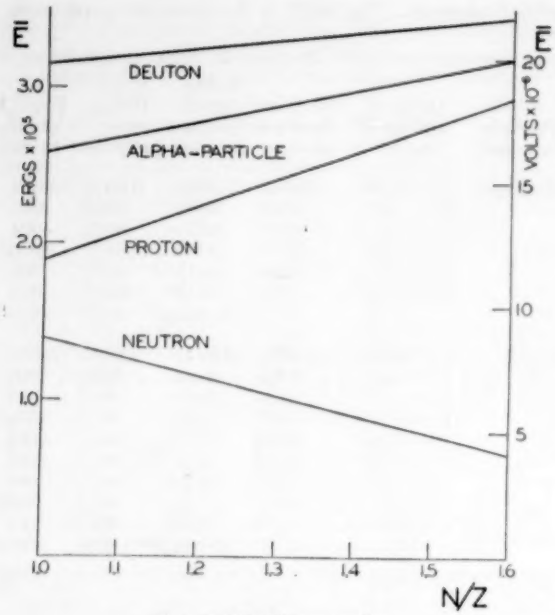

FIG. 5. Binding energies.

decrease with approach to the region in which the original assumptions are likely to be more closely valid. It is believed therefore that the equations afford reliable approximations, of greater accuracy than now obtainable from isotopic masses, for nuclei of large mass number.

NUCLEAR REACTIONS IN COLLISIONS WITH PARTICLES

General characteristics deducible from binding energies

Certain deductions of rough qualitative character concerning collision processes are obtainable from consideration of the binding energies alone of the various particles. This is facilitated by Fig. 5, where graphs[22] are shown of binding energies as functions of N/Z, based on Eqs. (1), (2), (20) and (21).

One of the features of the diagram is the large magnitude at all values of N/Z of the binding energy of the deuton. This implies relatively marked effectiveness of this particle in ejection of others.

According to the diagram, the alpha-particle should always be more effective, from a purely energetic standpoint, than the proton in producing disintegrations, though for equal kinetic energy of the particles the proton has a higher probability of surmounting or penetrating the Coulomb barrier. The two curves approach each other at large values of N/Z. There is also some indication from Table IV that the alpha-curve should be lowered somewhat relative to that of the proton among light elements.

Neutrons of low kinetic energy will, according to Fig. 5, be incapable of liberating other particles in their interactions with nuclei. They should be ejected readily by any of the other particles, especially if the struck nucleus is of high neutron-proton ratio, as it is, relative to neighboring elements, in Li^7, Be^9 and B^{11} for example.

The question of capture or escape of any projectile particle which has caused a disintegration is also answered, in part, by Fig. 5. Excluding the neutron, the smallest of the binding energies is of the order of 12 million volts. Neither natural particles nor artificially accelerated particles of such high energy have yet been employed in nuclear experiments. Disintegration without capture is therefore improbable or impossible in most cases. The ejection of a neutron without capture of the colliding particle is, on the other hand, indicated to be quite possible in many cases as far as total energy, independent of questions of transfer, is concerned.

The above qualitative conclusions seem to be borne out by experience. They are of some value for orienting purposes, but many other factors enter any more detailed consideration. Adequate quantitative treatment from the energetic standpoint of any nuclear collision requires a complete formulation of the process. Given such a formulation, equations applicable to the process can readily be deduced, as illustrated below.

Energy of particles ejected in nuclear disintegration by collision

With symbols previously employed and subscripts 1 and 2 to denote the projectile and emitted particles, respectively, the energy of the ejected particle is

$$W_2 = W_1 - V_1 + \bar{E}_1 - \bar{E}_2 + V_2. \qquad (28)$$

This equation assumes the capture of the impinging particle, neglects the kinetic energy and

[22] The lines of this figure represent, of course, mean positions about which the points of the system fluctuate.

excitation of the residual nucleus, and assumes that only one particle and no photon is ejected in the process. Strictly, the quantities V_1 and $\bar{E}_1$ are taken to correspond to the original struck nucleus, and $\bar{E}_2$ and V_2 to the residual nucleus. If, however, the nucleus is sufficiently large, the differences between the original and residual nucleus may be neglected without significant error. This has been done in the present calculations.

Substitution in (28) of the expressions previously obtained ((1), (2), (20) and (21)) for the appropriate binding energies leads to equations covering any type of capture-ejection process. A series of such equations for processes of current interest are recorded below.

$$W_P = W_a + 1.434 - 0.741N/Z - 0.142Z/M^{1/3}, \quad (29)$$

$$W_P = W_D + 2.499 - 1.237N/Z, \quad (30)$$

$$W_a = W_P - 1.434 + 0.741N/Z + 0.142Z/M^{1/3}, \quad (31)$$

$$W_a = W_D + 1.065 - 0.496N/Z + 0.142Z/M^{1/3}, \quad (32)$$

$$W_N = W_a - 1.037 + 2.229N/Z - 0.284Z/M^{1/3}, \quad (33)$$

$$W_N = W_P - 2.471 + 2.970N/Z - 0.142Z/M^{1/3}. \quad (34)$$

These equations do not depend in any way upon the mechanism of the assumed processes (penetration or surmounting of barriers, resonance, etc.), and they of course can yield no information as to the probability of occurrence of the various reactions.

The principal data suited to the tests of these equations are the observations of Rutherford and Chadwick[23] on protons ejected by alpha-particles. These are compared in Table V with the calculated values. In addition to these there are fragmentary data relating to other reactions. Lewis, Livingston and Lawrence[24] report the ranges of alpha-particles ejected from magnesium and aluminum by deutons, and Lawrence and Livingston[25] found long range protons ejected from aluminum by deutons. Only elements above atomic number 10 are included in the table.

TABLE V. *Energy of ejected particles in collision processes.* (Energies[17] are in 10^6 electron-volts.)

Projectile particle	Projectile energy	Struck nucleus	Ejected particle	Equation applied	Energy of ejected particle Calc.	exp't'l	Diff.
Alpha	7.68	Na^{23}	Proton	(29)	8.2	6.9	1.3
Alpha	7.68	Mg^{24}	Proton	(29)	8.3	5.6	2.7
Alpha	7.68	Mg^{26}	Proton	(29)	7.6	5.6	2.0
Alpha	7.68	Al^{27}	Proton	(29)	7.8	8.8	1.0
Alpha	7.68	P^{31}	Proton	(29)	7.5	7.7	0.2
Deuton	2.7	Al^{27}	Proton	(30)	10.	7.5	2.5
Deuton	1.2	Mg^{24}	Alpha	(32)	8.5	7.0	1.5
Deuton	1.2	Mg^{26}	Alpha	(32)	7.9	7.0	0.9
Deuton	1.2	Al^{27}	Alpha	(32)	8.4	7.0	1.4

Threshold energies of projectiles and critical characteristics of the struck nuclei in disintegrations by collision

For ejected particles of any arbitrarily fixed energy, calculation of the threshold energy of the projectile (or critical composition of the struck nucleus) can be made by Eq. (28), independently of any assumption as to mechanism. As the probability of occurrence of a process depends greatly upon this factor it is, however, often desirable to consider it. In illustration, suppose that a process of capture of a particle with ejection of a single particle of another sort is in question. Assume that the external Coulombic barrier can be penetrated frequently by the projectile particle if the total energy effect is favorable to its capture, and that for the ejection of the second particle a quantity of energy essentially equal to its binding energy must be supplied. Simple considerations then lead to the following modification of (28);

$$W_1 - V_1 + E_1 = \bar{E}_2. \quad (35)$$

Applying (35) to the ejection of protons on capture of alpha-particles there results

$$N/Z = (1.515 + W_a)/0.741 - 0.383Z/M^{1/3}, \quad (36)$$

where N, Z and M pertain (with the approximation introduced in a similar case previously), to the struck nucleus. If these variables are given in magnitude, the value of the critical energy of the alpha-particle may be solved for. If the energy of the alpha-particle is fixed, the critical characteristics of the struck nucleus can be determined. This is most conveniently done by calculating from (36) values of $Z/M^{1/3}$ corresponding to two arbitrarily chosen values of N/Z. On placing the resulting values on a plot like that in Fig. 2, it will be found that the line

[23] Reference 11, p. 293. The "observed energies" in Table V correspond to the maximum range of the protons in the forward direction.

[24] Lewis, Livingston and Lawrence, Phys. Rev. **44**, 55 (1933).

[25] Lawrence and Livingston, Phys. Rev. **45**, 220 (1934).

determined by them separates the nuclei for which the assumed reaction is indicated to be possible from those for which it is not. On carrying out this process for the alpha-particle of Ra C′ (of 1.222×10^{-5} erg energy) it is found that all isotopes of elements below $_{25}$Mn meet the condition. This necessarily rough result may be compared with the experimental one of Rutherford and Chadwick, who found disintegrations of this type as high as $_{19}$K, but not in heavier elements.

The possibilities predicted by Eq. (35) applied to capture of a deuton with ejection of a neutron or a proton are interesting. So far as total energy is concerned, neutrons might be ejected in this way from every element in the periodic system by million volt deutons. With the same assumption as to mechanism as employed above, Eq. (35) predicts that proton ejection should cease, again for million volt deutons, in the neighborhood of $_{33}$As. This is the limit at which sufficient energy is supplied on capture to carry a proton completely over the internal barrier. If this condition is abandoned as a necessary feature of the process, emission may occur even among very heavy elements. For example, if a deuton is captured by $_{78}Pt^{195}$, there is 1.645×10^{-5} erg available for excitation of a proton in the nucleus. Of this amount, 0.802×10^{-5} erg $=5.04\times10^{6}$ e.v., represents the excitation above the zero of energy. A nucleus excited to this extent should have a pretty short life and might eject a proton immediately after capture of the deuton.

Stability Relationships

Conditions for spontaneous emission of protons, deutons and neutrons

The question often arises as to whether protons are ever ejected from the nucleus in any spontaneous disintegration. The answer given by the present theory is obtained by making the energy, ΔE_P, zero in Eq. (24). The resulting equation in N/Z as a function of $Z/M^{1/3}$ represents the borderline of stability in such processes. The graph of this line is shown in Fig. 6, together with the similar curves[22] for other processes, including the beta- and alpha-curves determined previously. Points to the left of the proton line in the diagram represent nuclei that are stable with respect to emission of this particle. All existing species lie in the region between the dotted lines. Radioactivity of the type in question is therefore not expected among them. Experimentally, of course, no such spontaneous proton emission has ever been detected. Measured packing fractions negate the idea also in all cases where decisive accuracy is attained. (Compare Table IV.) Such accuracy is lacking in the heavy elements. The result above is therefore of some interest in this region.

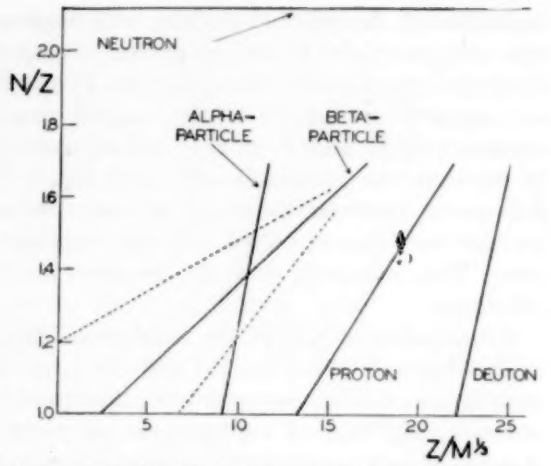

FIG. 6. Stability boundaries for emission of various particles.

Judging from Eq. (26), no existing nuclear species need ever be remotely suspected of spontaneous emission of deutons. The boundary curve for this process lies far from all others, as shown in Fig. 6. The region to the left is again the stable one. Eq. (25) shows that in the average case N/Z must exceed about 2.13 for instability with respect to the emission of neutrons. Unless Chadwick's mass of the neutron is 3 or 4 million volts too high no known nucleus can spontaneously disintegrate in this way.

Factors determining the maximum atomic number and field of existence of nuclei

The point at which the periodic system of the elements "ends" has also been the subject of much speculation. If the discussion is limited to the nuclear species that are stable under conditions existing at present on the earth, the limit for such stability is found to be in the vicinity of atomic number 51 (Sb). The alpha-

and beta-boundaries intersect each other in this region. Applying the present ideas strictly, every element above this point should be unstable with respect to one of these disintegrations and those in the region between the two curves above their intersection should be unstable with respect to both. Actually the fluctuations and periodic variations which are found vitiate this as a rigid deduction. It remains, however, strongly supported so far as the average tendencies are concerned, by the very fair agreement found in the quantitative tests of the hypotheses. The relative abundance of the elements above the intersection of the alpha- and beta-curves, and the likelihood of existence of elements above uranium, are resolved, therefore, into questions of rate of decay, or balance between decay and synthesis.

Judging from Fig. 6, the increasing instability with respect to alpha-emission may be the factor finally terminating the system of elements. The heaviest elements are farther from the indicated stable positions for the alpha than for the other changes. Periodic tendencies against the general trend may displace the breaking off point beyond the position where it might be expected that life periods would in the average case become very short. With the ultimate reversal of an opposed tendency such as this, after the completion of a period, for example, the break from relatively long to extremely short life might be sharp. This may happen above uranium.

The approach and final intersection of the dotted lines of Fig. 6 would also determine and "end" of the system. This approach seems too gradual to account for the breaking off at $Z=92$. However, the provisional interpretation given previously of these borders of the field of existing nuclei has been well supported by the results based upon it. This aspect of the situation may be outlined as follows. Stability with respect to the beta-change and its reverse determines a single line along which all nuclei should lie. Very slow rates of change make possible the existence of unstable isotopes. The "spread" of the field of points is then determined by the deviation allowable from the stable composition before the electron transfer becomes rapid. Near the point $Z=51$ the rate of the alpha-change constitutes an additional factor determining the width of the field. This appears to be of secondary importance, however, until the radio-elements are reached.

Spontaneous changes among "non-radioactive" elements

The point $Z=51$ determined above as the mean position at which stability with respect to the alpha-change ends, is surprisingly low. It is in agreement, however, with a similar conclusion from Gamow's[26] curve of nuclear energies against number of alpha-particles composing the nucleus, which goes through a minimum in this region. The large gap between this point and the lowest alpha emitter, $Z=83$, of the radio-elements, is considerably reduced by the recent discovery[27] of the alpha-activity of samarium, $Z=62$. Other alpha-changes, that have hitherto eluded discovery because of very low energies or slow decay, are to be anticipated in this region.

Concerning the beta-change, any species lying much above or much below the beta-curve of Fig. 6, may reasonably be suspected of activity involving loss or gain of an electron by the nucleus. There is, indeed, indirect but strong evidence that such changes are actually occurring in certain elements. The mass-spectrograph reveals a number of isobars. Of the total of 34 such isobaric pairs hitherto reported, only 9 are of unit difference in atomic number, and only a few of these are established beyond reasonable doubt. The relatively infrequent occurrence of this type of couple has been employed in the previous argument. We may, however, take the pair ${}_{49}\mathrm{In}^{115}-{}_{50}\mathrm{Sn}^{115}$ as a probable example of two atomic systems of the same total composition (in protons and electrons), but of different energies. The conclusion is inevitable that in such a system a spontaneous change, which in effect is the transfer of an electron between the nucleus and the exterior, is in progress in one direction or the other. The speed of the change must be finite, though perhaps immeasurably slow, or of undetectably low energy. Mass determinations sufficiently accurate to decide the direction of this change are lacking. Eq. (23) gives an energy of about 4×10^5 e.v. favoring

[26] Reference 10, pp. 19, 23.
[27] Hevesy and Pahl, Nature **130**, 846 (1932); Libby and Latimer, J. Am. Chem. Soc. **55**, 433 (1933).

the change from Sn to In, but this is no larger than the error likely in such calculations.

There are 24 isobaric couples reported of two units difference in atomic number. In such cases the energy of the change from one member of the pair to the missing intermediate element may be opposite in sign from that between the two members of the couple.[9] A double transfer would then be required to effect the change. A simultaneous emission or absorption of two electrons would no doubt be of extremely low probability, removing such pairs from the list of possibly detectable changes. If, however, the absence of the intermediate isobar merely indicates that this species is of very short life, the overall change need not be so slow. It may be remarked that for the couple $_{34}Se^{80} - _{36}Kr^{80}$, Aston gives the atomic weights 79.941 and 79.926, respectively. The mass difference is not large compared to the possible uncertainty of measurement, yet seems sufficient to justify the belief that Se^{80} is unstable with respect to Kr^{80}. Eq. (23) also leads to this result.

Conclusion

The very simple postulates of Heisenberg appear to have been substantiated as fairly close, though purely numerical, approximations over a surprisingly wide range of elements and in diverse phenomena. In their present form they cannot reproduce faithfully the individual characteristics of the various nuclei. Nevertheless, the values of the constants derived may be used with confidence for approximate calculations in many fields of nuclear physics, and for convenient general predictions and comparisons.

The relations utilized and deduced deal solely with the energy of the nucleus as a function of its composition. They might have been expressed equally well if the nuclear composition had been represented by any suitable "components." For this reason the success (or lack of it) of the relations obtained is without bearing upon the truth of the neutron-proton picture of the nucleus. These relations remain, however, as valid approximations in terms of physically real and determinable quantities.

There are two points at which the development may require modification in the future. It is not yet established that the rôles of the neutron and proton as complex and elementary particle should not be exchanged. Secondly, regardless of this, there is some evidence that the beta-ray change is more complicated than is generally assumed. If the existence is admitted of sharp and finite upper limits in the "spectra" of beta-particles, the failure of the conservation of energy in the individual occurrences can no longer be used to explain the variation in energy of the particles. The simultaneous emission of a second particle of some kind must then be assumed. Reformulation of the beta-process would be required in either case if present assumptions prove incorrect.

In conclusion, I desire to express my appreciation of valued suggestions received from Professor Heisenberg, who, in October, 1932, kindly criticized a preliminary and incomplete form of the manuscript of this paper. I have also benefited greatly from discussions with my colleagues.

On the Paramagnetic Rotation of Tysonite

J. H. Van Vleck and M. H. Hebb, *University of Wisconsin*

(Received May 12, 1934)

It is shown both theoretically and by examination of the Leiden experimental data on CeF_3 and tysonite that in rare earth compounds the Verdet constant V should exhibit the same dependence upon temperature as does the magnetic susceptibility χ, even when Curie's law is not obeyed. In consequence of the similarity in the mode of variation with temperature for V and χ, existing data on the temperature variation of χ can be considerably enhanced by drawing upon the Faraday measurements of Becquerel and de Haas. In particular, information concerning the χ's for individual crystallographic axes thus becomes available in tysonite and the tests of calculations of the susceptibility with crystalline potentials become correspondingly severe. The triclinic field proposed by Kramers for tysonite does not appear to account for the behavior of individual principal susceptibilities, although adequate for the mean characteristic of a crystal powder. It is shown that somewhat better agreement with experiment can be achieved by assuming tentatively that the local field has rhombic symmetry, with three possible orientations for the rhombic axes differing from each other by 120°, so that all told the crystal has the desired hexagonal symmetry. Such staggered rhombic fields are compatible with Oftedal's x-ray analysis of the crystallographic structure of tysonite, except that the deviations of the fields from axial character seem rather large.

Introduction

THE well-known measurements on the Faraday effect of paramagnetic salts at low temperatures, made at Leiden by Becquerel and de Haas,[1] are valuable as an alternative means of determining effective magneton numbers and other magnetic properties usually found from experiments on suceptibilities. Hitherto only the saturation properties of the magnetic rotation appear to have been generally[2] correlated with susceptibility. It is the purpose of the present paper to show, both by theory and by calculation from experimental data that, under certain conditions, the temperature variation of the Verdet constant V (rotation per unit length, divided by field strength) is, apart from an additive constant, the same as that of the magnetic susceptibility χ. Then

$$V = A\chi + K, \tag{1}$$

where K is a constant independent of temperature. Becquerel and Kramers confined[3] their analysis to temperatures so low that they could take $K=0$, and appear to have always regarded A as an undetermined function of the temperature, so that they could only utilize relations of the form

$$V(H_2, T_1)/V(H_1, T_1) = \chi(H_2, T_1)/\chi(H_1, T_1), \tag{2}$$

whereas we propose to show that it is often allowable to take

$$\frac{V(H_2, T_2)-K}{V(H_1, T_1)-K} = \frac{\chi(H_2, T_2)}{\chi(H_1, T_1)}. \tag{3}$$

Here H_1, H_2 denote two arbitrary field strengths, and T_1, T_2 two temperatures. As compared with (2), Eq. (3) greatly enhances the utility of the Faraday data, for (2) is of no value unless the field H is so great and the temperature so low as to permit observation of the saturation effect $\chi(H, T_1) \neq \chi(O, T_1)$.

[1] Jean Becquerel and W. J. de Haas, Proc. Amsterdam Acad. **32**, 523 (1929); J. Becquerel and W. J. de Haas, ibid. **32**, 536, 578, 590, 733, 874, 913, 926, 937 (1929–30); or Leiden Communications, Nos. 191, 193, 199, 211.

[2] It was mentioned long ago by Becquerel, and somewhat later independently by Ladenburg, that V and χ are both often linear in $1/T$, in which case Eq. (1) is obviously valid. Our emphasis, however, is on the applicability of (1) in the general case that Curie's law is not obeyed and it is primarily in this non-linear case that we find (1) particularly useful.

[3] H. A. Kramers, Proc. Amsterdam Acad. **32**, 1176, **33**, 959 (1929–30); H. A. Kramers and J. Becquerel, ibid. **32**, 1190 (1929); or Leiden Communications 204 and supplement 68.

1. Theory for Rare Earth Ions

The Verdet constant V for light of frequency ν is given by the expression[4]

$$V=(4\pi^2\nu^2B/Hch)\Sigma_{mn'j'm'}\tau(n'j'm';njm)[P_x(n'j'm')P_y]_{mm}e^{-W_{njm}/kT}, \tag{4}$$

where

$$B=N/\Sigma_m e^{-W_{njm}/kT}, \qquad \tau(n'j'm';njm)=1/[\nu^2-\nu(n'j'm';njm)^2]. \tag{5}$$

The matrix elements of the x component of electric moment are denoted by $P_x(n'j'm';njm)$ etc. To avoid excessive explicit printing of these elements, we find it convenient to introduce the abbreviation

$$[P_x(n'j'm')P_y]_{mm''}=i[P_x(njm;n'j'm')P_y(n'j'm';njm'')-P_y(njm;n'j'm')P_x(n'j'm';njm'')]. \tag{6}$$

The direction of the magnetic field H we take to be the z axis. The indices j and m denote respectively the inner and magnetic quantum numbers, while n signifies all quantum numbers other than j, m. The effect of n and j on the energy W is supposed large compared to kT. This supposition is warranted for all the rare earths except Sm, Eu, to which elements Eqs. (1) and (3) are consequently not applicable. It permits us to neglect, as is usual, the part of the Zeeman effect arising from elements non-diagonal in j.

If we disregard modulation of frequencies by the magnetic field we may set

$$\nu(njm;nj'm')=\nu(nj;n'j'), \qquad \tau(n'j'm';njm)=\tau(n'j';nj). \tag{7}$$

Actually this modulation is not negligible and gives rise to well-known, so-called "diamagnetic" terms, which have been calculated by Kuhn, Rosenfeld[5] and others. As long as H is the only external field, these terms are independent of T and unimportant at low temperatures. The Kronig-Hönl formulas for Zeeman components yield relations of the form[6]

$$[P_x(n'j'm')P_y]_{mm''}=m\delta_m{}^{m''}C_{nj}, \tag{8}$$

where C_{nj} depends on n, j but not on m.

The paramagnetic susceptibility is

$$\chi=(Bg\beta/H)\Sigma_m me^{-W_{njm}/kT}, \tag{9}$$

with the understanding that W_{njm} is inclusive of Zeeman energy. Here g is Landé's factor, and β is the Bohr magneton $he/4\pi mc$. If we substitute (7) and (8) in (4), then the terms in (4) corresponding to every value of n, j have the same dependence on T and H as does (9), except for a constant proportional factor and consequently (1) is proved, with so far $K=0$. (The dependence on H is mainly implicit, through W_{njm}.)

Introduction of a Crystalline Field. The preceding argument is essentially the same as Rosenfelds', but now we must go further, and insert a crystalline field, of the type treated by Bethe,[7] Kramers,[3] Penney,[8] Schlapp[8] and Van Vleck.[9] This complication is necessary for it is precisely what makes the temperature variation complex and interesting. The Hamiltonian function will cease to be diagonal in the original, equatorial system of representation. Instead, to diagonalize the crystalline plus Zeeman energy, one must make a canonical transformation to a new system, symbolized by indices j^*, m^*. We shall assume that the crystalline potential may be considered diagonal in n. This is doubtless a good approximation, for any perturbations due to non-diagonal elements in n are of the unimportant, high-frequency type. We shall also assume that in the ground state the non-diagonal elements of this potential in j can be disregarded, as here the Stark effect is smaller and the spin

[4] H. A. Kramers, Proc. Amsterdam Acad. **33**, 959 (1930); R. Serber, Phys. Rev. **41**, 489 (1932).

[5] W. Kuhn, Math. Phys. Comm. Dan. Acad. vii, **12**, 11 (1926); L. Rosenfeld, Zeits. f. Physik **57**, 835 (1930).

[6] Cf. L. Rosenfeld, Zeits. f. Physik **57**, 838–839 (1930).

[7] H. Bethe, Ann. der Physik **3**, 133 (1929).

[8] W. G. Penney and R. Schlapp, Phys. Rev. **41**, 194 (1932); R. Schlapp and W. G. Penney, ibid. **42**, 666 (1932).

[9] J. H. Van Vleck, *The Theory of Electric and Magnetic Susceptibilities*, Chap. XI.

multiplets wider than for the excited states. The new index m^* may, in a certain sense, still be regarded as a spatial quantum number but it ceases to have the usual axial significance of quantizing a component of angular momentum. For example, m^* will be nearly a "cubic" rather than equatorial quantum number if the external field is of cubic symmetry except for the magnetic portion H. Under our hypotheses, the transformation matrix from the old to new system is of the form

$$S(n'jm; n^*j^*m^*) = \delta_{n'n^*} S_{n'}(jm; j^*m^*), \qquad S(njm; n^*j^*m^*) = \delta_{nj^*} S(m; m^*), \tag{10}$$

and the susceptibility is

$$\chi = (Bg\beta/H)\Sigma_{m,\, m^*} m\, |S(m; m^*)|^2 e^{-W_{njm^*}/kT}, \tag{11}$$

with, of course, the understanding that now the letter m^* rather than m is to be used in connection with the definition of B. The Verdet constant is still given by (4) except that m^*, $j^{*\prime}$, $m^{*\prime}$ everywhere replace m, j', m'. If it is allowable to neglect the effect of m^*, $j^{*\prime}$, $m^{*\prime}$ on the frequency, and thus set

$$\tau(n'j^{*\prime}m^{*\prime}; njm^*) = \tau(n'j'; nj), \tag{12}$$

then one can take τ outside the summations over m^*, $j^{*\prime}$, $m^{*\prime}$. When this simplification is possible, use can be made of the relation

$$\Sigma_{j^{*\prime},\, m^{*\prime}} [P_x(n'j^{*\prime}m^{*\prime})P_y]_{m^*m^*} = \Sigma_{j',\, m'} [P_x(n'j'm')P_y]_{mm}\, |S(m; m^*)|^2, \tag{13}$$

which is essentially a special case of the principle of spectroscopic stability and is readily established from the orthogonality properties of the transformation (10) and the occurrence of the Kronecker δ factor in (8). In virtue of (12), (13) and (8), the new version of (4) becomes

$$V = (4\pi^2\nu^2 B/Hch)\Sigma_{n'j'}\{C_{n'j'}\tau(n'j'; nj)\ \Sigma_{m,\, m^*} m\, |S(m; m^*)|^2 e^{-W_{njm^*}/kT}. \tag{14}$$

Eq. (14) differs from (11) only by factors independent of H, T, and so (1) retains its validity, with $K = 0$ as yet. The K term should, however, be added to allow for the well-known diamagnetic rotation which arises from the modulation of the frequency factors, and also sometimes of the amplitude factors, by the magnetic field. Besides diamagnetic contributions, the K term may be regarded as including also the effect of the matrix elements of the magnetic moment which are non-diagonal in j. This term is really independent of temperature only as long as the effect of the crystalline potential is negligible, i.e., as long as this potential is small compared with kT. At low temperatures this condition will not be fulfilled but then the paramagnetic rotation far overshadows the diamagnetic. Hence, little harm is done if K is treated as independent of temperature.

The crux of the whole matter is whether (12) is a legitimate approximation. Naturally (12) is a much more severe restriction than (7), for the dependence of ν on m^* is due to crystalline Stark as well as Zeeman effect and is so much larger than the purely Zeeman dependence discarded in assuming (7). We shall consider specifically the case of Ce^{+++}. Here most of the rotation appears to be due to a band at 2500A, which, as first noted by Freed,[10] is doubtless to be attributed to the transition $4f-5d$. The Stark effect for the ground level $4f$ cannot amount to over 1000 cm^{-1} or so, as otherwise the susceptibility would not conform as well as it does to Hund's formula.

[10] S. Freed, Phys. Rev. **38**, 2122 (1931); It has often been suggested by spectroscopists that the ground state of Ce^{+++} is perhaps a $5d$ rather than $4f$ state. Such an alternative, however, seems entirely incompatible with the conformity of the susceptibility of cerium salts to Hund's formula at high temperatures. The spectroscopic evidence favoring $5d$ is an extrapolation from the spectrum of Cs I and Ba II (cf. Gibbs and White, Phys. Rev. **33**, 157, 1929). Such an extrapolation, however, is not really applicable, because the $4f$ orbit is of a different nature in Ce than in Ba, as in Ce^{+++} it is situated in the interior rather than exterior of the atom. In other words an extrapolation cannot be used to compare states located in different potential valleys. The theoretical calculations of Wu (Phys. Rev. **44**, 727 (1933) are not open to this objection, and still place $5d$ below $4f$ but the potential field utilized by Wu may not be accurate enough to make this conclusion reliable. On the other hand, very recently Roberts, Wallace and Pierce (Phil. Mag. **17**, 934, 1934) have found that the magnetic rotary dispersion of aqueous solution of $Ce_2(SO_4)_3$ favors a $4f$ rather than $5d$ ground level for the Ce^{+++} ion.

The Stark splitting for the $5d$ level can be somewhat greater, as this is an excited state. Unfortunately the series limit for the spectroscopic terms of Ce^{+++} is unknown but this may be approximately located from the known[11] separation of the $5d$ and $6d$ terms if we assume that these terms conform approximately to the Rydberg formula $16R/(n+\Delta)^2$. This gives $\Delta=-2.1$ for d terms, making $5d=215{,}000$ cm^{-1} and hence $4f=255{,}000$ cm^{-1}. Thus there is little relative difference between the firmness of binding of the $4f$ and $5d$ orbits. The Stark splitting should be somewhat greater, though, for a $5d$ than for a $4f$ orbit of equal firmness, due to the greater eccentricity of $5d$. It seems plausible that the crystalline Stark effect for $5d$ does not greatly exceed 10^3 cm^{-1} in magnitude. Since $4f-5d$ is about 40,000 cm^{-1}, it is seen that (12) is approximately true if this is the case. Strong experimental evidence that the Stark effect for $5d$ is not excessive is furnished by the mere existence of absorption bands for Ce^{+++} at approximately 2500A in a variety of compounds. Freed, for instance, finds that the position of the band does not differ by more than 100A or so, for the ethyl sulphate and for the hydrated chloride of cerium.

The absorption observed by Freed for Ce^{+++} near 2500A is diffuse rather than discrete in structure. As he mentions, this is probably because of the complicated modulations of the $5d$ state due to interaction with the inter-atomic vibrations in the crystal. Such interaction is, of course, not covered by the Bethe-Kramers method of static crystalline potentials. The amplitudes of the inter-atomic vibrations, of course, vary with temperature and this will mean that the absorption frequencies ν are to a certain extent a function of the temperature. It is partly for this cause that Kramers regards the proportionality factor A in (1) as an undetermined function of the temperature. However, we believe that any variation of A due to this cause is a relatively unimportant factor, particularly below room temperatures. This, for one thing, is indicated by the fact that Freed finds no great shift of absorption frequency with temperature. He finds that the absorption near 2500A can usually be divided into three component bands, occurring at roughly 2575, 2450, and 2300A. Possibly the three components are to be correlated with different Stark and spin components of the $5d$ state, each component being diffuse because of spread due to vibrational modulation. If so, the Stark splitting of $5d$ is of about the order estimated in the preceding paragraph.

Besides the above rotation due to $4f-5d$, we must also in Ce^{+++} consider that due to $4f-5g$. (The higher members $4f-md$, $m=6,7,\cdots$ and $4f-mg$, $m=6,7,\cdots$ are definitely less important, as the higher d members have much smaller τ factors than that for the first member $5d$, while the higher g members have much smaller amplitudes than for $5g$.) The $5g$ state is probably closely hydrogenic and then $4f-5g$ is about 185,000 cm^{-1}. The Stark effect for $5g$ is undoubtedly much larger than for $5d$, perhaps of the order 10^4 cm^{-1}. Even with this estimate, however, Eq. (12) is still approximately valid as applied to the transition to $5g$, thanks to the large value of the frequency $4f-5g$. The sign of the observed Faraday effect in solutions containing cerium shows quite definitely that $4f-5d$ is a much more potent line for the Faraday effect than $4f-5g$.[12] This fact presents an interesting theoretical problem. The magnitude of $\tau(4f;5d)$ is, to be sure, much greater than that of $\tau(4f;5g)$. The ratio of the two τ's is, for instance, about 30 if the incident light has a wave-length of 5000A. However, the amplitude $a(4f;5g)$ is much greater than $a(4f;5d)$, in fact over ten times greater if one makes a calculation with hydrogenic wave functions.[13] This is because the bulk of the $4f-g$ absorption intensity is concentrated in the first line $4f-5g$, whereas $4f-5d$ consumes only a small part of the $4f-d$ absorption. The departures from hydrogenic conditions must thus be such as to make $a(4f;5d)^2/a(4f;5g)^2>1/30$ rather than $<1/100$. That such departures may be large is clear from the fact that the $4f$ orbits in the rare earths occupy inner rather than peripheral regions of the atom. In Ce^{+++}, in particular, the $4f$ state has an effective quantum number $n^*=2.6$ and so is bound over twice as firmly as one would calculate for a hydrogen-like atom with $Z=4$. That actually the amplitude for $4f-5d$ is more important relative to other amplitudes emanating from $4f$ than in a hydrogen-like atom is shown by the following consideration. The squares of the amplitudes emanating from a given state sum to the mean square radius of this state. Since $r\sim n^{*2}$ the mean square radius for $4f$ differs from the hydrogenic value by a factor roughly $(2.6/4)^4=0.2$. On the other hand, Gorter's[12] measurements on the absolute amount of Faraday rotation indicate that the amplitude for $4f-5d$ has approximately the hydrogenic value. Hence the relative importance of this amplitude is increased by

[11] J. S. Badami, Proc. Phys. Soc. London **43**, 53 (1931).

[12] C. J. Gorter, Phys. Zeits. **34**, 238 (1933); Roberts, Wallace and Pierce, reference 10.

[13] Cf. calculations of hydrogenic amplitudes by Slack, reported by L. R. Maxwell, Phys. Rev. **38** 1685 (1931).

a factor $5^{\frac{1}{2}}$. On the other hand, a corresponding increase for $4f-5g$ is impossible and this amplitude must be about $5^{-\frac{1}{2}}$ the hydrogenic value, since otherwise the squares of the amplitudes for $4f-g$, already due almost entirely to $4f-5g$, would sum to more than the mean value of r^2 for $4f$.

Salts of the iron group are not in general amenable to any of the preceding theory, as here the crystalline potential is large compared to the spin-orbit energy, and produces a large electric Paschen-Back effect on the ground state. J. H. Van Vleck and W. G. Penney[14] will show elsewhere that a possible exception is furnished by manganous and ferric compounds for which the crystalline fields have cubic symmetry. In such ions the ground state is ${}^5S$ and the important absorption lines are ${}^5S-{}^5P$. Cubic fields do not decompose either S or P states, except for spin-orbit complications. Thus in cubic ferric or manganous crystals, V and χ are possibly sometimes proportional.

2. Experimental Confirmation in Tysonite

Tysonite is the rare earth mineral for which the most comprehensive rotational data are available at present. It is a mixed crystal (La, Ce, Nd+Pr, F_3). Cerium is known to be responsible for most of the rotation, probably because of the comparatively low value of the frequency $4f-5d$ in Ce^{+++} (cf. section 1). To make a proper test of (1), one must compare the Verdet constant of tysonite with the susceptibility of CeF_3 rather than of tysonite, since the susceptibility of tysonite arises only partially from Ce. The x-ray measurements of Oftedal[15] reveal that tysonite and CeF_3 are similar in crystal structure and dimensions, except, of course, for the variable cation (La, Ce, Nd, Pr) in the former. Hence the crystalline fields surrounding Ce^{+++} are nearly similar in the two materials.

The suceptibility of CeF_3 crystal powder has been measured by de Haas and Gorter.[16] The Verdet constant $V_\perp$ perpendicular to the crystal (i.e., optic) axis has been determined recently by Becquerel,[1] while that parallel to this axis has been available for some time. Since tysonite has hexagonal symmetry, the Verdet constant should have the same value for all directions orthogonal to the crystal axis, except for saturation effects which will be deferred until sections 3 and 6. For weak fields, the mean Verdet constant analogous to that for a powder equals $(V_{||}+2V_\perp)/3$. The comparison of susceptibility with rotation is given in Table I, along with the

Table I. *Comparison of susceptibility with rotation.*

Temperature	Tysonite $V_{||}\times10^6$	Tysonite $V_\perp\times10^6$	CeF_3 $\chi\times10^6$	$\left[\frac{\chi\times10^6}{\frac{1}{3}(V_{||}+2V_\perp)}\right]$	$\left[\frac{\chi\times10^6}{\frac{1}{3}(V_{||}+2V_\perp)}-.67\times10^{-3}\right]$
293°K	−6.17	−5.11	11.2	−2.05	−1.83
77.5°	−22.17	−12.84	29.3	−1.84	−1.76
20.4°	−73.3	−24.4	75.8	−1.86	−1.83
14.4°	−101.9	−30.3	100.8	−1.86	−1.84

underlying experimental data.[17] The constancy of the ratio in the next to last column is a test of Eq. (1) with $K=0$. The deviation at the highest temperature might be expected, since here the diamagnetic correction K will be most important. In the last column, the Verdet constant is modified by subtraction of a term $K=0.67\times10^{-3}$ independent of T. This value of K has been so determined as to make the ratio in the last column have the same value at 20.4°K as at 293°K.

The slight variation of the entries in either of the last two columns is gratifying when it is remembered that the experimental determination of $V_\perp$ is exceedingly difficult and that tysonite and CeF_3 are, after all, not exactly identical crystals. The approximate validity of (1) enables us to translate measurements of Verdet constants

[14] J. H. Van Vleck and W. G. Penney, Phil. Mag. **17**, 961 (1934).

[15] I. Oftedal, Zeits. f. physik. Chemie **B5**, 272 (1929); **13**, 190 (1931).

[16] W. J. de Haas and C. J. Gorter, Proc. Amst. Acad. Sci. **33**, 349 (1930) (or Leiden Communication 210c).

[17] Just as the present paper was completed, an article appeared by J. Becquerel, W. J. de Haas and J. van den Handel, Physica **1**, 383 (1934), giving a value of $V_{||}$ at 293°K 4.6% higher than that shown in Table I. This reduces $-(\chi/V)10^3$ from 2.05 to 2.01. Unfortunately, new measurements on the perpendicular component are not available but if they should increase $V_\perp$ in the same ratio, the value of $-(\chi/V)10^3$ at 293° would be lowered from 2.05 to 1.96. The corresponding change at 77°K is only slight, *viz.*, from 1.84 to 1.82. At temperatures below 20°K we have always utilized the new measurements on the parallel component, as these were communicated to us by Professor Becquerel in advance of publication. We wish to take this opportunity of expressing our indebtedness to Professor Becquerel for this material. Use of the new data does not affect our points on Fig. 2 at 293° if we assume that Becquerel's old value for the anisotropy $V_\perp/V_{||}$ is still correct.

into determinations of magnetic susceptibility and so greatly enriches our magnetic data, since the V of tysonite, unlike the χ of CeF_3, has been determined for individual crystallographic axes.

It is probably better to take the diamagnetic correction K to be negligible, i.e., of order 10^{-5}, rather than to be 0.67×10^{-3}, for the following reasons. First, in cerium ethyl sulphate, which should presumably be comparable with tysonite as regards the rough order of magnitude of K, Becquerel and de Haas[18] have presented fairly convincing evidence that K is only 3×10^{-5}. Second, it is hard to understand how χ/V could be lower at 77°K than at 20° and 293°, as would be required if $K=0.67\times10^{-3}$. On the other hand, the anomaly in χ/V at room temperatures which is concomitant to taking $K=0$ might be blamed on a shift of absorption centers with temperature or something of the kind. Hence in the following work we shall not use the value of V at 293° except that we shall make the reasonable assumption that the anisotropy in χ at 293°K is the same as that in V. This is necessary in order to have data available on individual axes at room temperatures and is tantamount to raising the values of V at 293° in the ratio 2.05/1.86. If, instead, one preferred to take $K=0.67\times10^{-3}$, the only material change would be to raise the values of n_B slightly at 77°K as shown by the solid circles in Fig. 2.

3. Evidence for a Demagnetizing Molecular Field in Tysonite

Unless the crystalline field has unusual symmetry, the Boltzmann factor is negligible at low temperatures for all but one pair of levels in an ion with an odd number of electrons such as Ce^{+++}. Such a pair we shall call a Kramers doublet. Because of Kramers' theorem,[19] the components of a doublet separate only in virtue of the magnetic field and have Zeeman energies $W_0\pm\mu\beta H$ $(+H^2)$. The susceptibility is given by the expression

$$\chi=I/H=(N\mu\beta/H)\tanh\left[\mu\beta(H-\gamma I')/kT\right]$$
$$+2N\left(\frac{H-\gamma I'}{H}\right)\sum_{n'(n'\neq n)}\frac{|m_H(n;n')|^2}{h\nu(n';n)}, \quad (15)$$

where the matrix elements of the magnetic moment in the direction of the field H are denoted by $m_H(n;n')$ and n' always refers to other doublets than the basic pair n. The term involving the hyperbolic tangent originates with Kramers and Becquerel[3] and is inclusive of the correction for saturation. On the other hand, we always neglect saturation in writing the second term, which represents the contribution of the high frequency elements. This is allowable, for surely βH is small compared with the crystalline Stark separation.

In writing Eq. (15) we have taken the argument of the hyperbolic tangent to be $\mu\beta(H-\gamma I')/kT$ rather than $\mu\beta H/kT$, in order to allow for the exchange effects which couple together the spins of the various paramagnetic ions. It is a well-known result of Heisenberg's theory of magnetism that these effects are approximately equivalent to superposition of a Weiss molecular field $-\gamma I'$ upon the applied field H, so that the total effective field is $H-\gamma I'$, where I' is the intensity of magnetization. The prime is affixed to I to indicate that it refers to the entire mixed crystal, rather than just to the cerium ingredient. Some of the coupling between the magnetic moments of the different ions may be due to "orbital valence," since the mutual energy of two ions certainly depends on the relative orientation of their orbital angular momentum vectors. The orbital coupling is likewise capable of description by a molecular field in the first approximation.[20] Thus, strictly speaking, $-\gamma I'$ represents the field arising from both exchange and orbital coupling. The constant of proportionality γ turns out to be positive in tysonite. This is the common sign behavior for non-ferromagnetic bodies and means that the molecular field has a demagnetizing effect, since then $H-\gamma I'<H$. In a crystal such as tysonite the concentration of paramagnetic ions is, of course, much greater than for the hydrated sulphates. Hence it is not unreasonable that the exchange correction should be appreciable in

[18] J. Becquerel and W. J. de Haas, addendum to supplement 74 of the Leiden Communications.

[19] H. A. Kramers, Proc. Amsterdam Acad. **33**. 959 (1930).

[20] The subject of orbital coupling will be discussed more fully in a future paper by the writer. Cf. also H. A. Kramers, Physica **1**, 182 (1934). It is to be clearly understood that the exchange integrals themselves depend on the alignment of the orbital angular momentum vectors; in fact this dependence is perhaps the most important manifestation of orbital coupling.

tysonite though it is known to be negligible in $Gd_2(SO_4)_38H_2O$ even at 1.4°K.[21]

In the discussion of magnetic data, it is often convenient to use in place of the susceptibility the effective Bohr magneton number defined by

$$n_B^2 = 3k\chi(T+\Delta)/N\beta^2. \tag{16}$$

The relation between V and χ, established in the preceding section, shows that in tysonite, n_B is then given in terms of the Verdet constant V by the relation

$$n_B^2 = -2.91\,V(T+\Delta). \tag{17}$$

One must use in (16) and (17) only the values of V and χ appropriate to weak fields, where saturation can be neglected. If there is no saturation, we may replace the hyperbolic tangent by its argument in (15), and also we may consider the ratio of the intensity of magnetization to the effective field to be approximately proportional to $1/T$ at temperatures where the demagnetizing correction is appreciable. Hence

$$\gamma I'/(H-\gamma I') = \Delta/T, \tag{18}$$

where Δ is a proportionality constant, and so

$$H-\gamma I' = H/(1+\Delta T^{-1}). \tag{19}$$

Thus the effective magneton number should be a linear function

$$n_B^2 = 3\mu^2 + BT \tag{20}$$

of T provided Eq. (15) is valid. The constant B equals $6k/\beta^2$ times the sum in the second term of (15). The linear relation (20) should hold up to at least the temperature of liquid hydrogen but, at still higher temperatures, more than one Kramers doublet becomes inhabited and then (15) and (20) cease to be valid.

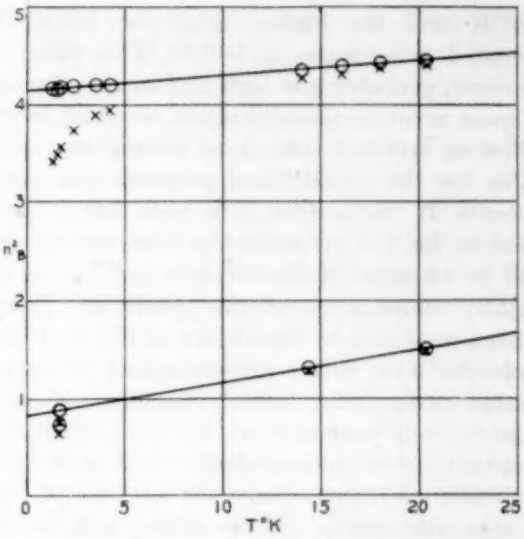

FIG. 1. Experimental values of the square of the effective Bohr magneton number n_B for tysonite at low temperatures, obtained from the data of Becquerel and de Haas by means of Eq. (17). The crosses are for $\Delta=0$; the circles for $\Delta=0.29$. The upper curve and corresponding points relate to the parallel component; the lower to the perpendicular component.

The values of n_B^2 deduced with the aid of (17) from Becquerel's data on the Verdet constants of tysonite are shown in Fig. 1. It is seen that with $\Delta=0.29$ there is the desired linearity (20) but that if $\Delta=\gamma=0$ there are pronounced deviations from linearity. Hence the introduction of the demagnetizing molecular field γ has been necessary in order to secure the proper variation with temperature for small T. In drawing Fig. 1 we have been aided by a letter from Professor Becquerel[17] informing us of new measurements on $V_{\|}$. He has independently concluded that introduction of a demagnetizing field is necessary to secure the proper linearity (20) at low temperatures and finds that 0.29 is the best choice for Δ, which we hence adopt. Prior to his letter we had obtained $\Delta=0.17$ on the basis of the older data and less thorough examination of the numerical fitting.

The determination of Δ for the perpendicular component is less certain, because here the experimental error is considerable. Note particularly the large divergence between the points at 1.7°K. If the values for $V_\perp$ at 14.3,

[21] According to P. W. Selwood, J. Am. Chem. Soc. **55**, 4869 (1933), the value of Δ in $GdCl_3$ is 14°. This, however, is not necessarily inconsistent with a Δ of only 0.29 in tysonite as gadolinium has a much larger spin vector s. Because only the component of spin along the total angular momentum j is effective with wide multiplets, the relation connecting Δ with the exchange integral J per electron can be shown to be

$$\Delta = -2Jz(\mathbf{s}\cdot\mathbf{j})^2/3k\mathbf{j}^2 = -Jz(s^2+s+j^2+j-l^2-l)^2/6kj(j+1).$$

Here z is the number of paramagnetic neighbors possessed by an ion. If this formula is used, and if J is the same in tysonite as in $GdCl_3$, the value of Δ should be 88.2 times larger for the latter than for the former. Actually J should be larger in tysonite than in $GdCl_3$ because the Gd and Cl ions are larger than those of Ce, F, respectively, and because the greater nuclear charge of Gd than of Ce tends to reduce the overlapping of the wave functions.

20.3°K and the higher value for 1.7°K be accepted as accurate, $\Delta_\perp$ is 0.62. This value is, however, probably too high and in the absence of more accurate measurements, we shall in the following sections take Δ as having the same value for the parallel and perpendicular components. If this is done, it is seen that a fairly good fit for the perpendicular components can still be obtained if the straight line be drawn slightly above some of the points and below others, as shown by the circles in Fig. 1. If the molecular field arises predominantly from exchange rather than orbital coupling, one may take $\gamma_{||}=\gamma_\perp$ inasmuch as the proportionality constant γ is independent of direction in Heisenberg's theory. Since the left side of (18) is approximately $\gamma I'/H$ the values of Δ for the two axes should then obey the relation

$$\Delta_{||}/\Delta_\perp=\chi_{||}'/\chi_\perp', \tag{21}$$

where $\chi'=I'/H$ refers to the total magnetic susceptibility of tysonite. Unfortunately, no information is available concerning $\chi_{||}'/\chi_\perp'$, since the ratio of the Verdet constants for the two axes supplies us only with the ratio $\chi_{||}/\chi_\perp$ for the part χ of the susceptibility due to the cerium ions only. As cerium is only one of the paramagnetic constituents of the mixed crystal tysonite, there is no reason why $\chi_{||}'/\chi_\perp$ should equal $\chi_{11}/\chi_\perp$. At helium temperatures, $\chi_{||}/\chi_\perp$ is about 5 but it is not unlikely that $\chi_{||}'/\chi_\perp'$ is smaller, since some of the other magnetic ingredients may behave more isotropically than cerium. Our choice unity for the ratio (21) seems about as reasonable as any which can be made at present, especially since Eq. (21) ceases to be valid when one considers the effect of directional valence on coupling between atoms.[22]

4. Saturation Effects in Tysonite

Instead of using Eq. (20) appropriate to weak fields, one can also deduce the numerical magnitude of the effective magneton number $n_B=3^{\frac{1}{2}}\mu$ at $T=0$ from the curvature of the graph of the rotation against field strength at a particular, very low temperature. This other, independent method based on saturation is that used by Kramers and Becquerel. At helium temperatures, the second term of (15) is of negligible importance, and the ratio of the rotations at two different field strengths will fix μ even if one assumes (2) instead of (3). Before one can use (15) it is necessary to make the assumption that the demagnetizing field $-\gamma I'$ is proportional to the paramagnetic rotation ρ, so that

$$H-\gamma I'=H-b\rho, \tag{22}$$

where b is a constant. The value of Δ is then connected with that of b by the relation

$$\Delta=b\rho_\infty\mu\beta/k$$

if ρ_∞ denotes the rotation at infinite field strengths, where the hyperbolic tangent may be replaced by unity. The assumption (22) may not entail serious error but certainly is not entirely correct, since the Faraday rotation ρ arises almost entirely from the cerium ions and so represents, except for a constant factor, the intensity of magnetization I of the cerium alone. On the other hand the demagnetizing field is proportional to the total intensity of magnetization I' of the mixed crystal. There is no reason why I' and I should be exactly the same functions of H, but possibly the difference between the two functions is not large.

If we assume (22) and that $\Delta=0.29$, Becquerel finds[17] that the value obtained from his latest saturation curves is $\mu=1.288$. The corresponding value obtained from (17) and (20), i.e., from the intercept in Fig. 1, is $\mu=1.18$. The agreement between the two methods is thus only moderate. The estimate obtained from the saturation effect is reduced to 1.22, thus removing a large part of the discrepancy, if one makes the approximation (19) rather than (22) in the argument of the hyperbolic tangent even at high field strengths. Eq. (22) would be an allowable approximation if one assumed that most of the magnetization of the mixed crystal arose from ions which do not exhibit appreciable saturation even at the highest field strength employed, so that I' is a nearly linear function of H even though I exhibits appreciable curvature. How-

[22] In terms of the vector model, the coupling energy connecting two ions a, b has the form $\sum_{i,k}c_{ik}j_i^a\cdot j_k^b$ where j_1^a, j_2^a, j_3^a are the components of the angular momentum of ion a along the three coordinate axes (cf. Kramers, reference 20). A simple calculation shows that the constant γ of the molecular field is approximately proportional to c_{ii} if H is applied along the direction of axis i. If we ignore orbital valence, as in Heisenberg's theory, then $a_{11}=a_{22}=a_{33}$, but actually the orbital effects may make $a_{11}\neq a_{22}$, etc. Then $\gamma_{||}\neq\gamma_\perp$, and so (21) ceases to be valid.

ever, it is hard to see any reason why I' should exhibit much less curvature than I, since the other paramagnetic ions in the crystal, unless they greatly outnumber the cerium ions, must have approximately as great values of μ and hence as much curvature as the cerium if they are to be important contributors to the magnetization.

In the case of the perpendicular component, the situation is still less encouraging. In the first place there is the difficulty that the experimental data are self-contradictory, for the experimental values of $V_\perp$ depend even in weak fields on the direction chosen for observation in the plane perpendicular to the crystal axis. Any sort of theory,[23] however, shows that such a variation is incompatible with the hexagonal symmetry of the crystal. (We shall later see, in section 6, that there might be some variation with direction in the saturation method but that this is too small to be appreciable at the field strengths used.) When we give experimental data or theoretical calculations aimed to fit these data on the perpendicular component near $T=0$ we shall always give two values. The first of these is based on measurements parallel to one of the diagonal axes of the crystal. The second of these will be inclosed in parentheses and is based on measurements still perpendicular to the crystallographic axis but at an angle of about 30° to the diagonal axis. The first and second directions are equivalent to horizontal and vertical axes in Fig. 3 of section 6. The difference between the two sets of measurements is perhaps due to crystalline flaws or to the fact that Becquerel used two different crystals. It disappears at hydrogen temperatures and higher.

With $\Delta=0.29$, the value of $\mu_\perp$ furnished by the saturation method is 0.874 (0.726) while (17) yields 0.523 (0.469). In connection with the saturation procedure, it makes little difference whether one uses (19) or (22), since in the perpendicular component only the beginnings of saturation are observed. Part of the trouble may easily be experimental error, since the saturation curvature in the perpendicular direction is slight and hence very difficult to determine. We shall show in section 6 that the value of $\mu_\perp$ obtained by the saturation method is reduced to 0.780 (0.726), if all the cerium atoms do not have the same crystallographic situations, in which case Eq. (15) must be modified.

In testing various types of crystalline fields in the next two sections, we shall use the values of n_B furnished by (17) rather than by the saturation curvature, since the former appear to be the more reliable. The discrepancy between the two methods of determining n_B is inherent in the existing data, and for the following reason cannot possibly be imputed to our use of (1) (i.e., correlation of the temperature variation of χ with that of V) rather than of the less drastic conventional hypothesis (2). Suppose that we admitted only (2) and assumed that saturation methods were reliable. Then the effective "powder" magneton number $(\mu_{||}^2+2\mu_\perp^2)^{\frac{1}{2}}$ would be deduced from saturation to be 1.78 (1.65) at 1.7°. On the other hand it is known from susceptibility measurements that n_B for CeF_3 powder has already dropped to 1.52 at 14.48°K. Now it is scarcely conceivable that the magneton number should actually increase as one lowers the temperature from 14.48° to 1.7°. In fact, examination of Fig. 2 shows that any reasonable sort of extrapolation of the direct experimental measurements of susceptibilities, indicated by crossed circles in Fig. 2, to very low temperatures demands that n_B be about 1.4 for the powder near $T=0$. We thus appear forced to accept the lower values of n_B given by (17) in preference to the greater values yielded by saturation.

Of course it is possible that the trouble may lie in a real difference between CeF_3 and tysonite for our purposes. The constancy of the ratio χ/V in Table I makes it appear probable that if the two materials are unlike, they manifest approximately the same percentage difference in their susceptibilities at all temperatures. If so, our use of (17) may be regarded as a convenient and allowable way to extend the data on CeF_3 to individual axes and very low temperatures. Our calculations in sections 5 and 6 would then be for the crystalline potential of CeF_3 rather than of tysonite. Because of the qualitative similarity of the two substances, our ensuing conclusions concerning the relative merits of the triclinic and staggered rhombic fields would also apply to tysonite.

[23] J. H. Van Vleck, Phys. Rev. **45**, 115 (L) (1934).

5. Failure of a Triclinic Field to Represent the Measurements in Tysonite

So far our discussion has consisted mostly in establishing the proportionality between χ and V. We now propose to examine what crystalline field will represent the observed behavior of χ, or equally well the related V. We thus enter upon a subject whose broader aspects have been developed by Kramers,[3] Bethe,[7] Penney,[8] Schlapp[8] and Van Vleck.[9] The only attempt at numerical calculations for tysonite has been made by Kramers.[24] When we refer to his work, we always mean his most recent paper[24] and not his earlier articles[3] on tysonite which involved the incorrect assumption that the multiplet width structure is small compared to the crystalline potential.

Tysonite is a hexagonal crystal, but this does not mean that the field on an individual atom possesses hexagonal symmetry. Instead the hexagonal symmetry need be achieved only from a macroscopic point of view. The x-ray measurements of Oftedal[15] indicate that the fields acting on individual atoms have nearly triclinic symmetry, i.e., nearly a period of 120° around the crystallographic axis. The simplest assumption, and the one made by Kramers,[24] is that these fields can be considered accurately triclinic. This facilitates the calculations, for the off-diagonal matrix elements of the crystalline potential are then entirely of the form $\Delta M=\pm 3$, with none between $M=3/2$, $M=-3/2$. Here M denotes the magnetic quantum number associated with spatial quantization relative to the crystallographic symmetry. The wave functions belonging to the Stark levels are then of the form

$$\Psi_{\pm \mathrm{I}}=\alpha\psi_{\pm 3/2}+(1-\alpha^2)^{1/2}\psi_{\mp 1/2},$$
$$\Psi_{\pm \mathrm{II}}=(1-\alpha^2)^{1/2}\psi_{\pm 3/2}-\alpha\psi_{\mp 1/2},$$
$$\Psi_{\pm \mathrm{III}}=\psi_{\pm 3/2}, \quad (23)$$

where α is a constant and the fractional subscripts relate to M. The two sign choices yield the two components of a Kramers doublet. Kramers gives the formula for the mean χ corresponding to (23) and we need not repeat it here. He does not explicitly isolate $\chi_{\|}$, $\chi_{\perp}$ but this can be done without difficulty.

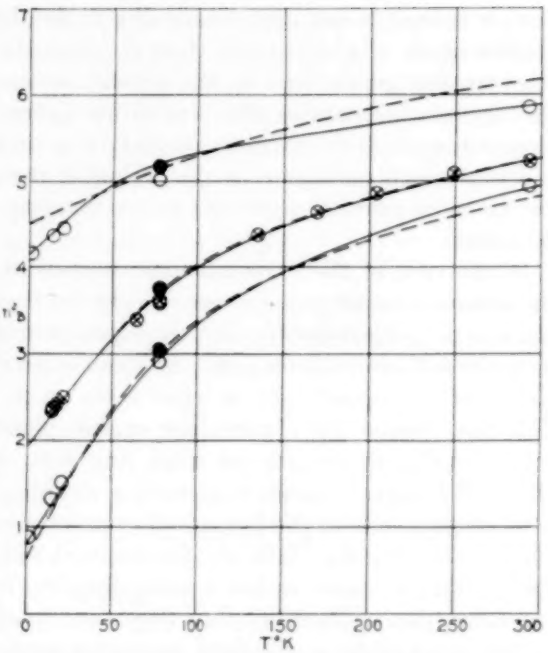

Fig. 2. The square of the effective Bohr magneton number as a function of temperature. The crossed circles ⊗ are experimental values deduced from Leiden susceptibility measurements on CeF_3 by means of (16) with $\Delta=0.29$, while the plain circles ○ give values obtained from the data of Becquerel and de Haas on the magnetic rotation of tysonite (with adjustment at 293°K mentioned in section 2). The solid circles ● at 77°K are obtained by using $K=0.67\times10^{-3}$ instead of $K=0$ in (1) and (17). The broken lines are theoretical curves based on Kramers' triclinic field, with constants chosen as in (25). The solid curves are for the staggered rhombic field described in section 6. The upper and lower curves refer, respectively, to directions parallel and perpendicular to the optic axis. The middle curve relates to the mean.

Kramers considered only the mean or powder susceptibility of CeF_3, which he shows can be fitted quite well with the following choice of constants

$$\alpha^2=2/3, \quad W_{\mathrm{III}}-W_{\mathrm{I}}=163\ \mathrm{cm}^{-1},$$
$$W_{\mathrm{II}}-W_{\mathrm{I}}=4\times163\ \mathrm{cm}^{-1}. \quad (24)$$

(Here and elsewhere we take the lowest Stark component as the origin of energy.) When, however, the proportionality between magnetic susceptibility and rotation is used, the measurements extend down to 1.5° rather than 14.3°K, and especially, data for individual crystalline axes become available. The test to be met by the theory then becomes considerably more

[24] H. A. Kramers, Proc. Amsterdam Acad. **36**, 1 (1933).

severe and it turns out that no wave functions of the form (23) are adequate. It is possible, to be sure, to represent the mean susceptibility over the entire range 1.5–293°K by modifying slightly Kramers' choice of the constants as follows

$$\alpha^2=0.644, \quad W_{III}-W_I=139\ \text{cm}^{-1},$$
$$W_{II}-W_I=5.5\times 139\ \text{cm}^{-1}. \quad (25)$$

However, the susceptibilities for individual axes are not then correctly represented as can be seen from examination of the broken lines in Fig. 2. Kramers notes that the powder susceptibility of CeF_3 can be fitted by still another choice of constants, which is similar to (24) except that W_{II}, W_{III} are interchanged. This or any neighboring choice of constants, however, gives even worse agreement on individual axes than does (25). It would require that n_B for the parallel component reach a maximum at around 500–600°K and then decline as the temperature is raised further.

This failure of purely triclinic fields is not surprising, for the following reason. If there is a center of symmetry the terms of the crystalline potential which yield matrix elements of the form $\Delta M=\pm 3$ arise, as Kramers shows, only from Tesseral harmonics of even order which change sign under reflection in the equatorial plane (e.g., T_4^3, T_6^3, etc.). Without such elements we can only have $\alpha=0$ or $\alpha=1$ in (23); i.e., wave functions of the same form as for a field of axial symmetry. Furthermore, the calculation of the susceptibility for a field of axial symmetry is particularly simple, and one easily convinces oneself that the data on the individual susceptibilities of tysonite are incapable of representation by a field of axial symmetry: in fact even the mean is fitted none too well. To give a situation like (24), the matrix elements $\Delta M=\pm 3$ must be quite important, and this in turn demands large terms in the harmonic expansion of the crystalline potential which change sign under equatorial reflection. However, according to the crystallographic structure tentatively proposed by Oftedal,[15] there is a plane of symmetry passing through each atom perpendicular to the crystallographic axis. If this is the case and if there is triclinic symmetry, there can be no such terms in the expansion of the potential function. Oftedal himself mentions that the crystallographic structure may be somewhat distorted from the diagrams which he gives. In fact, he even mentions the possibility that the atoms do not have planes of symmetry in their potential fields. This will be the case if the corresponding crystallographic planes "above" and "below" a given atom are not equidistant. However, one would expect any asymmetries of this type to be small, so that it seems rather unreasonable for surface harmonics which are odd under equatorial reflection to have as large an effect as postulated by Kramers.

FIG. 3. "Staggered" rhombic field, representing the three orientations of the local field about an individual Ce^{+++} ion.

6. REPRESENTATION OF THE SUSCEPTIBILITY OF TYSONITE BY A STAGGERED RHOMBIC FIELD

Instead of a trigonal field, we may essay calculations on the assumption that each atom is subject to a field of rhombic symmetry. One of the principal rhombic axes, *viz.*, the z axis, we shall suppose to be always parallel to the crystallographic or optic axis. One-third of the atoms will have their x and y axes directed in each of the fashions shown in Fig. 3, so that the field for one atom will differ from that of another only by a rotation through 120°, thus explaining our use of the term "staggered." A staggered structure of this type is precisely what is indicated in the tentative structure diagram for tysonite published by Oftedal. Hence our model is perhaps more reasonable than the triclinic one used by Kramers; we must, however, mention that to represent the susceptibility properly, the "rhombic" terms which represent the departures from effective axial symmetry (represented symbolically in Fig. 3 by the difference in length of the crossed arrows) turn out to be

surprisingly large, greater than one would *a priori* expect from the nearly triclinic symmetry in ionic surroundings reported by Oftedal.

The matrix elements introduced by a field of rhombic symmetry are of the form $\Delta M = M' - M'' = 0, \pm 2, \pm 4$ so that the wave functions may be taken to be

$$\Psi_{i\pm} = \alpha^i_{5/2}\psi_{\pm 5/2} + \alpha^i_{1/2}\psi_{\pm 1/2} + \alpha^i_{-3/2}\psi_{\mp 3/2}, \qquad i = \text{I, II, III}. \tag{26}$$

As previously, the two sign choices give the two components of a Kramers doublet. We have assumed the α's to be real, which involves no loss of generality since by proper choice of phases the matrix elements of the crystalline potential may all be made real if there is rhombic symmetry. The coefficients α are not all independent and must satisfy the orthogonality and normalization relations

$$\alpha^i_{5/2}\alpha^j_{5/2} + \alpha^i_{1/2}\alpha^j_{1/2} + \alpha^i_{-3/2}\alpha^j_{-3/2} = \delta_j{}^i. \tag{27}$$

In a system of representation appropriate to the wave functions (26), the matrix elements of the magnetic moment are

$$\mu_z(i\pm; j\pm) = g\left[\frac{5}{2}\alpha^i_{5/2}\alpha^j_{5/2} + \frac{1}{2}\alpha^i_{1/2}\alpha^j_{1/2} - \frac{3}{2}\alpha^i_{-3/2}\alpha^j_{-3/2}\right], \tag{28}$$

$$\mu_x(i\pm; j\mp) = g\left[\frac{5^{1/2}}{2}(\alpha^i_{5/2}\alpha^j_{-3/2} + \alpha^i_{-3/2}\alpha^j_{5/2}) + 2^{1/2}(\alpha^i_{1/2}\alpha^j_{-3/2} + \alpha^i_{-3/2}\alpha^j_{1/2}) + \frac{3}{2}\alpha^i_{1/2}\alpha^j_{1/2}\right] \tag{29}$$

$$-\mu_y(i-; j+) = \mu_y(i+; j-) = (-1)^{1/2} g\left[\frac{5^{1/2}}{2}(\alpha^i_{5/2}\alpha^j_{-3/2} + \alpha^i_{-3/2}\alpha^j_{5/2}) - 2^{1/2}(\alpha^i_{1/2}\alpha^j_{-3/2} + \alpha^i_{-3/2}\alpha^j_{1/2}) + \frac{3}{2}\alpha^i_{1/2}\alpha^j_{1/2}\right]. \tag{30}$$

These expressions follow from the well-known relations

$$(\mu_x \pm i\mu_y)(M; M\mp 1) = g[J(J+1) - M(M\mp 1)]^{1/2}, \qquad \mu_z(M; M) = g\beta M$$

characteristic of the usual M system of representation appropriate to a field of axial symmetry. Elements of the form $\mu_z(i\pm; j\mp)$, $\mu_z(i\pm; j\pm)$, $\mu_y(i\pm; j\pm)$ all vanish.

By standard principles of quantum magnetic theory, the square of the effective magneton number for the z direction in weak fields is

$$n_B{}^2(z) = \frac{3\Sigma_i\{|\mu_z(i+; i+)|^2 + 2kT\Sigma_{j\neq i}|\mu_z(i+; j+)|^2/(W_j{}^0 - W_i{}^0)\}e^{-W_i{}^0/kT}}{\Sigma e^{-W_i{}^0/kT}}. \tag{31}$$

The expressions for the x and y components are similar except that μ_x or μ_y replaces μ_z and that the indices are $(i+; i-)$, $(i+; j-)$ instead of $(i+; i+)$, $(i+; j+)$. Eq. (31) contains only one sign choice, as the summation over the two components of the Kramers doublet has already been performed.

The constants at our disposal must now be adjusted so as to yield agreement with experiment. These constants are five in number, *viz.*, the energy intervals $W_{II}{}^0 - W_I{}^0$ $W_{III}{}^0 - W_I{}^0$ and three of the coefficients α. Only three of the nine α's are arbitrary because of the six constraints imposed by (27). In place of $W_{II}{}^0 - W_I{}^0$, $W_{III}{}^0 - W_I{}^0$ it is convenient to introduce new parameters q, A defined by $W_{II}{}^0 - W_I{}^0 = A$, $W_{III}{}^0 - W_I{}^0 = qA$. If we plot $n_B{}^2$ against T, the effect of changing A is merely to expand or contract the scale of abscissa. There are obviously more complexity and more leeway in adjustment to experiment than in Kramers' triclinic case, where there were three adjustable constants. It should not, however, be inferred that with a rhombic field agreement can be achieved with almost any sort of experimental curve, for with data on two principal axes the material to be fitted is considerable. In fact most of the parameters are fixed simply by data in the hydrogen-helium range.

The simplest way to start is to fit the experimental values of the effective magneton number defined by (20) at $T=1.7°$, which is the same as $T=0$ to all intents and purposes. Using values appropriate to $\Delta=0.29$ quoted in section 4, we thus have

$$\mu_z(\mathrm{I}^+;\mathrm{I}^+)=\mu_{||}=1.18, \quad \tfrac{1}{2}[|\mu_x(\mathrm{I}^-;\mathrm{I}^+)|^2+|\mu_y(\mathrm{I}^-;\mathrm{I}^+)|^2]=\mu_\perp^2=(0.52)^2, \quad (\text{or } (0.47)^2) \tag{32}$$

with notation as in (27), (28), (29). The value of $\frac{1}{2}(\mu_x^2+\mu_y^2)$ is the same as that of $\mu_\perp^2$ because one must average over the three types of orientation of rhombic axes shown in Fig. 3. It is found that there are four sets of values of α^{I} which will fit (32), *viz.*

$$\alpha^{\mathrm{I}}{}_{5/2}=0.762,\ (0.736), \quad \alpha^{\mathrm{I}}{}_{1/2}=0.525,\ (0.592), \quad \alpha^{\mathrm{I}}{}_{-3/2}=-0.379,\ (-0.327), \tag{33}$$

$$\alpha^{\mathrm{I}}{}_{5/2}=0.122,\ (0.145), \quad \alpha^{\mathrm{I}}{}_{1/2}=0.187,\ (0.152), \quad \alpha^{\mathrm{I}}{}_{-3/2}=0.975,\ (0.978), \tag{34a}$$

$$\alpha^{\mathrm{I}}{}_{5/2}=0.095,\ (0.126), \quad \alpha^{\mathrm{I}}{}_{1/2}=0.217,\ (0.182), \quad \alpha^{\mathrm{I}}{}_{-3/2}=-0.972,\ (-0.975), \tag{34b}$$

$$\alpha^{\mathrm{I}}{}_{5/2}=0.680,\ (0.700), \quad \alpha^{\mathrm{I}}{}_{1/2}=0.713,\ (0.675), \quad \alpha^{\mathrm{I}}{}_{-3/2}=-0.167,\ (-0.234). \tag{35}$$

As explained in section 4, values in parenthesis relate to a choice of 0.47 rather than 0.52 for the experimental value of $\mu_\perp$.

The remaining constants are determined so as to fit the experimental data at higher temperatures and to yield proper values for the constant B in formula (20) at low temperatures. One relation between these other constants is immediately obtained by giving the ratio $B_\perp/B_{||}$ the proper value. This ratio has the advantage of being independent of the scale factor A. Too much reliance should not, however, be placed on endeavors to fit this ratio exactly, as experimentally it is not known with much precision because of uncertainty in the value of Δ for the perpendicular component. Nevertheless, study of the approximate magnitude of this ratio furnishes fairly conclusive evidence against the Kramers' triclinic field studied in section 5, since (25) yields a value 4.4 for $B_\perp/B_{||}$ which is excessively high compared with the experimental value 2.3.

It is impossible to choose the other constants so as to give good agreement with experiment if one uses (34a), (34b), or (35). It is disappointing that (34a), (34b) must thus be excluded, for wave functions of the type (34a) or (34b) would require only slight departures of the crystalline potential from axial symmetry, where the matrix of the α's is unity. No nearly axial field can be successful, since a perfectly axial field yields an infinite value of $B_\perp/B_{||}$.

With (33), the experimental data in weak fields can be fitted quite well for both the parallel and perpendicular components if one chooses the constants as follows for the upper states:

$$\alpha^{\mathrm{II}}{}_{5/2}=0.517, \quad \alpha^{\mathrm{II}}{}_{1/2}=-0.846, \quad \alpha^{\mathrm{II}}{}_{-3/2}=-0.134 \quad W_{\mathrm{II}}{}^0-W_1{}^0=130\ \mathrm{cm}^{-1}, \tag{36}$$

$$\alpha^{\mathrm{III}}{}_{5/2}=0.391, \quad \alpha^{\mathrm{III}}{}_{1/2}=0.095, \quad \alpha^{\mathrm{III}}{}_{-3/2}=0.916, \quad W_{\mathrm{III}}{}^0-W_1{}^0=754\ \mathrm{cm}^{-1}. \tag{37}$$

These values have, of course, been chosen in compliance with (27). The curves for the effective magneton number based on (33), (36), (37) are indicated by solid lines in Fig. 2 and are seen to agree with experiment better than do those for triclinic fields.

For simplicity, we have shown for the perpendicular component in Fig. 2 only the theoretical curves which are fitted to a value 0.523 for $\mu_\perp$ at $T=0$. If the experimental value is instead taken as 0.469, we would have to use the second set of constants in (33) and modify slightly the constants in (36), (37) and (25). These alterations, however, are not as important as in the discussion of saturation, and do not affect the conclusion that the staggered rhombic field fits the data better than does the triclinic.

Saturation for the perpendicular component. Since we must average over the three types of rhombic axes shown in Fig. 3, Eq. (15) does not yield directly the susceptibility for directions perpendicular to the crystallographic axis. Let us suppose that the magnetic field is applied perpendicular to this axis and makes an angle φ with one of the long axes in Fig. 3. Then one can show that the corre-

sponding type of atoms in Fig. 3 has first order Zeeman energies for the lowest Kramers doublet of the form

$$W = W_0 \pm H\beta\mu(\phi) \qquad \text{with} \qquad \mu(\phi) = (\mu_x^2 \cos^2\varphi + \mu_y^2 \sin^2\varphi)^{1/2}.$$

The formulas for the other two types of atoms are, of course, similar except that ϕ must be advanced by $2\pi/3$ or $4\pi/3$. Hence the proper formula for $\chi_\perp(\varphi)$ is

$$\chi_\perp(\varphi) = \frac{N\beta}{3H}\Sigma_{\psi=0,\,2\pi/3,\,4\pi/3}\ \mu(\varphi+\psi)\tanh\left[\frac{\mu(\varphi+\psi)\beta(H-\gamma I')}{kT}\right] + 2N\frac{(H-\gamma I')}{H}\Sigma_{n'(n'\neq n)}\frac{|m_x(n';n)|^2+|m_y(n';n)|^2}{2h\nu(n';n)}. \quad (38)$$

One notes that (38) is not independent of φ and immediately wonders whether this is the reason why Becquerel observes different rotations for $\varphi=0$ and $\varphi=30°$ (cf. section 4). Such an explanation, however, will not work, since if (38) is expanded as a Taylor's series in H, only the coefficients of H^4 and higher powers depend upon φ. At the field strengths used by Becquerel, little harm is done if the development is terminated at H^2 and if we neglect terms of the order $H^2\Delta^2$. Then (38) reduces to an expression[25]

$$\chi_\perp = \frac{N\beta^2}{k(T+\Delta)}\left[\frac{\mu_x^2+\mu_y^2}{2}\right] - \frac{N\beta^4H^2}{k^3T^3}\left(\frac{1}{3}-\frac{4\Delta}{3T}+\cdots\right)\left[\frac{(\mu_x^2+\mu_y^2)^2}{4}+\frac{(\mu_x^2-\mu_y^2)^2}{8}\right] \quad (39)$$

independent of φ. In writing (39), we have dropped the second or "high frequency" part of (38); this is allowable at very low temperatures, where saturation is important. As already stated, and as is also apparent from (39), the value of the effective magneton number appropriate to weak fields is $3^{1/2}\mu_\perp = [3(\mu_x^2+\mu_y^2)/2]^{1/2}$. Because of the term in $\mu_x^2-\mu_y^2$, the coefficient of H^2 in (39) is not the same as that which would be obtained by expanding (15) with $\mu=\mu_\perp$. When Becquerel measures the saturation curvature in the Faraday rotation at low temperatures, he determines empirically the ratio of the coefficient of H^2 to the term independent of H in $\chi_\perp$. The effect of the rhombic staggering is to make this ratio greater by a factor

$$a^2 = 1+\tfrac{1}{2}[(\mu_x^2-\mu_y^2)/(\mu_x^2+\mu_y^2)]^2 \quad (40)$$

than it would be if we used Eq. (15). Thus the saturation method really furnishes us with $a\mu_\perp$ rather than $\mu_\perp$, if inadvertently (15) is used, as is usually done. When this distinction is overlooked, the apparent values of $\mu_\perp$ furnished by saturation will thus be greater than those yielded by the Eq. (17) appropriate to weak fields. With the choice of constants (33), the magnitude of a is found from (29, 30) and (40) to be 1.12 (1.00). When (38) rather than (15) is used, the value of $\mu_\perp$ furnished by the saturation method is then reduced from 0.874 (0.726) to 0.780 (0.726). Hence the correction (40) removes part, but not all, of the discrepancy with the value 0.523 (0.469) deduced from (17) in section 4, provided we prefer the determinations not in parentheses.

With a triclinic instead of staggered rhombic field, not even a part of the discrepancy can be removed, since in the triclinic case no averaging over different types of atoms is necessary, and (15) can be used even for the perpendicular component.

Constants of the rhombic crystalline field. Let us suppose that the crystalline potential is developed as a series

$$V = \Sigma_{l,\,m} f_l^m(r)\,Y_l^m(\theta,\varphi) \quad (41)$$

in Tesseral harmonics $Y_l^m(\theta,\varphi) = F(\theta)e^{im\varphi}$ which we suppose normalized to unity. Because of the

[25] In deriving (39) from (38) one must remember that γ is involved implicitly through I' on the right side of (38) as well as explicitly. Otherwise the factor 4/3 multiplying Δ in (39) would be wanting.

rhombic holohedral symmetry, f_l^{-m} equals f_l^m and the coefficients vanish unless l and m are both even. If V satisfies Laplace's equation then $f_l^m(r)\sim r^l$. The Laplacian of V probably vanishes only approximately, since V, as we use it, is inclusive of the effect of the charge redistribution of the $5s^25p^6$ shell under the influence of the interatomic field, and so V may have a charge source even in the region occupied by the $4f$ orbits inasmuch as the inner parts of $5s$, $5p$ overlap $4f$. We wish to show that only certain choices of the coefficients in (41) will lead to wave functions and energy levels of the structure (33), (36), (37). In the "M" or axial system of representation, one finds by the Kramers' symbolic method,[28] or otherwise, that the matrix representing the potential (41) is

$$\begin{array}{c|ccc|} & \pm 5/2 & \pm 1/2 & \mp 3/2 \\ \hline \pm 5/2 & A_0^0+(A_2^0/6^{\frac{1}{2}})+(A_4^0/70^{\frac{1}{2}}) & (A_2^2/10^{\frac{1}{2}})-(3A_4^2/70^{\frac{1}{2}}) & A_4^4/5^{\frac{1}{2}} \\ \pm 1/2 & (A_2^2/10^{\frac{1}{2}})-(3A_4^2/70^{\frac{1}{2}}) & A_0^0-(4A_2^0/150^{\frac{1}{2}})+(2A_4^0/70^{\frac{1}{2}}) & (3A_2^2/50^{\frac{1}{2}})+(A_4^2/14^{\frac{1}{2}}) \\ \mp 3/2 & A_4^4/5^{\frac{1}{2}} & (3A_2^2/50^{\frac{1}{2}})+(A_4^2/14^{\frac{1}{2}}) & A_0^0-(A_2^0/150^{\frac{1}{2}})-(3A_4^0/70^{\frac{1}{2}}) \end{array} \qquad (42)$$

with $A_l^m=c_l\int_0^\infty f_l^m R^2r^2dr$, where c_l is a constant of proportionality independent of m and R is the radial wave function. Let $\mathbf{a}$ be the matrix of the coefficients α and let $\mathbf{H}$ be a diagonal matrix of characteristic values W_{I}, W_{II}, W_{III}. After the crystalline potential is diagonalized, its matrix is $\mathbf{H}$. In the original M system, before this diagonalization, its matrix is $\mathbf{a}H\mathbf{a}^{-1}$ inasmuch as $\mathbf{a}^{-1}$ is the inverse of the transformation from the axial to the final diagonal system of representation. Using (33), (36), (37), and the fact that $\mathbf{a}^{-1}$ is the same as the "transpose" $\tilde{\mathbf{a}}$ of $\mathbf{a}$, one finds

$$\mathbf{a}\mathbf{H}\mathbf{a}^{-1}=\mathbf{a}\mathbf{H}\tilde{\mathbf{a}}=\begin{vmatrix} 150 & -29 & 261 \\ -29 & 100 & 80 \\ 261 & 80 & 634 \end{vmatrix}\ \mathrm{cm}^{-1}. \qquad (43)$$

To obtain (33), (36), (37), the A's must be so chosen that (42) reduces to (43). The surprising feature is that the fourth order terms A_4 are thus seen to be fully as large as the second order ones A_2. Hence a second order rhombic field of the "asymmetrical top" type is entirely inadequate and the convergence of the Taylor's development of the potential is hence presumably poor, so that it is probably not allowable to terminate the development at the fourth order terms. When the higher order terms are included the identification of the A's ceases, of course, to be unique. A similar inadequacy of the second order terms is also found in the Kramers' triclinic theory, since α in (23) can differ from zero or unity only if fourth and higher order terms are admitted. Both in Kramers' theory and ours, the lowest diagonal element of the crystalline potential in the original axial system of representation belongs to $M=3/2$. This situation is impossible with only second order terms. If the crystalline field had cubic symmetry we would have $A_2^0=A_2^2=A_4^2=0$; $A_4^0=A_4^4(14/5)^{\frac{1}{2}}$. Actually these relations are not fulfilled, as is not at all surprising, since actually tysonite has hexagonal rather than cubic symmetry. The deviations from fulfillment are on the whole remarkably small, for (43) would satisfy these cubic conditions if, for instance, we replaced the elements 150, 634, -29, 80 by 217, 685, 0, 0 respectively, leaving 100, 261 unaltered. This probably is only a fortuitous coincidence, but, of course, it is conceivable that the microscopic environment of a given ion show some vestiges of cubic symmetry even though macroscopically the crystal is hexagonal.

It will be noted that our procedure is in a certain sense the reverse of that used by Penney and Schlapp.[8] Instead of first postulating a given crystalline potential (41), and then calculating the susceptibility, we first find the structure of the wave functions and energy levels which will represent the observed susceptibility. Then we transform "backwards" to the M system in the fashion (43) to find the characteristics of the crystalline potential. It is believed that this alternative, reverse procedure may become increasingly advisable for other materials than

[28] H. A. Kramers, Proc. Amsterdam Acad. **33**, 953 (1930); **34**, 965 (1931).

tysonite as the magnetic theory becomes increasingly refined through the development of improved experimental data on individual principal susceptibilities, etc., permitting more drastic tests and presumably requiring more complicated potentials than the simple ones used in the first approximations.

In conclusion, we do not wish to give any impression of finality to the rhombic potential represented in (43). It does seem to work better than the triclinic, and is fully as compatible with the known facts of the crystallographic structure. The departures from axial symmetry involved in (43) are rather large, and it is possible that they can be reduced by considering still more complicated potentials, notably those involving simultaneously both triclinic and staggered rhombic terms. Another possible modification is to have the z axis of the rhombic system spiral about the optic axis instead of being parallel to the latter. Then to compute the susceptibility in any given direction, a three-dimensional averaging process is required, rather than a two-dimensional one as in (38) for the directions perpendicular to the optic axis and none at all for the parallel direction. The attractive feature of this modification is that it makes the magneton number deduced from saturation greater than that deduced from (17) even in the case of the parallel component, thus tending to alleviate the discrepancy between the two methods emphasized in section 4. Furthermore, the effect of the matrix elements of the crystalline potential and of the moment which are non-diagonal in the inner quantum number j ought really to be considered if the separation of $F_{5/2}$ and $F_{7/2}$ in cerium is only 1600 cm^{-1}, as reported by Brunetti and Ollano.[27] However, it appears useless to make elaborate calculations based on these various ideas until better experimental data are available for the perpendicular component.

[27] R. Brunetti and Z. Ollano, Zeits. f. Physik **75**, 415 (1932).

Nitrogen Molecular Spectra in the Vacuum Ultraviolet

WILLIAM W. WATSON AND PHILIP G. KOONTZ, *Yale University*

(Received April 27, 1934)

Nitrogen molecular spectra in the region from 900A to 2300A have been photographed with a 10-foot vacuum spectrograph giving a dispersion of 5.5A/mm. Partial rotational quantum analyses have been made for several bands of the $a^1\Pi_u \rightarrow {}^1\Sigma_g^+$ system yielding the constants $B_0' = 1.632 \pm 0.002$, $B_0'' = 1.998 \pm 0.002$, $\alpha' = 0.021$, $\alpha'' = 0.018$. Many new bands in a nitrogen band system with an origin at 1847A discovered by Hopfield in a condensed discharge in a helium-nitrogen mixture are reported. This system is due to N_2^+, having the same lower state as that of the first negative system. The rôle of the helium is discussed. Birge and Hopfield's b' progression is found to consist of Q branches only with $B' = 1.147$. Several new N_2 ground state progressions among the bands in the 900A–1300A interval are presented.

INTRODUCTION

SEVERAL band systems assigned to the N_2 or N_2^+ molecules lie in the vacuum ultraviolet. The vibrational structure of the prominent $a^1\Pi_u \rightarrow {}^1\Sigma_g^+$ system, which extends through the whole Schumann region, has been investigated in detail by Birge and Hopfield.[1] Their analysis yielded accurate vibrational energy data for these two N_2 states, but the dispersion of their spectrograph was insufficient to reveal the rotational structure of the bands. That the upper state of this system is really ${}^1\Pi_u$ has been proved by Appleyard[2] who has made a rotational quantum analysis of the (5,13) and (5,14) bands which may be photographed with a spectrograph in air. The only determination of the rotational energy constant B_0 for the normal ${}^1\Sigma_g^+$ state, however, has been that of Rasetti[3]

[1] R. T. Birge and J. J. Hopfield, Astrophys. J. **68**, 257 (1928).

[2] E. T. S. Appleyard, Phys. Rev. **41**, 254 (1932).

[3] F. Rasetti, Phys. Rev. **34**, 367 (1929).

from the rotational Raman spectrum of nitrogen gas. An analysis of the rotational structure of bands at the origin of this system was therefore thought to be desirable.

Among the large number of emission bands of N_2 in the interval from 900A to 1300A Birge and Hopfield[1] recognized three normal state progressions (their b, b' and c series). We have investigated this region in the nitrogen molecular spectrum with considerably higher dispersion with a view to creating further order in this complex of bands. Finally, a considerable increase in the number of bands in an interesting N_2 system with an origin at 1846A discovered by Hopfield[4] in a helium-nitrogen mixture is reported, revised vibrational quantum assignments are given showing that the emitter is the N_2^+ molecule with the lower electronic state identical with the lower state of the first negative nitrogen bands, and the probable energy transfer from helium ions is discussed.

Experimental Procedure

The 10-foot, normal incidence, vacuum spectrograph used in this work was constructed in the shop of the Sloane Laboratory, following somewhat the design given by Sawyer[5] for a one-meter vacuum spectrograph. The grating is of speculum metal, 15,000 lines to the inch, giving a dispersion of 5.5A per mm in the first order. The plate-holder covers the entire vacuum region up to 2300A. We have used Schumann plates of our own manufacture, employing the process given by Hopfield and Appleyard[6] with entire satisfaction. Development with Eastman D-76 borax developer for $1\frac{1}{2}$ minutes is recommended. As wave-length standards we have taken revised values for the 1200A and 1134A NI triplets kindly furnished us by Dr. J. C. Boyce, the value 1742.749A for NI as determined by Hopfield, and the 1215A and 1025A H lines. The 1134A triplet is also present in the second order on all of our spectrograms.

As light source either a Π-shaped air-cooled tube 80 cm long and 2.5 cm diameter with an internal capillary of 1 cm diameter and 30 cm length mounted close to the slit with a current of 100 milliamperes or a water-cooled tube of 1 cm internal diameter and 30 cm length carrying 300 milliamperes was used. A constant flow of gas from a cylinder of nitrogen or helium passed through a capillary, a hot copper oxide tube and a liquid air trap into the discharge tube and thence through the slit into the body of the spectrograph. The pressure in the discharge tube was usually about 0.1 mm, while in the spectrograph the pressure was less than 0.01 mm. The liquid air served to eliminate effectively the CO spectrum, so that the only impurity bands on the spectrograms are some rather weak NO bands at the long wave-length end. It was found that the tank helium had a sufficient nitrogen content so that no additional nitrogen was needed for the mixture. Exposure times were usually about 24 hours with the air-cooled tube, the slit width being about 0.025 mm.

The $a^1\Pi_u - {}^1\Sigma_g^+$ System

In agreement with Appleyard[2] we find that the bands of this system are of the $^1\Pi \rightarrow {}^1\Sigma$ type. Since the normal state of N_2 is known to be $^1\Sigma_g^+$, this fixes the upper a state as $^1\Pi_u$. In the enlargement of the (0,4) and (1,5) bands in Fig. 1 the inner Q-branch head is easily seen, and one can observe at some distance from the head that the rotational lines fall into two branches, P and Q, each exhibiting alternating intensities. A partial rotational analysis of the (0,1), (0,4), (1,5), (1,6), (1,7) and (2,8) bands has been made. The incompleteness of the analysis is due to the impossibility of locating any R-branch lines in the heads of the bands or in the regions of the first lines of the P and Q branches, and to the fusion of many of the latter lines. Quantum assignments may be made for all of the available P and Q lines, however, on the basis of the comparison of the usual $Q(J)$–$P(J)$ and $Q(J)$–$P(J+1)$ combination differences between bands. Unfortunately there is exact superposition of successive P and Q lines in the range of intermediate and high J-values in most of the bands, a fact which limits the accuracy of the calculations of the rotational constants. Assignments of line frequencies for three of the bands as samples

[4] J. J. Hopfield, Phys. Rev. **36**, 789 (1930).
[5] R. A. Sawyer, J. O. S. A. and R. S. I. **15**, 305 (1927).
[6] J. J. Hopfield and E. T. S. Appleyard, J. O. S. A. **22**, 488 (1932).

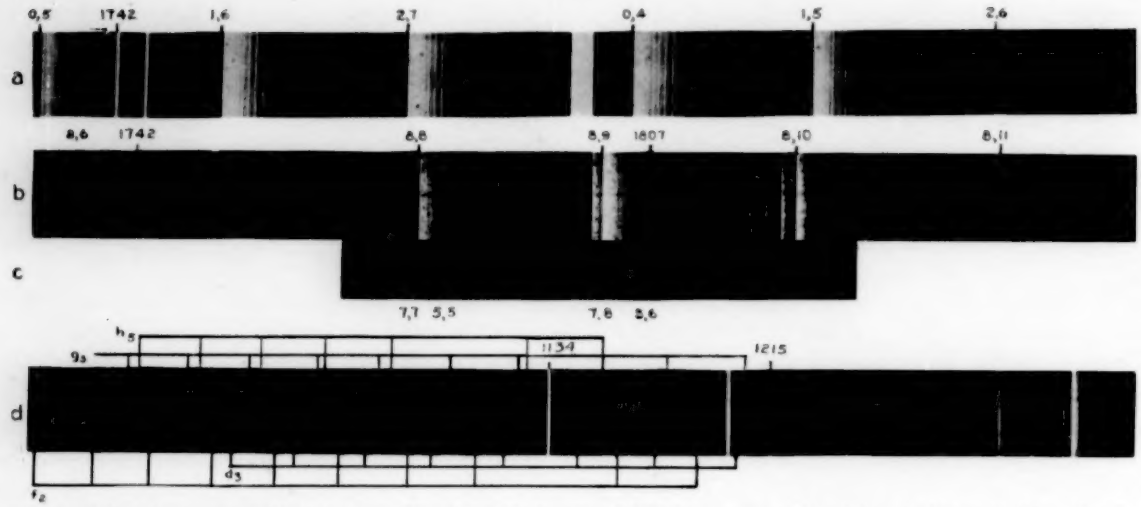

FIG. 1. (a) Enlargements (8.4 ×) of $a\ ^1\Pi_u \rightarrow {}^1\Sigma_g^+$ N_2 bands. (b) N_2^+ system with origin at 1847A, Helium-nitrogen mixture. (c) Condensed discharge in nitrogen showing additional bands of lower v-values in N_2^+ system. (d) Short wavelength end of N_2 band spectrum showing ground state progressions.

are given in Table I. The more intense lines have even J'' numbering. Notice that the superposition of Q and P lines preserves the alternating intensities in the (0,1) band but destroys them in the (1,7) band. In the (0,4) band the two branches are not fused.

Application of the P–Q–R combination difference with the fragmentary measurements on portions of the R-branches indicate that the Λ-doubling in the Π state is very small. The rotational energy constants B_v' and B_v'' are then correctly given by the Q–P combination differences. The values so obtained are presented in Fig. 2. We include also Appleyard's values (the crosses) from his analysis of the (5,13) and (5,14) bands. These indicate a departure of the B_v against v curve from linearity at high v values. Our analyses give $B_0' = 1.632$ cm^{-1} and $B_0'' = 1.998$ cm^{-1} with probable errors of ± 0.002. This value of B_0'' for the normal state of N_2 is to be compared with Rasetti's value 1.992 ± 0.005 from the rotational Raman lines. From Fig. 2 it is evident that $\alpha' = 0.021$, $\alpha'' = 0.018$.

TABLE I. *Assignments of frequencies in* $a\ ^1\Pi_u \rightarrow {}^1\Sigma_g^+ N_2$ *bands. Number following each frequency is estimated intensity.*

	0,1		0,4		1,7	
J''	$Q(J)$	$P(J)$	$Q(J)$	$P(J)$	$Q(J)$	$P(J)$
14	66,542.7 4	66,493.0 5			54,852.1 3	54,807.3 3
15	29.0 2	79.6 2			44.0 2	795.6 3
16	19.6 4	63.9 4	59,734.4 4		36.1 3	83.8 3
17	507.1 2	48.8 2	24.2 2	59,668.7 2	27.0 1	71.6 3
18	493.0 5	33.0 4	14.5 4	54.2 0	16.9 3	59.2 3
19	79.6 2	416.0 2	704.6 2	41.1 2	807.3 3	45.7 3
20	63.9 4	398.3 4	692.2 4	27.2 1	795.6 3	31.2 3
21	48.8 2	79.9 2	80.0 2	612.1 2	83.8 3	16.9 2
22	33.0 4	61.4 3	66.1 1		71.6 3	701.4 2
23	416.0 2	40.6 2	51.2 1		59.2 3	686.1 2
24	398.3 4	22.2 3	37.2 2		45.7 3	69.3 2
25	79.9 2	300.9 1	20.9 0	539.5 1	31.2 3	48.6 2
26	61.4 3	278.0 3	603.5 2	18.8 0	16.9 2	34.8 2
27	40.6 2	56.2 1	588.3 1	00.5 0	01.4 2	
28	22.2 3	31.6 2	73.6 2			
29	300.9 1		56.2 1			
30	278.0 3					

N_2^+ System in Helium-Nitrogen Mixtures

Fig. 1(b) is a reproduction of a spectrogram obtained with a condensed discharge in tank helium. The most intense bands in this system were discovered by Hopfield[4] who pointed out that the bands showed the alternating intensities expected for N_2 bands. Hopfield apparently did not observe, however, the $\Delta v = +3$ and -2 sequences

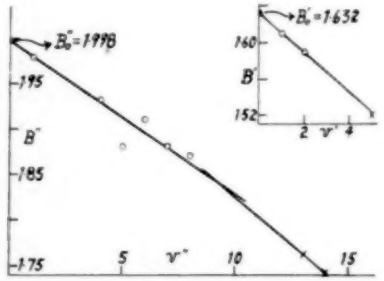

FIG. 2. B_v *vs.* v curves for $a\ ^1\Pi_u$ and $^1\Sigma_g^+$ N_2 states. Circles indicate our data, crosses Appleyard's.

and the extension of the $\Delta v = +1$ and $+2$ sequences to more than four members. Furthermore, a condensed discharge in nitrogen brings out additional bands (those with $v' = 5$, 6 and 7 in Table II) in each of the main sequences on the long

TABLE II. *Assignments of band heads in the N_2^+ system. d indicates double assignment. All bands degrade to the red.*

v', v''	Int.	νObs.	v', v''	Int.	νObs.
8,11	4	48,553.7	10,11	5	52,472.6
9,12	3	48,729.5	11,12	3	52,585.3
10,13	2	48,912.5	12,13	0	52,695.0
11,14	1	49,097.6	13,14	0	52,809.1
6,8	0	50,134.6	2,2; 3,3	1 d	53,974.7
7,9	1	50,257.6	1,1; 4,4	1 d	53,985.1
8,10	10	50,391.5	0,0; 5,5	2 d	54,006.1
9,11	8	50,530.6	6,6	2	54,046.9
10,12	6	50,675.7	7,7	1	54,100.2
11,13	4	50,824.2	8,8	6	54,165.3
12,14	1	50,975.2	9,9	3	54,233.4
13,15	1	51,127.0	10,10	1	54,308.6
14,16	0	51,285.2	5,4; 6,5	1 d	56,050.4
15,17	0	51,426.8	7,6	1	56,074.0
5,6	1	51,996.4	9,8	1	56,138.7
6,7	2	52,073.1	10,9	1	56,180.6
7,8	2	52,160.5	11,10	0	56,224.2
8,9	9	52,261.7	7,5; 8,6; 9,7	3 d	58,078.9
9,10	7	52,363.1			

wave-length side of the bands intensified in the helium discharge. These additional bands are almost completely masked in the spectrum of the helium-nitrogen discharge by the rotational structure of the intensified bands which degrade to the red in apparent violation of the empirical rule that in band spectra with $\omega' > \omega''$ the bands degrade to the violet.

Having suspected that this band system was due to the N_2^+ molecule because of the action of the excited helium atoms (21.11 to 24.46 volts energy as compared to 15.65 volts for the I. P. of N_2), comparison of the observed $\Delta G(v''+\frac{1}{2})$ values with those for the lower state of the first negative N_2^+ system as given by Coster and Brons[7] showed the two states to be the same.[8] There was the difficulty, however, that although the vibrational frequencies in the two states were very nearly equal, the $\Delta v = 0$ sequence seemed to begin with the (5,5) band. Calculation of the approximate positions of these missing bands by extrapolation of the course of the observed $\Delta G(v'+\frac{1}{2})$ values then showed that this sequence probably had a long-wave-length edge at about the (2,2) or (3,3) band and that the (0,0) and (5,5) bands should nearly coincide. Two additional bands have been found in this region on spectrograms taken with an uncondensed discharge in the helium-nitrogen mixture. Each of these agrees well within the experimental error with two of the predicted positions because of the reversal of direction in the sequence, and together with the use of the (5,5) band frequency also as (0,0) fills out the $\Delta v = 0$ sequence completely. There is no evidence of bands with $v < 5$ in the $\Delta v = +1$ or -1 sequences, however, and there remains to be explained the general lack of intensity among the bands of low v values.

TABLE III. *Additional normal state progressions at the short wave-length end of the N_2 emission spectrum.*

v''	d	Int.	e	Int.	f	Int.	g	Int.	h	Int.
1					107860.6	2	106606.5	1		
2					105548.8	1	104306.3	0		
3	98237.0	0			103270.0	1	102018.4	1		
4	95999.3	3			101044.9	2	99801.4	2 d		
5	93781.7	At			98829.8	4	97591.1	2	101414.0	2
6	91597.7	3			96641.8	2	95398.4	0	99226.1	2
7	89449.2	3			94489.4	1	93247.0	3	97071.1	1
8	87322.0	4			92355.2	1	91136.3	1	94953.5	2
9	85218.7	3			90265.3	3	89027.6	2	92836.2	3
10	83150.7	2	83874.5	1						
11	81115.6	1	81831.5	1	86176.0	1	84942.4	1	88713.6	3 d
12			79814.4	3	84151.4	1	82899.7	3	86721.8	1
13			77836.0	2			80919.9	1	84710.4	1
14									82769.9	0

The assignment of frequencies of band heads in this system is given in Table II. For the range $v' = 0$ to 7 inclusive these frequencies fit the following formula:

$$\nu = 54{,}024 + 2173.2\,(v'+\tfrac{1}{2}) - 10.43\,(v'+\tfrac{1}{2})^2 - 0.017\,(v'+\tfrac{1}{2})^3 - 2207.16\,(v''+\tfrac{1}{2}) + 16.136\,(v''+\tfrac{1}{2})^2 + 0.040\,(v''+\tfrac{1}{2})^3,$$

where the lower state terms are those given for the first negative system. At $v' = 8$, strangely enough just at the energy where the intensification by the helium takes place, the second differences between the successive $\Delta G(v'+\frac{1}{2})$ values

[7] D. Coster and H. H. Brons, Zeits. f. Physik **73**, 747 (1932).

[8] J. Kaplan kindly informed us in a private communication during the course of the present work that he had already noticed the similarity of the lower state vibrational differences in Hopfield's data with those for the lower state of the N_2^+ bands in the visible, but that he had had difficulty in establishing the identity of the two states because of the most peculiar intensity distribution then resulting among the bands as given by Hopfield (no bands with $v'' < 8$ and no bands of wave-length shorter than 1779A).

jump to about 32 cm^{-1}. This sudden change in the course of the ΔG's makes it impossible to represent all of the bands in the system by the same formula.

In Fig. 3 we give the distribution of intensities among the bands of this N_2^+ system. The $v'=8$ level at which the enhancement of intensities due to the helium occurs is 2.05 volts above $v'=0$.

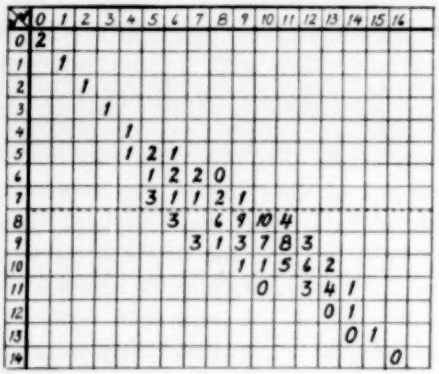

FIG. 3. Intensity distribution in the 1847A N_2^+ system.

Adding to this 6.67 volts for the energy of the (0,0) transition and 15.65 volts (I. P. of N_2) for that of the ground state of N_2^+ with respect to normal N_2, there results 24.37 volts for the total. The close agreement of this value with that for the I. P. of He, 24.46 volts, would indicate that collisions of the second kind between He ions and normal N_2 molecules are responsible for the large production of N_2^+ with this or slightly greater energy. Since, according to Lozier,[9] the heat of dissociation of N_2^+ in its ground $^2\Sigma$ state is 6.73 volts, the upper (apparently $^2\Sigma$, judging from the single-headed appearance of the bands) state of this system is in a favorable position in its lower vibrational levels for interaction with one of the several probable repulsion states arising from $N(^4S)+N^+(^3P)$ atoms. Such predissociation may be the cause of the very low intensity of bands with $v'<5$.

N_2 Bands of Shorter Wave-Length

Between 900A and 1300A there are more than 150 emission bands of N_2. Among these Birge and Hopfield[1] recognized three ground state progressions—their b, b' and c series—, each apparently coming from a different upper electronic level. With a certain condition of excitation of the discharge tube they noted the complete absence of the b' progression, and speculated as to the possibility of its being due to NO rather than to N_2 even though the vibrational intervals agreed fairly well with those of the N_2 normal state. Our higher dispersion spectrograms reveal clearly an alternating intensity among the rotational lines of these bands, however, which definitely decides in favor of N_2 as the emitter. Several of these b' bands seem to consist of but a single branch emanating from the head, and each has one rotational line at some distance from the head showing a marked intensity perturbation. Now if each of these bands consisted of an exactly superposed Q and P branch, as in some of the $a^1\Pi-{}^1\Sigma$ bands discussed above, one would expect that proceeding along some four or five bands in the progression the two branches would necessarily get out of step with each other. This is not the case. Furthermore, if superposed P and R branches were involved there should be two lines, separated by, say, four others since the fractional change in B is evidently large in these bands, showing the intensity anomaly. We therefore conclude that the b' progression consists of a set of single Q branches, the upper state being thus $^1\Pi_u$. This absence of P and R branches in a long progression of $^1\Pi-{}^1\Sigma$ bands forms a striking example of an already discovered type of predissociation.[10]

The frequency interval between each rotational line of these Q branches and the origin (head) divided by $J(J+1)$ should be a constant for each band (if $(D'-D'')J^4$ may be neglected) and equal to $B'-B''$. Numbering the perturbed line $J=25$ and the other lines accordingly in each band, these quotients are very constant. Then knowing B'' for each from the data for the $^1\Sigma$ ground state, we compute B' to be 1.148, 1.145 and 1.147 for the b' 14, b' 15 and b' 16 bands, respectively. The average of these, 1.147, one may assume to be B_0 for this $^1\Pi$ N_2 state lying 103,677.7 cm^{-1} above $v=0$ of the N_2 normal state.

[9] W. W. Lozier, Phys. Rev. **44**, 575 (1933).

[10] R. deL. Kronig, Zeits. f. Physik **62**, 300 (1930).

From the magnitude of this B_0 one would estimate that if other vibrational levels in this same $^1\Pi$ state existed they should be spaced at about 1400 cm^{-1} intervals. We list in Table III some further ground state progressions we have found among the N_2 bands in this region. One of these, that labelled d, is 1474 cm^{-1} above the b' level, and there are indications of excited state vibration frequencies of about 740 cm^{-1} and about 1250 cm^{-1}, but we have been unable to establish any upper state vibrational frequency definitely. Nitrogen absorption spectra taken at a number of rather low nitrogen gas pressures in the receiver of the spectrograph should aid greatly in the complete ordering of the N_2 levels in this higher frequency region. Experiments with this objective are in progress.

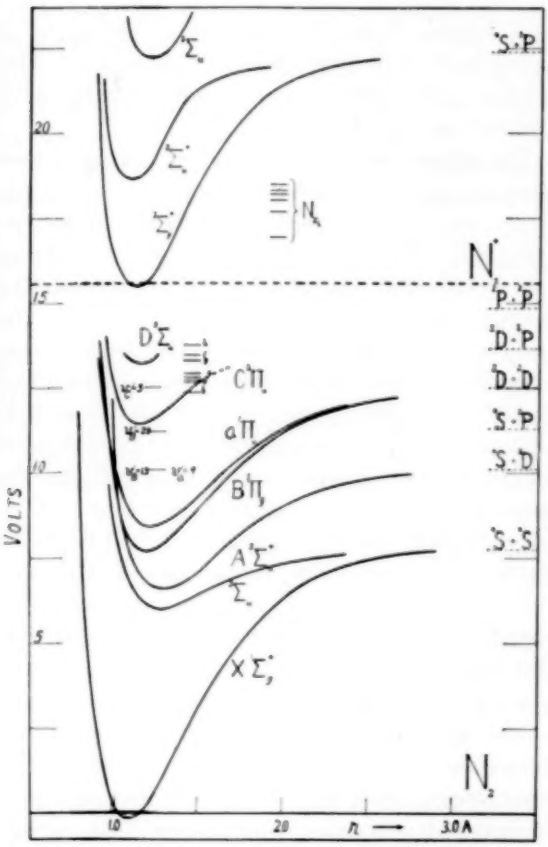

FIG. 4. Potential energy curves drawn with the aid of Morse functions for known N_2 and N_2^+ states.

N_2 AND N_2^+ ELECTRONIC LEVELS

Lozier has shown[9] that the heat of dissociation D for the normal state of N_2 is 7.90 ± 0.02 volts. Kaplan[11] from his study of the energy relations between predissociation regions in the triplet band systems of nitrogen and the products of dissociation has pointed out that the energy of $v=0$ of the $A\ ^3\Sigma_u^+$ state must be $\geqq D-1\cdot2$ volts. This level must then come at or slightly higher than 6.7 volts above $v=0$ of the normal state. Placing it exactly at this energy, we may then plot the potential energy curves for all the known states of N_2 and N_2^+, for the first time placing the singlet and triplet levels in very closely their correct relative spacing. In Fig. 4 we present such a plot, the form and position of the curves having been computed with the aid of Morse functions. Since the b' level comes just above the energy of $^2D+^2D$ atoms, it may well be a repulsion curve from this limit which is responsible for the observed predissociation.

Note added in proof: The lowest $^3\Sigma_u$ curve in Fig. 4 was drawn according to the results recently published by J. Kaplan.[12] Kaplan's later revision of these results gives the $A\ ^3\Sigma$ state as the upper state of his new N_2 bands. The $^3\Sigma$ state arising from two ^4S atoms is therefore as yet undiscovered. Because of these new data on the $A\rightarrow X$ intercombination system, it may be necessary to use 7.4 volts for the heat of dissociation of N_2.[13] In that event all of the triplet levels in our Fig. 4 must be lowered by 0.5 volts.

---

[11] J. Kaplan, Phys. Rev. **42**, 97 (1932).
[12] J. Kaplan, Phys. Rev. **45**, 675 (1934).
[13] Cf. W. W. Lozier, Phys. Rev. **45**, 840 (1934).

The Transmutation of Fluorine by Proton Bombardment and the Mass of Fluorine 19

M. C. Henderson, M. S. Livingston and E. O. Lawrence, *Radiation Laboratory, Department of Physics, University of California*

(Received May 1, 1934)

Fluorine has been transmuted by bombardment with protons into oxygen and helium. The number of transmutations has been followed from a proton energy of 0.675 to 1.63×10^6 electron-volts. The alpha-particles emitted have a range greater than 6 cm. Their range increases with proton energy in the expected manner. The short range alpha-particles observed both by us and by other workers are probably due to a boron contamination. Professor Oppenheimer has calculated, along the lines of the Gamow theory, the manner in which the probability of transmutation should vary with the energy of the protons. The measurements are in excellent agreement with the theory. The mass of the fluorine atom that is calculated from the reaction, 19.0031, is in excellent agreement with other transmutation data, but not with the value usually accepted, namely 19.000.

Introduction

USING 450,000 volt protons in their pioneer experiments on the artificial transmutation of the elements, Cockcroft and Walton[1] observed the emission of 3.0 cm alpha-particles from a target of CaF_2. They attributed this emission to the transmutation of fluorine with the formation of oxygen. Later Oliphant and Rutherford,[2] in careful experiments with much greater numbers of protons at lower voltages, observed 4.1 cm alpha-particles from a target of FeF_2, which also were attributed to fluorine. In our preliminary experiments[3] using protons of much greater energy, we observed the emission from CaF_2, in addition to the particles of short range, of alpha-particles of about 7 cm range. We have in the interim carried out a more thorough experimental investigation and have come to the conclusion that the long range group alone is emitted by fluorine,[4] and that the particles of shorter range were the result of a contamination, probably by boron.

Method and Apparatus

The apparatus used in this work was the larger of the two that have been developed in this laboratory for the production of high speed light ions without the use of high voltages. It has already been described[5] in this journal. The smaller apparatus has been used for work with lithium[6] and boron.[7]

The apparatus is so constructed that only ions having a particular value of e/m are accelerated. Heretofore we have used the hydrogen molecular ion, $(H)_2^+$. The disadvantage inherent in using this ion is that the deuton, $(H^2)^+$, has almost exactly the same e/m, and, if present in the apparatus, is accelerated at the same time. Since the deuton has proved to be a very reactive projectile in transmutation work and since it is always present in our apparatus in considerable numbers, the apparatus was adjusted for the present experiments to accelerate protons, $(H)^+$, only. Proton beams of energies up to 1.63 MEV (million electron-volts) were used.[8] Although currents of as much as 0.8 microampere were obtainable, generally much smaller currents than this were used because the yield of transmutations is very large at high voltages.

The energy of the bombarding protons was determined, whenever possible, by measuring their range when scattered into the ionization chamber by a platinum target. To obtain energies different from the one for which the apparatus was adjusted, mica foils of known stopping power were inserted in the path of the

[1] J. D. Cockcroft and E. T. S. Walton, Proc. Roy. Soc. **A137**, 229 (1932).

[2] M. L. E. Oliphant and Lord Rutherford, Proc. Roy. Soc. **A141**, 259 (1933).

[3] E. O. Lawrence and M. S. Livingston, Phys. Rev. **44**, 316A (1933).

[4] We have just seen the abstract of a paper by M. A. Tuve, L. R. Hafstad and O. Dahl presented at the April, 1934, meeting of the American Physical Society, in which they report finding 60 mm alpha-particles from fluorine, in agreement with our results.

[5] E. O. Lawrence and M. S. Livingston, Phys. Rev. **45**, 608–612 (1934).

[6] M. C. Henderson, Phys. Rev. **43**, 98 (1933).

[7] M. G. White and E. O. Lawrence, Phys. Rev. **43**, 304 (1933).

[8] We have included in the results two runs in which the molecular ion beam was used. The deutons present do not seem to cause spurious effects with this particular target.

primary beam—thus the lowest value of the energy was obtained by inserting a 21 mm air-equivalent mica foil in the path of a 1.2 MEV beam.

The target was a piece of calcium fluoride melted onto a piece of platinum mesh and placed on the target-mounting in the Faraday chamber. It was one of twelve targets, any one of which could be rotated into the path of the proton beam by turning a ground joint. The targets included nearly all the elements in the first two rows of the periodic table and calcium hydroxide as well. Only from the calcium fluoride target was there any evidence of a 6 to 7 cm alpha-particle. As no alpha-particles of this range could be detected from any other target at the highest currents obtainable, they are certainly to be attributed to the transmutation of fluorine.

The alpha-particles were detected in a shallow ionization chamber by a four stage amplifier[9] of the type described by Wynn-Williams.[10] The Geiger counter used in earlier work was discarded for obvious reasons. The plate circuit of the third stage of the amplifier operated two separate output tubes. One of them actuated a cathode-ray oscillograph and the other a "scale of eight" thyratron counter.[11] The cathode-ray tube was a new type having a brilliant spot that is easily visible in daylight. It was kept under continuous visual observation during a run. We were thus able to keep close track both of all radiations that entered the ionization chamber and of the performance of the amplifier.

Visual observations with a cathode-ray oscillograph (combined with a counting device) have a twofold advantage. On account of the very long time scale, about two inches per sixtieth of a second, spurious impulses that are recorded by the counter are readily distinguished from the characteristically shaped potential pulses caused by alpha-particles. Also, with the oscillograph time scale oscillating in synchronism with the 60 cycle alternating potential that is applied to the plate of the main oscillator, it is possible to observe whether any pulses occur after the proton bombardment ceases. (The proton bombardment is confined to about 50 percent of the positive half of each cycle, or about 1/4 of the whole.) It should thus be possible to detect such effects as radioactivity of very short life. All alpha-particles or disintegration protons thus far observed have appeared simultaneously with the proton beam. None have been observed later than 1/300 sec. after its disappearance.

[9] The amplifier and recording mechanism are to be described in more detail elsewhere.

[10] C. E. Wynn-Williams and Ward, Proc. Roy. Soc. **A132**, 391 (1931).

[11] C. E. Wynn-Williams, Proc. Roy. Soc. **A136**, 312 (1932).

Range of the Alpha-Particle

Fig. 1 is a number-range curve for the alpha-particles from a target of calcium fluoride. The two scale of ordinates are given in absolute terms—that is, they represent the numbers of transmutations per 10^9 protons incident on the target. In calculating numbers of transmutations from numbers of alpha-particles it is assumed that the alpha-particles are emitted isotropically. Curves I, II and III are plotted on the 0 to 10 scale, the remainder on the 0 to 100 scale.

For comparison the number-range curves of alpha-particles from boron and lithium are given, curves VII and VIII. The extrapolated range of the lithium and boron curves are larger than the values given by other workers[1, 2]

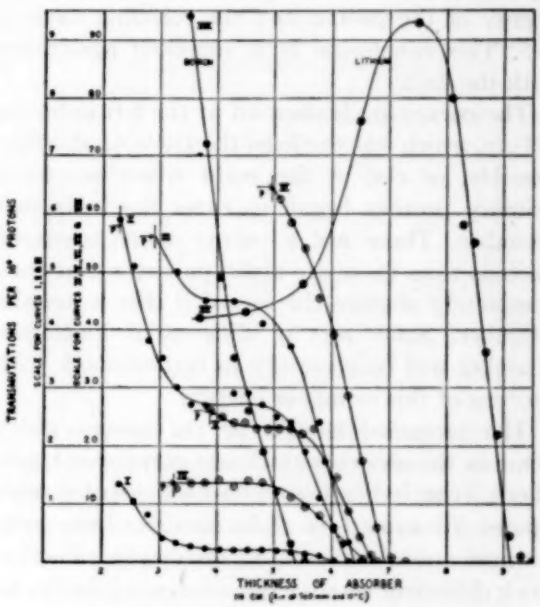

FIG. 1. Number of transmutations per 10^9 protons vs. absorber thickness for different proton energies.

because the energy of the bombarding proton is considerably greater. The increase in range agrees well with the amount calculated from the increase in proton energy. The difference in range between the boron or lithium alpha-particles and the fluorine alpha-particles should be more accurate than the actual measured range of either.

In calculating the curves for the three different elements, account has been taken of the fact that the mechanism of transmutation is different in each case. Thus, for fluorine one alpha-particle is emitted per transmutation. For lithium, however, there are twice as many, and for boron, three times as many alpha-particles as transmutations.

Curves I to VI were obtained when fluorine was bombarded by protons of the following energy: Curve I—0.675 MEV, II—0.975, III—1.10, IV—1.20, V—1.33, VI—1.63. Curve VII is lithium bombarded by 1.5 MEV protons, and Curve VIII boron bombarded by 1.2 MEV protons.

From the six curves of fluorine alpha-particles it can readily be seen that the range of the alpha-particle increases with the energy of the proton that produces it. From the mechanism of the transmutation it may be inferred that the alpha-particle receives approximately 4/5 of the energy of the proton and the recoiling nucleus 1/5. This conclusion is in excellent agreement with the data.

The curves are broken off at the left either at 2.3 cm, which was the least thickness of absorber possible, or else at the point where scattered primary protons began to enter the ionization chamber. There are so many more scattered protons than there are alpha-particles that they completely obscure the record if they enter the chamber. Some sort of differential ionization chamber will be necessary in further work with protons of this or higher energy.

The increased heights in the curves which come as the absorber thickness is reduced below about 3 cm, indicating alpha-particles of shorter ranges, are caused by alpha-particles from some contamination common to all targets. Further work definitely showed this contamination to be boron. Compared to other substances the yield of alpha-particles from boron is enormous. Each disintegration produces three alpha-particles and the number of disintegrations itself is about ten per million protons at a million volts. The peculiar form of the boron range curve makes contamination with boron particularly treacherous, as has already been emphasized by Oliphant and Rutherford[2] and by Tuve.[12] The exponential increase in number of alpha-particles makes it easy to determine a false alpha-particle range for an element that, in point of fact, yields no alpha-particle. Any alpha-particle with range less than four cm is suspect, unless special precautions are taken to ensure that no boron is present. The alpha-particles of short range that we detected from a number of targets in our early work are almost certainly the result of boron contamination.[3]

On the other hand, there is a very definite end to the boron range curve, as may be seen from Fig. 1, Curve VIII, or from Oliphant and Rutherford,[2] p. 270. The alpha-particle yielded by a calcium fluoride target goes at least a centimeter further than the boron alpha of longest range.

Voltage Transmutation Function

Fig. 2 shows the voltage transmutation functions of two targets: calcium fluoride and lithium. The lithium target was originally a piece of metallic lithium, but by the time the measurements were taken its surface had probably become lithium hydroxide, or even lithium carbonate. The ordinates in this figure are the heights of the plateaux of the number-range curves in Fig. 1. The plateau for Curve VI was estimated in an obvious manner by comparison with the others.

In this figure the number of transmutations is plotted against the range of the protons producing the transmutation and not against their energy directly. There is given a second scale of abscissas showing the proton energy in kilovolts to which the proton ranges correspond. This method of plotting shows at once in the case of lithium where the initial exponential rise with voltage ceases, and the increased number of transmutations becomes a result simply of the

[12] Tuve, Hafstad and Dahl, Phys. Rev. **43**, 942L (1933).

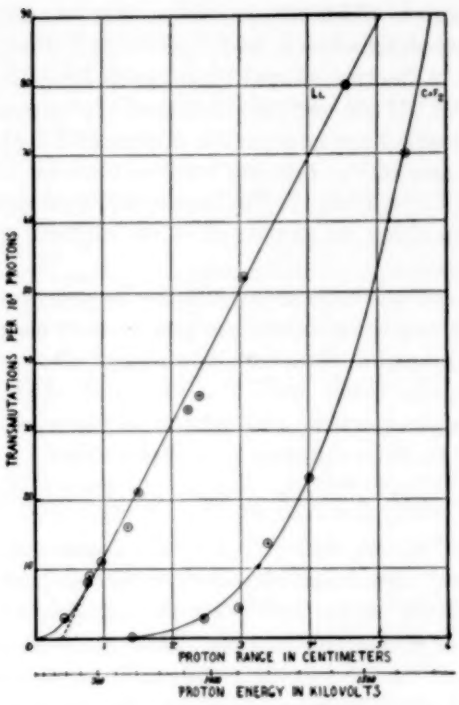

FIG. 2. Transmutations per 10^9 protons *vs.* proton range (energy) for Li and CaF_2.

increased penetration of protons into the target. The relation between proton range and proton energy was taken from data given by Blackett.

The lithium curve was taken from the work of Henderson.[6] The highest point (filled circle), however, was determined separately in the larger apparatus in the course of the present experiments.

We are greatly indebted to Professor Oppenheimer for working out, along the lines of the Gamow theory* of the nucleus, a theoretical formula for the voltage transmutation function of fluorine. Approximations that were sufficient in the case of lithium[6] are no longer so for fluorine. The assumptions underlying the theoretical formula are: (1) the peak in the potential barrier is high compared to the proton energy; and (2) the barrier is nearly impenetrable. The probability of transmutation is the product of two exponentials, corresponding to the two terms in the brackets, one representing the probability of a proton penetrating the barrier and the other the probability of transmutation after penetration. The fact that the target is "thick" also is taken into account. The formula is

$$N=kVe^{-S}(1+V^{\frac{1}{2}}/6+V/24+V^{\frac{3}{2}}/72+\cdots)$$

where

$$S=(4\pi^2e^2/h)\{Z_F[M_F/2E_p]^{\frac{1}{2}}+Z_\alpha Z_0[M_\alpha\cdot M_0/2(M_\alpha+M_0)(E_d+E_p^*)]^{\frac{1}{2}}\}.$$

Z_F, Z_0 and Z_α are, respectively, the atomic numbers of fluorine, oxygen, and the alpha-particle; M_0, M_α, and M_p are the masses, in grams, of the oxygen atom, alpha-particle and proton; E_d and E_p are the disintegration energy and proton energy, in ergs; $E_p^*=E_p(M_F/(M_F+M_P))$.

Numerically,

$$S=(+8.92/V^{\frac{1}{2}}+28.3/(8.2+V)^{\frac{1}{2}}),\ V \text{ in MEV}.$$

There is thus only one arbitrary constant, k. This constant was calculated to make the curve pass through the point 1.63 MEV and 70. As may be seen from the table, the fit is excellent except for one point that is obviously in error experimentally. It is remarkable that a formula of this character should fit so well, and the fit affords good evidence for the correctness of the underlying assumptions.

TABLE I. *Comparison of theoretical and experimental values for voltage transmutation function of fluorine.*

Voltage (MEV)	Transmutations per 10^9 protons N (Obs.)	N (Calc.)
0.675	0.20	0.34
0.975	2.7	3.7
1.10	4.3	7.7
1.20	13.5	12.8
1.33	23	22.9
1.63	70	70.
0.625		0.20
0.50		0.04
0.25		9×10^{-5}

An error of 50 EKV in determining the energy at the lowest point would make the observed value coincide with the calculated. We were not able to observe scattered protons at less energy than 900 EKV so the energy may well be in error by as much as 50 EKV.

The "threshold" for transmutation seems to be no better defined for fluorine than for lithium

*See Gamow, *Atomic Nuclei and Radioactivity*, p. 97, formula 42.

or boron. Extrapolating the theoretical curve to 500 EKV shows that one would need a current of about 10^{-7} amperes of protons of that energy to detect 10 alpha-particles per minute in a solid angle of $4\pi/60$ (our solid angle), or 50 microamperes at 250 EKV.

From the transmutation function may be calculated a nuclear cross section effective for transmutation. At 1.5 MEV there are about 50 transmutations for an equivalent centimeter of proton track. From the number of fluorine atoms present in such a layer and the stopping power of CaF_2, one may calculate that the effective radius of the fluorine nucleus, within which a proton must strike to produce a transmutation, is 3.5×10^{-14} cm. This value is quite small compared to the nuclear radius deduced from scattering experiments. In other words, the chance of transmutation in a close collision is small. For lithium the corresponding radius is 2×10^{-14} cm.

The Mass of F^{19}

The mechanism suggested by Cockcroft and Walton[1] for this transmutation is ${}_9F^{19}+{}_1H^1={}_8O^{16}+{}_2He^4+E$. The energy available in this reaction, if the mass of the neutral fluorine atom is assumed to be 19.000, is about 5 MEV. Dividing this energy between alpha-particle and recoiling oxygen nucleus gives the alpha-particle 4 MEV, corresponding to a range of about 4.5 cm. This range is consistent with the measurements of Oliphant and Rutherford.[2] However, Bainbridge[13] has shown from his measurements of the mass of Ne^{22} and from the transmutation of fluorine with alpha-particles, as in the experiments of Chadwick and Constable,[14] that the mass of fluorine should be between 19.0022 and 19.0034. If we use our measured alpha-particle range of 6.7 cm at a proton energy of 1.2 MEV, the mass of the fluorine nucleus may be calculated to be 19.0031. This calculation, of course, assumes that no gamma-rays are emitted in the reaction.

In our work the energy of the incident proton is not negligible in comparison to the energy of transmutation. The complete equation for calculating the latter from the measured energy of the alpha-particle and proton is therefore important. This equation is the following:

$$E=\tfrac{1}{2}MU^2+\tfrac{1}{2}MU^2\cdot M/M'-\tfrac{1}{2}mu^2(1-m/M')$$

where m, M and M' are the masses of the proton, alpha-particle, and recoil nucleus, respectively, and u and U are the velocities of the proton and alpha-particle. This equation takes account of the fact that the recoil nucleus must carry off the momentum of the proton and therefore does not recoil in a direction directly opposite to that taken by the alpha-particle. It is calculated on the assumption that the alpha-particle is observed in a direction at right angles to the path of the proton. For lithium the correction term amounts to one-quarter of the proton energy. At low proton energies or higher recoiling masses this correction is not important.

We acknowledge with sincere thanks the continued financial support of the Research Corporation and the Chemical Foundation and the valuable assistance of Commander T. Lucci.

[13] K. Bainbridge, Phys. Rev. **43**, 424 (1933).

[14] J. Chadwick and J. E. R. Constable, Proc. Roy. Soc. **A135**, 48 (1932).

Photoelectric Measurements of the Absorption of Fused and Crystalline Quartz Between 1633 and 1463A

W. M. POWELL, JR., *Research Laboratories of Physics, Harvard University*

(Received April 30, 1934)

The transmission of eight sections of one specimen of crystalline quartz, eleven sections of another crystal, and six sections of a piece of fused quartz from the General Electric Company was determined between 1633 and 1463A. The method is the same as that used for fluorite, except that the photoelectric currents are measured by an FP-54 Pliotron with a galvanometer in the plate circuit. The fused quartz and the first crystal showed large variations in the coefficient of absorption. The other crystal was much more homogeneous, and from it the percentage of light removed at the surfaces was determined. The extraordinary variations in the coefficient of absorption show the importance of actually testing a piece of quartz in the ultraviolet before incorporating it in an instrument for use in that region.

THE procedure and the apparatus employed in these measurements are nearly the same as those used in the study of the absorption of fluorite.[1] The vacuum spectrograph is used as a monochromator, wave-lengths being changed by rotating the grating. Two alterations have been made, one in the apparatus for measuring the photoelectric currents and the other in the method of polishing.

MEASUREMENT OF THE CURRENT

Dr. J. C. Street very kindly turned over to me an amplifier tube circuit which he had used in measurements of cosmic rays in Peru last summer. This circuit is a simplification of one described by DuBridge,[2] and replaces the Compton electrometer used previously. A diagram of the circuit is shown in Fig. 1. The filament-to-plate resistance of the FP-54 Pliotron acts as one arm of a Wheatstone bridge. The variable resistance A, is the opposite arm while the two 10,000 ohm resistances form the other two arms. A variation in the potential of the sensitive grid changes the balance of the bridge. This grid is connected to the external shielding through a 5×10^{10} ohm resistance. In operating the circuit the bridge is balanced first when there is no light entering the photoelectric cell. Then the light is turned on and the resultant current causes a change in the potential of the grid. The potentiometer P is adjusted to bring the bridge back into balance again. Thus the tube circuit is used as a null instrument and the currents are strictly proportional to the voltage across the high resistance. This voltage is read directly from the potentiometer P.

The dotted lines in Fig. 1 represent shielding. All resistances except the one connected to the grid are mounted on a Bakelite panel which is inclosed in a metal lined box. Leads to the FP-54, the galvanometer, and the tube batteries B, are made of shielded wire. This allows the FP-54 and the galvanometer to be placed at any convenient distance from the controls. The two six volt storage batteries B, can be placed in a shielded box but this was found to be unnecessary. The Leeds and Northrup Type R galvanometer G, has a period of 2.6 seconds and sensitivity of about 3×10^{-9} amp./mm scale deflection at one meter distance. The photoelectric cell batteries D, were not shielded in any way. The voltage sensitivity of the electrical system is about 4000 mm/volt. The currents from the photoelectric cell range from 10^{-11} to 10^{-13} ampere. Since the capacity of the grid circuit is small, readings can be made as fast as they can be written down. There is one objection to the circuit. The FP-54 and photoelectric cell are located only three inches away from the hydrogen discharge tube which, though run on direct current, has a tendency to oscillate. This causes a disturbance in the amplifying circuit which it was found possible to reduce by shielding the discharge tube and its leads in galvanized iron. With a hydrogen discharge this effect was very small but with oxygen the effect

[1] W. M. Powell, Jr., Phys. Rev. **45**, 154 (1934).
[2] L. A. DuBridge, Phys. Rev. **37**, 392–400 (1931).

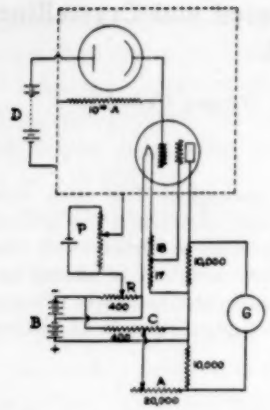

FIG. 1. Schematic diagram of apparatus.

became much greater. However, since all measurements were made with the hydrogen discharge this trouble did not affect the accuracy of the results.

The amplifying circuit is very easy to use. There are only three resistances to adjust before using the Leeds and Northrup Student Potentiometer *P*. The 20,000 ohm variable resistance *A*, is set to have approximately the same value as the filament-to-plate resistance of the FP-54. Resistance *R* is adjusted to give the proper grid voltage, -4 volts. Then resistance *C* is changed until the galvanometer reads zero. Resistances *A* and *C* remain fixed after the first adjustment. *R* alone is altered to counteract the zero shift as the tube warms up. As in reference 1 fourteen alternate readings were taken with and without the quartz in the beam. After the tube warmed up for an hour the zero drift reduced to about 0.004 volt per hour. This was almost negligible since the usual voltages measured ran between 0.05 and 0.2 volt. The complete set of readings for one point were taken in about ten minutes.

PREPARATION OF THE QUARTZ

The quartz was polished entirely mechanically on a machine made by Mr. David Mann. The specimens were mounted with Canada balsam on a suitable support and surrounded by other pieces of quartz to prevent rounding of the edges. The lap was an ordinary pitch lap charged with the same fine rouge employed previously[1] in preparing fluorite. The polishing was continued for about an hour after all pits and scratches had disappeared from the surfaces. All the specimens were prepared in this way and as far as could be seen the polish was always the same. No variation was observed between consecutive polishings. The quartz was cut into slices and the pieces numbered in the order in which they came off. Since not more than three mm of quartz were removed in cutting, it was possible to observe the change of absorption with change in the position of the slice in the original specimen.

RESULTS

The ratio of the intensity of the light passing through the specimen, I, to that of the direct beam, I_0, is $I/I_0=(1-r)^2e^{-\mu x}$ where r corresponds to the reflecting power only if the surfaces are perfectly polished, μ the coefficient of absorption, and x the thickness of the specimen in centimeters. If μ is constant and if $(1-r)^2$ is the same for specimens of different thicknesses, then both quantities can be determined. In only one quartz crystal was this true. This piece was cut into eleven slices arranged in the following way. Two thin pieces about 0.05 cm through were cut off, and then one thick piece 0.1 cm through, then two thin pieces and so on until there were three thick pieces altogether and eight thin ones. The slices were cut with their faces perpendicular to the optic axis. Their transmissions were plotted against thickness on a logarithmic scale, and numbered according to their position in the original crystal. It was possible to choose two of the thick pieces in preference to the third for homogeneity from the behavior of their neighboring thin control pieces. All thick pieces were then cut down to 0.02 cm and remeasured. Thus each thick piece gave two values for the transmission for each wave-length. R was determined from each pair of values. The two pieces which appeared to be the most homogeneous from the behavior of the controls gave practically identical results for r. The difference between the two values of r was never greater than 5 percent. Their average is given in column 1 of Table I. The third piece gave values for r which were considerably different, but since the controls had indicated a much greater change in absorption at that particular part of the original crystal these values were discarded.

TABLE I. *Measured absorption coefficients of quartz.*

Wave-length (Å)	r (%)	Maximum absorption coefficient 1st crystal	Minimum absorption coefficient 1st crystal	Maximum absorption coefficient 2nd crystal	Minimum absorption coefficient 2nd crystal	Maximum absorption coefficient fused quartz	Minimum absorption coefficient fused quartz
1633.6	10.7	3.51	0.48	0.191	0.167	10.2	5.5
1613.3	11.0					10.9	6.2
1585.7	11.6	3.98	0.51	0.196	0.172	13.7	7.8
1569.7	12.0					16.6	9.5
1547.1	12.8	5.51	0.82	0.49	0.201	24.1	14.6
1533.2	13.1					37.6	25.8
1523.4	13.5					57.3	44.4
1517.4	13.7	11.05	1.86	2.92	0.70		
1489.3	14.3	26.1	5.06	4.87	2.39		
1473.9	15.7			8.92	5.15		
1462.9	16.2	35.3	18.16	19.40	14.08		

The other piece of crystalline quartz was less transparent and much more inhomogeneous. Eight pieces were cut from it with their faces parallel to the optic axis. In order to give a practical idea of the variation in transmission μ was calculated by using the values of r given by the good crystal. The maximum and minimum values of μ are given in columns 2 and 3 in Table I. F. Zernike[3] has taken some interesting shadow photographs through large quartz prisms and lenses showing the sudden changes in absorption which can be expected in crystalline quartz of the highest quality. There is no indication of this behavior in visible light. Columns 4 and 5 show the maximum and minimum values of μ for the "clearer" crystal.

Both crystals were twinned, with sharp boundaries between the different orientations of the crystal formation. There seemed to be no correlation between the amount of twinning and the inhomogeneity.

The fused quartz was part of a large piece of the best quality which had been poured by the General Electric Company for a lens. Six sections were cut from it. It proved to be very inhomogeneous to ultraviolet light, though showing no signs of inhomogeneity in the visible. The strains in it were not sufficient to be seen by polarized light. The inhomogeneity of the fused quartz destroyed the possibility of determining the true value of r. Therefore the same procedure was adopted as before, namely, using the values of r obtained from the crystalline quartz in calculating μ for the fused specimen. Since Gleason[4] found that fused quartz reflects less light than crystalline quartz this approximation would give a lower value for μ. However, the variations in μ are so great that nothing of practical value is lost by this approximation. Columns 6 and 7 give the maximum and minimum values of μ calculated in this way for fused quartz.

DISCUSSION

The values of r can be compared with those obtained by Gleason.[4] His measurements were made at an angle of 45 degrees and no mention is made of the amount of light reflected from the back surface of the piece of quartz. Assuming no light to have been reflected back from the rear surface, and calculating the reflecting power, r, for normal incidence from his values taken at 45 degrees, we get the following: Gleason's value at 1474A is 10.8 percent while that found here is 15.7 percent; at 1634A his value is 9.36 percent while the present is 10.7 percent. The latter values agree within experimental error, but at shorter wave-lengths there is a distinct increase in my values over his. This discrepancy can be explained by poor polish on one or both specimens. A poor polish in Gleason's specimen would lower the reflecting power while a poor polish on the specimen tested here would raise the value of r. The effect of poor polish would be more pronounced at shorter wave-lengths. However, not much weight can be attached to the

[3] F. Zernike, Physica **8**, 81–7 (1928), No. 2.

[4] P. R. Gleason, Proc. Am. Acad. Sci. **64**, 121 (1930).

apparent agreement at 1634A since the effect of the back surface is not taken into account in Gleason's values of r.

If I_1 is the intensity of the light traversing a crystal with absorption coefficient μ_1 and thickness x, and I_2 the same quantity for a crystal of the same thickness and absorption coefficient μ_2, then the ratio of the intensities is $I_1/I_2 = e^{-(\mu_1-\mu_2)x}$. It is the difference between the values of the absorption coefficients which is significant in determining this ratio. In the first crystal $\mu_{(max)}-\mu_{(min)}$ is 21 at 1489A. This is the most marked case of inhomogeneity. At longer wave-lengths this difference is always less, and at 1633A for the second or clearest crystal it is as low as 0.024. In fused quartz this difference never gets below 4.7. These extraordinary variations in μ show the importance of actually testing a piece of quartz in the ultraviolet before incorporating it in an instrument for use in that region of the spectrum.

There is no doubt that the values of r obtained for quartz indicate a better condition of the surface than in the case of fluorite. Because of its greater hardness quartz should take a better polish than fluorite. Furthermore the quartz surfaces are much more rugged and insensitive to abrasives which appear to destroy a fine polish on fluorite.

Experiments are now under way to make simultaneous measurements of transmission and reflecting power directly.

Magnetic Susceptibilities of Dilute Solid Solutions of Nickel in Copper at Various Temperatures

WILLIAM H. ROSS,* *Sloane Physics Laboratory, Yale University*

(Received May 7, 1934)

New data on the magnetic susceptibilities of the low nickel content end of the nickel-copper alloy series present two main features. At low temperatures an approximation to the usual Curie-Weiss decrease in χ with increasing T is established, while above room temperature there is an abnormal paramagnetism, χ increasing with increasing T. The variations are continuous with respect to both concentration and temperature. Certain assumptions applied to the Curie-Weiss part of the curves lead to a magnetic moment per Ni atom in the lattice of 0.3 to 0.4 Bohr magnetons.

INTRODUCTION

NICKEL and copper have face-centered cubic crystals with nearly equal lattice constants. The two elements form a complete series of solid solutions. Since pure copper is diamagnetic the series seems ideal for studies on the magnetic moment per atom of nickel and also on the various interactions which modify susceptibility. Previous studies,[1] all of which extend to high nickel content, do not give precise information regarding the low percentage nickel alloys. For dilute solutions the expected variations with concentration and temperature are small, requiring sensitivity of such order as is used for the study of the noble metals.

APPARATUS

A Weiss-Foëx pendulum offers sufficient sensitivity. A light balsa wood beam is suspended by fine copper wires. At one end of the beam is the specimen, located at maximum HdH/dx. The force on the specimen due to the field is just balanced by that between currents in two small concentric coils, one attached to the far end of the beam and the other stationary. Motion of the beam from the null position causes a mirror, reflecting the image of an illuminated cross-hair on a distant scale, to rotate about a vertically stretched quartz fiber. Necessary data consist in

* Part of a Dissertation presented to the Faculty of the Graduate School of Yale University in Candidacy for the Degree of Doctor of Philosophy.

[1] E. H. Williams, Phys. Rev. [2] **38**, 828 (1931). R. Gans and A. Fonseca, Ann. d. Physik [4] **61**, 742 (1920). M. Alder, Thesis, Zürich (1916).

the current readings for the specimen, for the holder, and for a suitable standard. A resistance furnace heating to 600°C, or a double-walled liquid-air container, fitted into the gap (with centers at maximum HdH/dx) without moving the pole pieces. Both high and low temperature runs were made in flowing hydrogen.

The method being comparative, a gold cylinder which showed no temperature variation of χ from 20 to 600°C, was chosen as a standard. The average of Vogt's recent values,[2] 144.7 $\times(10)^{-9}$ for gold relative to air, was accepted.

Specimens

The alloys were cast from electrolytically deposited nickel and copper. The melting was done in quartz tubing in a wire-wound vacuum furnace. The operation was performed in flowing hydrogen, the pressure being reduced to a few millimeters as the samples were slowly cooled through the solidifying point and down to room temperature. Aside from two definitely polycrystalline specimens, the cylinders (5 mm diameter, 10 mm length) showed the etched surface lines of single crystals. Since the loss in weight in preparation was negligible, the 9.75 atomic percent alloy excepted, the percentage composition of the specimens was taken from the synthesis. For field strengths from 6000 to 14,500 gauss no specimen showed a variation in χ as great as $1\times(10)^{-9}$.

Results

The numerical values in Table I can best be discussed in connection with Fig. 1. All curves for high temperature show the equivalent of an abnormal increase in paramagnetism with increasing temperature. The curves for 9.75 and 8.35 atomic percent nickel show a decided minimum, and from room temperature down to that of liquid air there is rough agreement with the usual Curie-Weiss Law. This led to attempts to plot values of $1/\chi$ against T. The results were far from linear at high temperature. The asymptotes to the $\chi-T$ curves were then drawn and a quantity, $\Delta\chi$, was obtained by subtracting the ordinate of the asymptote from the ordinate of the curve at the same abscissa. Values of the reciprocal, $1/\Delta\chi$, when plotted against temperature gave a straight line from 90 to 900°K. Interpreting this as a permanent moment to be attributed to the Ni present, the values of the magnetic moment per Ni atom calculated were 0.40_5, 0.36_6, and 0.2_8 Bohr Magnetons from the 9.75, 8.35, and 5.48 atomic percent specimens, respectively.

Fractional Moments per Ni Atom

At the ferromagnetic end fractional values of the magnetic moment per Ni atom have already received treatment by Stoner.[3] While it should be emphasized that the effects measured in the present experiment would be hopelessly masked by any actual ferromagnetism, certain of Stoner's considerations may apply. Eighteen electrons are considered to be in closed shells, eight electrons to be in d-orbits, and two electrons to belong to the metal as a whole. In normal interaction the d-electrons pair off with the spins anti-parallel. This tendency is opposed, however,

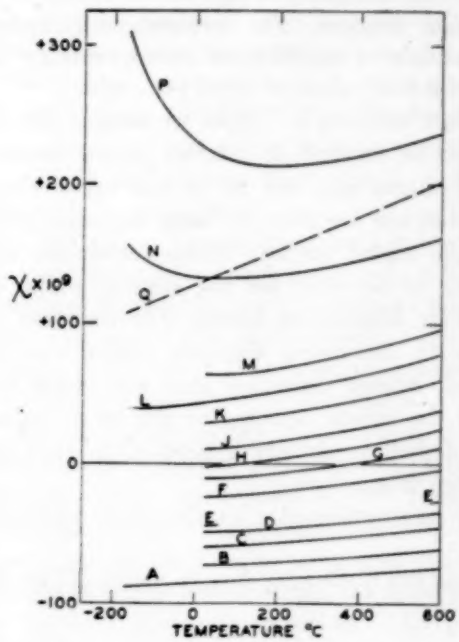

FIG. 1. Mass susceptibility vs. temperature. Letters on curves refer to Table I.

[2] E. Vogt, Ann. d. Physik [5] **14**, 1 (1932). H. J. Seemann and E. Vogt, Ann. d. Physik [5] **2**, 976 (1929).

[3] E. C. Stoner, Phil. Mag. [7] **15**, 1018 (1933). E. C. Stoner, Proc. Leeds Phil. Soc. **2**, 391 (1933).

TABLE I. *Mass susceptibilities relative to vacuum.* Column "dev." indicates the mean deviation for all values where a specimen was completely removed and replaced several times. The high temperature values were taken from smooth curves drawn through the points, these not lying on even temperatures. In some cases the value at 600°C is an extrapolation.

No.	Mass g	Wt.% Ni	At.% Ni	Susceptibility $\times(10)^6$ 22°C	dev.	−183°	200°	400°	600°	Curve
M2	5.355	0.00	0.00	−85.8	0.5	−88.8	−83.2	−79.5	−75.6	*A*
M4	5.633	0.00	0.00	85.6	0.3	—	—	—	—	—
S1	6.012	0.51	0.55	72.6	0.3	—	70.6	66.7	61.5	*B*
T2	5.560	1.01	1.09	60.5	—	—	57.0	51.8	46.0	*C*
M3	5.407	1.42	1.54	49.9	—	—	46.9	41.2	33.7	*D*
B3	6.403	1.62	1.75	45.2	—	—	—	—	27.4	*E*
T3	5.643	2.48	2.68	24.8	0.4	—	19.2	−12.2	−3.8	*F*
S2	6.261	3.04	3.29	10.3	—	—	−5.5	+2.5	+12.0	*G*
T1	5.248	3.38	3.66	−1.8	—	—	+3.5	13.0	24.9	*H*
B2	5.207	3.84	4.16	+10.0	—	—	17.2	26.3	40.0	*J*
M1	5.838	4.56	4.84	28.5	0.1	—	36.2	47.1	60.6	*K*
B1	6.493	5.06	5.48	42.5	0.7	+38.9	50.5	63.1	78.2	*L*
Asymptote						8.5			72.0	
—	—	—	—	—	—	—	—	—	—	
SI	4.161	5.45φ	5.91	62.8	0.5	—	67.5	80.2	95.2	*M*
SII	4.329	7.72φ	8.35	132.5	1.2	157.0	135.5	144.1	164.0	*N*
Asymptote						59.5			142.0	
SIII	2.013	9.05*	9.75	222.8	—	311.8	212.5	220.5	236.5	*P*
Asymptote						106.0			202.5	*Q*

φ indicates a polycrystalline specimen.
* 9.08 percent by analysis, 9.02 percent at synthesis.

in the uncompleted shell, by one for parallel settings due to the lower potential energy resulting from the positive sign of the Heisenberg interaction integral. For ferromagnetic nickel the condition of equilibrium corresponds to an excess of 0.6 unbalanced spins per atom.

In dilute solution in copper we assume the Ni atoms to be located at random in the lattice. The Ni atoms are not all in the same sized aggregates, nor are they the same distance apart as in the nickel lattice. These conditions are sufficient to account for the smaller value of 0.40_5 Bohr Magnetons found. The decrease in value with increasing dilution might also be expected. Stoner estimates that for nickel the ratio of the atomic spacing to the mean radius of the *d*-shell is already greater than that for maximum interaction.

Vogt[4] has published a similar study of dilute solutions of nickel in gold. His curves for low temperature are similar to those of Fig. 1, and yield fractional values for the magnetic moment that are still smaller than those of the present work. (Gold has a larger lattice constant than copper, just as copper has than nickel.) He also finds a tendency toward decreasing moment with increasing dilution.

HIGH TEMPERATURE EFFECTS

Vogt's work was not carried above room temperature since the $\chi - T$ curves were already horizontal. This may be significant in connection with the anomalous paramagnetism of the present alloys at high temperature. Pure gold is one of the few elements with constant susceptibility over all ranges of temperature.[5] Pure copper has a decreasing diamagnetism from 17 to 1000°K, and the alloys have larger and larger decreases in diamagnetism, or the equivalent—increases in paramagnetism.

A change in susceptibility of the order of $10\times(10)^{-9}$ per 100°C change in temperature may be accounted for by almost any variation. The number of paramagnetic carriers may increase, Cu^{++} being paramagnetic. The magnetic moment of the nickel may vary since the interatomic distance varies. The effect may be a decrease in underlying crystal diamagnetism. The conductivity changes rather rapidly with the addition of nickel and this may help in deciding between hypotheses. Comparison with Vogt's results merely indicates that conditions in copper are not entirely abnormal.

In performing the present experiment the apparatus was set up in a constant temperature room and controlled from outside, partly to avoid tremors. Thanks are due to those working in the Sloane Physics Laboratory for cooperation in minimizing vibration, and to Professor McKeehan in particular for suggesting the problem and for subsequent advice.

[4] E. Vogt and H. Krueger, Ann. d. Physik [5] **18**, 755 (1933).

[5] W. J. de Haas and P. M. van Alphen, Proc. K. Ak. van Weten. Amster. **36**, 263 (1933).

Arcs in Inert Gases.* II

G. E. Doan† and A. M. Thorne,‡ *Lehigh University*

(Received May 3, 1934)

Arcs in *pure* inert gases between electrodes of pure metals have been found impossible to maintain under ordinary conditions, whereas they are easy to maintain if the gas is slightly contaminated. (1) For highly purified iron in argon, helium and neon, and highly purified silver and zinc in argon, the arc discharge is inherently unstable. The cathode spot darts rapidly up and down the electrode, and finally goes out at values of open circuit voltage, short circuit current, pressure of the arc atmosphere, and electrode separation at which a stable arc is ordinarily obtained when slightly less pure elements are used. We conclude, therefore, that the degree of purity of the elements of metallic arcs in inert gases, and particularly the degree of purity of the gas, determines the boundaries within which stable arcing may occur. Further, for elements of a high degree of purity the boundary values of the region of unstable operation are quite definite and readily determinable experimentally; beyond these boundaries much more stable arcs are encountered. (2) The extinction of an unstable arc is not characterized by any marked change in the current or voltage of the arc at the instant immediately preceding extinction. (3) Higher purity of the electrode material and of the inert atmosphere appears to move the voltage *versus* current curve in the direction of higher voltage.

Introduction

A PREVIOUS investigation[1, 2] revealed the impossibility of obtaining a stable, low current arc discharge between pure iron electrodes in a pure argon gas atmosphere. The arc was found to go out spontaneously. In the present paper certain of the boundary conditions of this previously observed phenomenon are reported, and in addition the phenomenon is found to extend also to silver and zinc arcs in argon, and to iron arcs in helium and neon.

The boundary conditions reported are the limiting values of three parameters: open circuit voltage, electrode separation, and pressure of the arc atmosphere—limiting in that they could not be exceeded without the authors' obtaining an arc which persisted for *at least five seconds. Such an arc the authors have arbitrarily classed as "stable."*

Purity of the Materials. Apparatus Details

The purest obtainable metals and gases were used for the tests. The iron was supplied by the magnetic testing division of the Westinghouse Company, and was guaranteed to have an oxygen content of less than 0.01 percent in addition to being particularly free from solid inclusions. The silver was obtained from Handy and Harmon of Bridgeport, and was declared to be 99.999 percent pure silver. Nothing was known of its gas content as received, but it was vacuum baked at about 600°C before use. The zinc was furnished by the New Jersey Zinc Company, and was stated to be spectroscopically pure. It too, however, was vacuum baked at 360°C before use in the experiments.

The argon was supplied in high pressure cylinders by the Cleveland Wire Works of Nela Park, Ohio, and was stated to have an impurity content of not greater than thirty parts per million, but before final use it was purified as described below. The neon and helium used were the spectroscopically pure grade which the Air Reduction Sales Corporation supplies sealed in glass, and were used as received. (The neon actually contained 0.8 percent of helium, but was otherwise spectroscopically pure.)

Two refinements of the apparatus used in the previous investigation consisted in adding a mercury vapor pump behind the rotary oil pump and in inserting a liquid air trap in the vacuum line at the inlet to the arcing chamber.

In the previous investigation the glass system was torched during evacuation. The present authors attempted to extend this precautionary measure by providing for the baking out of the arcing chamber as a whole, and the chamber design they finally adopted is shown to scale in

* Communicated by Karl T. Compton.
† Associate Professor of Physical Metallurgy.
‡ Research Fellow.
[1] Doan and Myer, Phys. Rev. **40**, 36–39 (1932).
[2] Doan and Myer, Elect. Eng. September, 1932.

Fig. 1. Unfortunately, the baking operation had to be dispensed with, for it was found that it could not be carried out, even under vacuum, without its producing on the freshly cleaned electrodes a thin film, apparently of oxide. The authors assume that the film was produced by active gases thrown off the glass walls or other parts during the baking. In the tests the arc was never run so long that the walls became hot enough to give off gas, and the electrodes were never found to have developed an oxide film.

The misch metal arc shown attached to the arc chamber proper (Fig. 1) constitutes the scavenger eventually adopted. It was used, however, only for the argon tests. The solenoid pick-up used to move the anode assembly was another refinement adopted in the present work.

The duration of a discharge was measured with a stopwatch, and the five second criterion for stability was selected in part because arcs of much longer duration melted the electrode tips. The possibility of melting also caused the authors to fix ten amperes as the maximum current to be used.

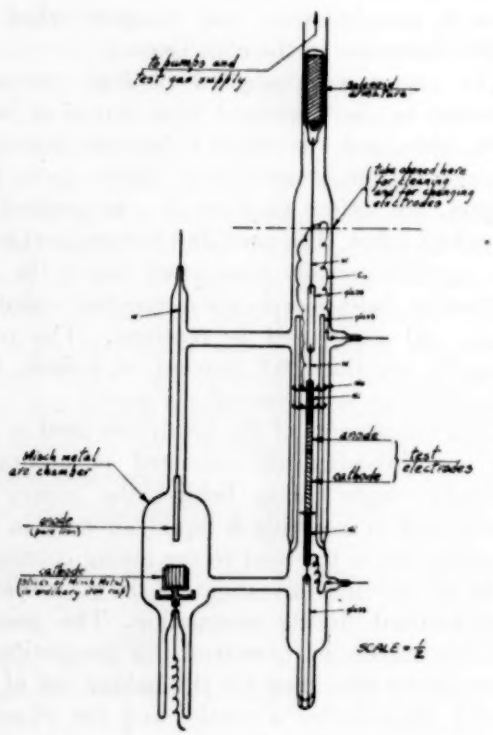

FIG. 1. Arcing chamber and misch metal arc chamber.

The measuring circuit followed the conventional arrangement, and the variable voltage source and series resistance enabled either open circuit or short circuit current to be held constant while the other was being varied. The vacuum pump and adjustable solenoid provided for variation of the other two parameters—the arc atmosphere and electrode separation, respectively.

Observations and Results

The general character of the unstable arcing effect was described in references (1) and (2). A similar description fits the present arcing effects. Thus, during the five second interval immediately following the strike the unstable arc would vary its length by several hundred percent as the cathode spot darted up and down the side of the electrode, and then suddenly would go out.

Only for iron electrodes were all three parameters varied independently in each of the three gases, A, He and Ne. The maximum possible values of voltage and current for unstable arcing (which are, of course, also the minimum required values for stable arcing) are shown in Figs. 2 and 3.

Fig. 2 shows the effect of varying the pressure of the arc atmosphere. The effect is small in argon and also in neon so long as the discharge remains that of an arc. At 19 cm in neon, however, the discharge becomes a glow, and the minimum required open circuit voltage for stable arcing at once increases by a factor of more than two. All of the helium curves represent a glow type of discharge and the minimum re-

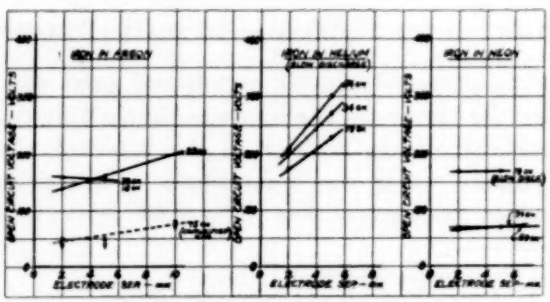

FIG. 2. Minimum open circuit voltage required for stable arcing; effect of pressure of arc atmosphere. (Short circuit current = 3.0 amperes.)

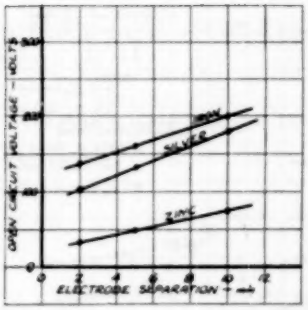

FIG. 3. Minimum open circuit voltage required for stable arcing; variation with electrode material. Gas = argon, pressure = atmospheric, short circuit cur. = 3.0 amp.

quired voltage for stability is seen to increase with the pressure.

The argon curves also show the effect of contamination in the atmosphere of the arc. For unpurified argon the minimum required open circuit voltage is only about one-third that required for purified gas.

Fig. 3 shows the variation of open circuit voltage requirements with electrode material. Zinc is seen to yield a stable arc at much lower open circuit voltages than will iron and the requirements for silver lie intermediate between those for the other two.

The current boundary of stable arcing was studied up to 8.5 amperes short circuit current, but the measurements are not yet completed.

OSCILLOGRAMS AND MOTION PICTURES

In exploring the cause of extinction some twenty-two oscillograms were taken. Fig. 4 shows the initial strike between pure iron electrodes in a slightly impure argon atmosphere—it represents a stable arc. Iridescent oxide colors appeared about the cathode tip for several millimeters below the usual sputtered region indicating that an oxide film had formed during the discharge, and showing that the gas was impure. Twenty subsequent strikes were made with these electrodes in the same atmosphere, the first four lasting more than 20 seconds, and all lasting longer than 7 seconds with an average around 15 seconds.

Fig. 5 shows the seventy-first strike in a system which was scavenged by the misch metal arc. The strike is seen to have lasted only about

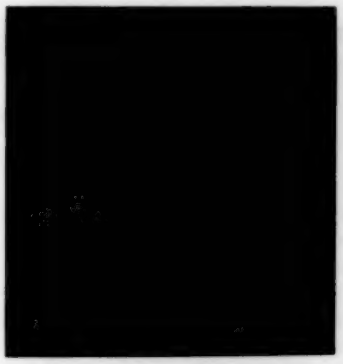

FIG. 4. Initial strike—pure Fe electrodes in unscavenged A. Stable arc.

1.1 seconds, with the final break occurring very suddenly and at very high speed. The zero of voltage (E_{sc}) and short circuit current (I_{sc}) were not drawn separately in this film, but were about where the arrows indicate.

Sufficient of the 60 cycle trace shows at the lower right for the time of the discharge to be calculated. This trace shows particularly well the rapid and random variations of current and voltage in the unstable arc, and the extremely rapid and sudden final break of the arc.

Motion pictures of the typical arc recorded in Fig. 5 were taken also in the hope of correlating the wandering of the cathode spot down the side of the electrode with voltage and current changes in the arc. The motion picture camera was, however, of only standard speed, and not nearly fast enough to record the rapid fluctuations in arc length as the cathode spot wandered. Three successive pictures on the film were found, however, which caught the arc immediately before and immediately after the cathode spot had wandered way down the side of the cathode, and Fig. 6 gives some idea of the long arcs which this erratic wandering sometimes involved.

FIG. 5. Seventy-first strike—unstable arc.

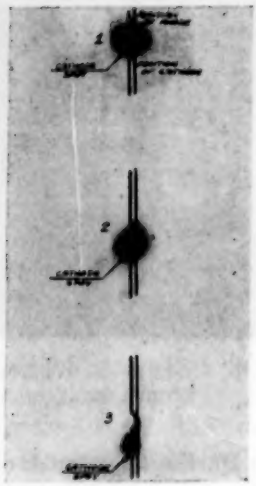

FIG. 6. Successive standard speed motion pictures of an unstable arc. Arc struck in same system as that for arc of Fig. 5—arc is seen to be lengthening at cathode end.

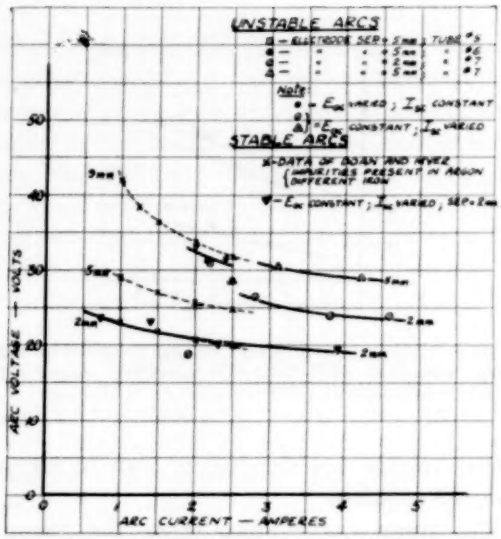

FIG. 7. Static characteristics of stable and unstable arcs; effect of impurities in the gas. Pure iron in argon, atmospheric pressure.

Further examination of Fig. 5 shows that the *minimum* values of arc voltage and maximum values of arc current lie on straight lines which are parallel with the "zero lines." It seemed logical to assume this minimum voltage (and maximum current) condition to be that obtaining when the arc was as short as possible, that is, when the cathode spot was on the tip of the cathode rather than somewhere down its side. (The anode end of the discharge always emanated from the tip of the electrode and, accordingly, need not be mentioned in considerations of arc length. The latter is always taken as the luminous path to the cathode spot.) Adopting this assumption we have at once an accurate method of locating the *E versus I* curve for arcs which last even only a fraction of a second, and which, therefore, could not be observed on dead beat instruments.

This method of locating the *E versus I* curve looked so promising that it was decided to use it to check the *E versus I* curves determined in reference 2 for pure iron in slightly impure argon in which investigation it had been necessary to use dead beat instruments and two observers. For the attempted confirmation the present authors used argon from the tank, that is, without scavenging it, and oscillograms taken at 2 mm separation. Four different short circuit currents yielded the static characteristic shown by solid inverted triangles in Fig. 7. The close check of this curve with the data of the previous investigation is somewhat surprising since the iron of the electrodes used this time was distinctly different from that used previously, having been prepared by a different company under a different process, and known to have only 0.01 percent of oxygen whereas the electrodes used previously contained some 0.07 percent of oxygen. Apparently, the condition of importance for non-arcing is the purity of the inert gas; the purity of the electrodes seems to be relatively unimportant.

Three oscillograms of unstable pure iron arcs in scavenged argon for 5 mm electrode separations were taken and eight for 2 mm separations. On calibrating the oscillograms of these unstable arcs and plotting their traces as static characteristics (see Fig. 7) we find the characteristics located at definitely higher voltages than the corresponding curves for stable arcs.

The Mean Life of the 7^3S_1 State of Mercury from Polarization Measurements on the Visible Triplet

ALLAN C. G. MITCHELL AND EDGAR J. MURPHY, *New York University, University Heights*

(Received May 7, 1934)

Fluorescence of the visible triplet lines of mercury (4047, 4358, 5461) was obtained by exciting a mixture of mercury vapor and a small amount of nitrogen by radiation from a quartz mercury arc. The fluorescence was observed at right angles to the exciting light beam and the polarization of each line, isolated by suitable filters, was measured by the method of crossed Wollaston prisms. Measurements in zero magnetic field (polarized excitation) gave 88.2 percent for 4047, −65.5 for 4358, and 14.55 for 5461, compared to theoretical values (broad line excitation) of 84.7, −67.0, and 8.7 percent, respectively. Measurements were then made of the polarization as a function of a magnetic field applied in the observation direction and the mean life of the 7^3S_1 state calculated from the data. The mean life of this state as measured by 4047 and 4358 was $0.8\pm0.1\times10^{-8}$ sec. at about 3.0 mm nitrogen pressure. The mean life as measured by the line 5461 was about $0.6\pm0.1\times10^{-8}$ sec. The collision cross section for the 7^3S_1 state against nitrogen was measured by measuring the polarization of 4358 at a field of 3 gauss and varying nitrogen pressures, giving the result $\sigma_q^3=1.3\times10^{-16}\,\text{cm}^2$.

INTRODUCTION

SEVERAL attempts have been made to measure the mean life of the 7^3S_1 state of mercury by various methods. This state gives rise to the lines of the visible triplet (4047, 4358 and 5461) and experiments have been performed on the three lines which give a measure of the mean life of the 7^3S_1 state. One would expect theoretically that, as a result of measurements on each of the three lines, the value obtained for the mean life of the upper state should be a constant and not depend on the line used for the measurement. In two experiments which have been performed to date, the results have not been in agreement with the expectation. For example, Randall,[1] using a resonance lamp with electrical cut-off, found the mean life of the 7^3S_1 state to be 5.75×10^{-8} sec., when measured by 4047 and 4358, and 2.37×10^{-7} sec. when measured by 5461. A similar result was found by Richter,[2] who measured the polarization of the three lines obtained as fluorescence when a mixture of mercury vapor and nitrogen was irradiated by light from a mercury arc. By measuring the rotation of the plane of polarization of each line caused by the application of a small magnetic field in the direction of observation Richter calculated the following values of τ as measured by the three lines: from 4047, 0.5×10^{-8} sec.; from 4358, 0.6×10^{-8} sec.; and from 5461, 2.2×10^{-8} sec. Mitchell[3] has pointed out certain mistakes in Richter's calculations mainly arising from erroneous theoretical considerations. Since neither Richter nor Randall obtained results that could be accounted for on the basis of any reasonable theoretical assumptions and since the authors felt that improvements on Richter's method could be made, they undertook the following investigation.

APPARATUS AND METHOD OF MEASUREMENT

The method used is similar to that of Richter and consists of optically exciting mercury vapor in the presence of a few millimeters of nitrogen with light from a quartz mercury arc lamp. Mercury atoms in a resonance tube absorb the line 2537 from the arc, thereby reaching the 6^3P_1 state. On collision with nitrogen molecules some mercury atoms are transferred to the 6^3P_0 state from which they may reach the 7^3S_1 state by absorption of the line 4047 from the arc. The fluorescence of the visible triplet occurs when mercury atoms in the 7^3S_1 state revert to the $6^3P_{0,1,2}$ states. If the direction of observation of the fluorescence is at right angles to that of the exciting beam, and if the resonance tube is situated in a region of zero magnetic field, the fluorescence lines will be polarized. The applica-

[1] R. H. Randall, Phys. Rev. **35**, 1161 (1930).
[2] E. F. Richter, Ann. d. Physik **7**, 293 (1930); **17**, 463 (1933).
[3] A. C. G. Mitchell, Phys. Rev. **43**, 887 (1933). Hereafter referred to as II.

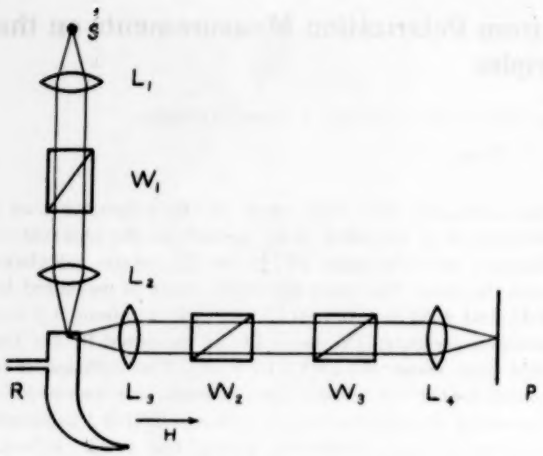

FIG. 1. Diagram of apparatus.

tion of small magnetic fields, applied in the direction of observation, will cause the polarization of the lines to decrease. From these measurements the mean life of the 7^3S_1 state can be calculated.

The light from a water-cooled and magnetically deflected quartz-mercury arc (Fig. 1) was made parallel by the lens L_1 and passed through the Wollaston prism W_1, which was transparent to wave-lengths greater than 2200. The two polarized images of the source were focussed on the resonance tube R, which was surrounded by a shield by means of which one image could be cut out. The resonance tube was made of glass and had a fused quartz window cemented to the front end with picein wax. An all quartz tube could not be used since quartz fluoresces in the blue-green when irradiated with ultraviolet light. The fluorescence light, escaping from a square hole in the shield (about 1 mm on each side), was made parallel by the lens L_3 and sent through the two Wollaston prisms W_2 and W_3. The prism W_2 was fixed while W_3 could be rotated so that its axis could make any desired angle with that of W_2, and the angle could be read to 1 minute with a scale and vernier. The polarized images of the hole were then brought to a focus on the photographic plate P. The various lines were isolated by means of filters[4] placed at the lens L_4. All lenses were of fused quartz.

A large Helmholtz coil placed about the apparatus served to neutralize the earth's field to less than 0.01 gauss. A smaller Helmholtz coil, placed with its axis along the direction of observation, was used to apply known magnetic fields to the resonance tube. This coil was calibrated by the standard inductance method with the help of a Brooks inductometer, so that the field produced by a given current flowing through the coil was known to 0.5 percent.

The nitrogen used in the experiment, made by heating NaN_3, was stored in a flask over metallic sodium. Any desired pressure of nitrogen could be admitted to the apparatus by means of stopcocks. Pressures were read on a McLeod gauge. The pressure of mercury vapor in the apparatus corresponded to the vapor pressure of mercury at room temperature.

The determination of the degree of polarization of any line under given experimental conditions was made photographically by taking four or five exposures and varying the angle made by the Wollaston prism W_3 with respect to W_2 for each exposure. At a certain angle α, two of the images will be of equal intensity, for which conditions the polarization is given by $P = -\cos 2\alpha$. The approximate positions for equal angles was found by taking exposures at angular settings differing by several degrees and examining the plates visually. In the final measurements exposures were made at angle settings one degree apart and the plates run through a recording microphotometer. On the resulting tracing the heights of the two peaks corresponding to the two images were measured. Calling these two heights a and b, a curve was drawn in which $(a-b)/(a+b)$ was plotted against the angle setting, and the position of equal images determined from the curve. Only exposures taken on one plate were used for the determination of a given angle. The zero position of the two Wollastons, i.e., the angle reading for which the principal planes of the two prisms were parallel, was determined to within 5 minutes of arc.

In the determination of the degree of polarization the time of exposure varied from thirty minutes to two and a half hours depending on the

[4] The filters used for the lines were: For 5461, Corning filters No. 351, 2 mm thick and No. 512, 4.39 mm thick; for 4358, Corning filters No. 038, 2.55 mm thick and No. 585, 4.52 mm thick; for 4047, Corning filters No. 585, 4.52 mm thick and No. 305, 3.62 mm thick together with 3 cm of a solution of 2.5 g I_2 in 500 cc CCl_4. For a discussion of these filters see E. J. Bowen, J. Chem. Soc. 2236 (1932).

line being measured, the pressure of nitrogen, and the strength of the depolarizing magnetic field. Frequent exposures were made to test for the presence of scattered light by placing a glass plate between the exciting light source and the resonance tube. Plates showing any trace of scattered light were, of course, discarded.

In all experiments the current through the arc lamp and that through the magnet used to deflect the arc stream was kept constant. The temperature of the water used to cool the arc was measured as it left the cooling chamber and arrangements were made to keep this temperature fairly constant to within about two degrees. Later experiments showed, however, that variations of the temperature of the cooling water from 15°C to 25°C had no measurable effect on the degree of polarization obtained.

Polarization in Zero Field

With a pressure of 3 mm of nitrogen in the resonance tube, the degree of polarization of the three lines was measured in zero magnetic field. For the lines 4358 and 5461 the exciting light was polarized with electric vector vertical while for 4047, on account of the low intensity of this line, unpolarized exciting light was used. The values of the degree of polarization for the line 4047, obtained with unpolarized light, were placed on a basis for comparison with the other lines, which were obtained using polarized excitation, by employing the well-known relation $\bar{P}_0=P_0/(2-P_0)$, in which $\bar{P}_0$ is the degree of polarization measured with unpolarized exciting light and P_0, that to be expected if the exciting light is polarized with electric vector vertical. The values of the percentage polarization in zero field using polarized excitation (P_0) for the three lines are given in Table I. The theoretical values of the percentage polarization calculated from the known hyperfine structure are given in column 3 of the table. The minus sign before the value for the line 4358 denotes that this line is polarized with its electric vector at right angles to that of the exciting beam.

Table I. *Percentage polarization in zero field with polarized excitation.*

Line	*Polarization (percent) P_0* Measured	calculated With hfs	Without hfs	Mean life 7^3S_1 state (sec.)
4047	88.3 ±0.1	84.7	100	0.8×10^{-8}
4358	−65.7 ±0.9	−67.0	−100	0.8×10^{-8}
5461	14.57±0.16	8.6	14.3	0.6×10^{-8}

Polarization in Applied Magnetic Fields

With a nitrogen pressure of 3 mm in the resonance tube the polarization of each line was measured when a magnetic field was applied in the direction of observation. Measurements made for various values of the intensity of magnetic field up to 5 gauss are shown in Fig. 2, in which the percentage polarization $P(H)$ is plotted against the intensity of the magnetic field. In the figure the experimental data are given by the circles (4047), triangles (4358), and squares (5461), while the curves are theoretical ones whose significance will be discussed later. In making the measurements of the percentage polarization in applied fields the same procedure was adopted as in those made in zero field. In order to be sure that no fluctuations in the arc lamp were occurring which might change the value of the percentage polarization obtained, a test exposure was made on every plate. This was accomplished by taking an exposure in zero applied field with the Wollaston set at an angle α for which images of equal intensity had been obtained for the previous experiments in zero field. In the series of experiments represented by the points in Fig. 2, no significant variation in the zero field polarization was observed.

As in the case of the zero field measurements, the results for the line 4047 were obtained using unpolarized excitation. The points shown in Fig. 2 were obtained by computing the degree of

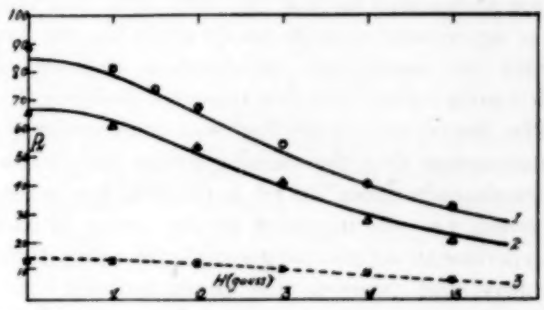

Fig. 2. Percentage polarization as a function of magnetic field. Circles, 4047; triangles, 4358; squares 5461.

polarization which would have occurred had polarized excitation been used. The method of computation given by Breit[5] consisted in multiplying the observed polarization $\bar{P}(H)$, obtained with unpolarized excitation, by $(2-P_0)$ where P_0 is the polarization in zero field obtained from the experimental values given in Table I.

Finally, experiments were performed to show the effect of nitrogen pressure on the degree of polarization. With a magnetic field of 3 gauss applied to the resonance tube, the degree of polarization of the 4358 line was measured at several nitrogen pressures. The results are given in column 2 of Table II. It will be noted that, at

TABLE II. *Percent polarization of the 4358 line at various nitrogen pressures.* H = 3 gauss.

N_2 Pressure in mm Hg	Polarization percent $P(H, p)$ Line 4358	$\frac{1}{f(\bar{P})}$
2.50	40.19	1.261
3.20	41.20	1.302
3.95	43.35 42.26 } 42.81	1.368

constant magnetic field, the degree of polarization increased with increasing nitrogen pressure, in agreement with similar experiments performed by Richter. Other experiments showed that the degree of polarization in zero field was independent of the nitrogen pressure over the range examined.

Discussion of Results

(a) The zero field polarization

A comparison of the percentage polarization obtained with that to be expected from the known hyperfine structure of the lines in question shows that for the two lines 4047 and 4358 the agreement is quite good, while for the line 5461 the percentage polarization observed is definitely higher than that expected theoretically. The theoretical calculation[3] was made under the assumption that the exciting source had "broad line characteristics" as far as the 4047 line is concerned, i.e., the intensity at the center of each hyperfine structure component is the same. If the source had "narrow line characteristics" (i.e., the intensity of each component is that which would be given by a source entirely free from self-absorption), the degree of polarization expected should have been much higher.

The high polarization of the 5461 line is not understood at present. Since the 4047 line is the only line absorbed to any appreciable extent by the mercury vapor in the resonance tube, and since the fluorescent lines 4047 and 4358 do not show a degree of polarization too high to be accounted for on the basis of a broad line source, it is probable that the characteristics of the source cannot account for the result obtained in the case of 5461.

The apparatus was carefully checked to be sure that no systematic error of measurement could be operative in making the observed polarization too high. With this object in view the zero position of the two Wollaston prisms was rechecked using the fluorescent line 5461, depolarized by a magnetic field of 20 gauss, as a source, and the results were in agreement with those previously obtained. The resonance tube was observed between crossed Nicol prisms to see if strains might be causing erroneous results, but no strains were found.

It is conceivable that the fluorescence radiation is partially absorbed in getting out of the resonance tube and that this might account for the observed results. The light path through the vapor in our apparatus was less than 5 mm, and a calculation made with the help of the data of Pool and Simmons[6] on the absorption coefficient of the various hyperfine structure components of the 4047 line shows that no appreciable effect can arise from this source.

(b) The mean life of the 7^3S_1 state

The mean life of the 7^3S_1 state may be obtained from curves of the polarization $P(H)$ against the magnetic field as shown in Fig. 2. Provided such a series of points is at hand the mean life may be obtained by fitting the data to the theoretical curve

$$P(H)=\sum_{\alpha}\sum_{\varphi}\frac{P_0(\varphi\alpha)}{1+[(eH/mc)g_{\varphi}(\alpha)\tau]^2}. \qquad (1)$$

[5] G. Breit, Rev. Mod. Phys. **5**, 91 (1933), see p. 124.

[6] M. L. Pool and S. J. Simmons, Phys. Rev. **44**, 997 (1933).

The use of this method has been discussed in detail in II. Curves 1 and 2 of Fig. 2 were obtained from Eq. (1) using the hyperfine structure values of $P_0(\varphi\alpha)$, the correct values of $g_\varphi(\alpha)$ for the various hyperfine states of 7^3S_1 and a value of $\tau=0.8\times10^{-8}$ sec. Curve 3 was obtained using $\tau=0.6\times10^{-8}$ sec. and not taking into account hyperfine structure.

It was pointed out in II that, while P_0 is quite sensitive to the hyperfine structure of the line in question and also to the nature of the source, the value of the mean life obtained from a curve of $P(H)$ against P_0 is quite insensitive to these factors. This is especially true in the case of mercury where most of the light comes from the isotopes of even atomic weight. If, now, $P(H)/P_0$ is plotted against H discrepancies in the values of P_0 cancel out and a value of τ can be obtained. Fig. 3 shows curves of $P(H)/P_0$ against H for the line 4047. Curves 1, 2 and 3 are drawn for mean lives of 0.7, 0.8 and 0.9×10^{-8}, respectively, under the assumption that there is no hyperfine structure. The dotted curve is obtained when hyperfine structure is considered for the mean life $\tau=0.8\times10^{-8}$ sec. With this method of calculation the mean life of the 7^3S_1 state, obtained from the observations on the three lines 4047, 4358 and 5461, measured at a nitrogen pressure of 3 mm, is 0.8×10^{-8}, 0.8×10^{-8} and 0.6×10^{-8} sec., respectively, to within about 10 percent.

The results for the mean life of the 7^3S_1 state seem to be the same whether measured by the line 4047 or 4358. The value for the mean life obtained from the measurements on the 5461 line appears to be smaller than that measured by the other two lines by about 25 percent. This discrepancy would seem to lie outside of the experimental error of this investigation. The discrepancy is, however, not very great and in view of the anomalous value obtained for the percentage polarization of 5461 in zero field, the three results for the mean life may be considered to be essentially the same. There is no evidence from this investigation that the mean life as measured by 5461 is four times as large as that measured by the other two lines, as has been reported in the other two investigations.

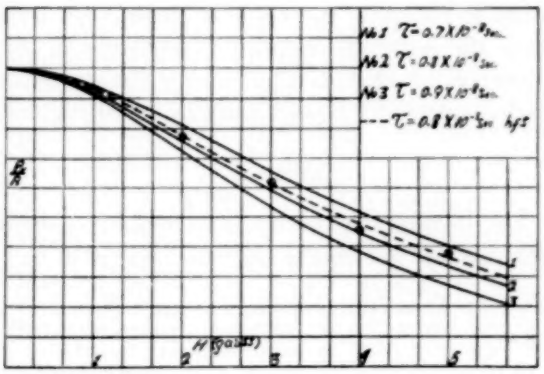

FIG. 3. $P(H)/P_0$ as a function of magnetic field.

(c) The effect of nitrogen on observed values of $P(H)$. Collision cross section

It was found in the above experiments that $P(H)$ at a given value of the magnetic field increases with increasing nitrogen pressure. This may be explained by letting the mercury atom in the 7^3S_1 state be represented by a damped classical oscillator of mean life τ. The oscillator will precess in the magnetic field H. If there were no foreign gas present to disturb the oscillator, the amplitude of the oscillator should decrease to $1/e$ of its original value in a time τ, and the plane of the oscillation should be rotated through an angle φ calculated from the Larmor precession velocity. The net result of this process is that the polarization observed, $P(H)$, should be given by

$$P(H)=P_0/\{1+[(eH/mc)g\tau]^2\}, \qquad (2)$$

which is similar to (1). If, now, nitrogen is present it may quench the mercury atom in the 7^3S_1 state. The result of collisions of nitrogen with the classical oscillator in a magnetic field would be to damp the amplitude of oscillation before the oscillator had a chance to precess very far. A calculation, similar to that made by Turner[7] for the quenching of resonance radiation, shows that a formula similar to (2) may be used provided τ is replaced by $\tau T/(\tau+T)$, where T is the time between collisions, and provided that nitrogen has no effect on the polarization in zero field.

If the polarization at a given magnetic field and pressure of nitrogen, $P(H, p)$ be measured as a function of the nitrogen pressure and the quantity

[7] L. A. Turner, Phys. Rev. **23**, 464 (1924).

$$\frac{1}{f(P)}=\left(\frac{1-P(H,\,p)/P_0}{P(H,\,p)/P_0}\right)^{-1}$$

be plotted against the pressure p, a straight line should result whose intercept is $mc/eHg\tau$ and whose slope, $(A\sigma_q^2/g)(mc/eH)$, where σ_q^2 is the quenching cross section and

$$A=2666.6\left(\frac{2\pi N}{kT}\cdot\frac{m_1+m_2}{m_1m_2}\right)^{\frac{1}{2}}.$$

If the values of $1/f(P)$ for the experiments on the line 4358 taken from Table II are plotted against the corresponding nitrogen pressures a straight line results which gives a value of $\tau=0.88\times10^{-8}$ sec. and of $\sigma_q^2=1.3\times10^{-16}$ cm². This result must be taken as only an approximation to σ_q^2 and τ, since in the theoretical treatment hyperfine structure was not considered. The experiments were performed, however, at such a magnetic field ($H=3$ gauss) that the value of $P(H)/P_0$, calculated on the basis of hyperfine structure, is not essentially different from that calculated neglecting hyperfine structure.

Finally, it must be emphasized that, in the experiments in which the mean life of the 7^3S_1 state was measured by observations on the three fluorescent lines, $\tau T/(\tau+T)$ was measured and not τ. Since, however, the nitrogen pressure was kept constant at 3 mm in these experiments, a short calculation shows that the values of the true mean life as measured by the three lines should have the same relation to each other as do the values given in Table I.

In conclusion, the authors wish to acknowledge their indebtedness to Dr. R. L. Garman, of the Chemistry Department of the Washington Square College who kindly made the intensity measurements with the microphotometer.

A Calculation of Mass Scattering Coefficients

L. M. HEIL, *Ohio University*

(Received February 28, 1934)

By means of graphical integration, the mass scattering coefficients of the substances carbon, aluminum, iron, tin and gold have been calculated over the wave-length range $\lambda=0.4$A to 1.1A. The results show: (1) the mass coefficients obtained agree reasonably well with those obtained experimentally by Coade, Mertz, Hewlett, Statz and Allen; (2) the mass scattering coefficients may be expressed by the relation, $\sigma/\rho=0.0230Z^{1.16}\lambda$, over a wave-length range $\lambda=0.4$A to 1.1A and upwards from atomic number 12; (3) the part of the scattering coefficient due to incoherent scattering averages 20 percent lower than that value expressed by the Dirac or the Klein-Nishina formula.

INTRODUCTION

EXPERIMENTAL values of the mass scattering coefficients of x-rays have been determined for a number of elements directly by Coade,[1] Mertz,[2] Statz[3] and Hewlett[4] and indirectly by Allen.[5] As yet no satisfactory theoretical calculations have been made that agree with the experimental values. It was the purpose of this study to calculate the value of these coefficients from the existing accurate knowledge of the intensity of x-rays, as a function of the scattering angle, scattered by gases and powdered crystals.

METHOD

The intensity of x-rays scattered by a single electron is given by the classical theory[6] as

$$I_{\theta}=I_0(e^4/2m^2c^4R^2)(1+\cos^2\theta),$$

[1] E. H. Coade, Phys. Rev. **36**, 1109 (1930).
[2] P. Mertz, Phys. Rev. **28**, 891 (1926).
[3] Statz, Zeits. f. Physik **11**, 304 (1922).
[4] Hewlett, Phys. Rev. **20**, 688 (1922).
[5] Allen, Bull. Am. Phys. Soc. **8**, Nos. 5, 6.

[6] J. J. Thomson, *Conduction of Electricity Through Gases*, 3rd Ed., p. 321.

where R is the distance from the scattering electron to the receiver, e^4/m^2c^4 is 7.85×10^{-26}, I_0 is the intensity of the original x-ray beam and $\frac{1}{2}(1+\cos^2\theta)$ is the Thomson polarization factor.

According to the quantum theory this scattered radiation consists of two parts;[7] one part in which the wave-length of the x-rays scattered is changed, the modified or incoherent radiation, and one part in which the wave-length is the same, the coherent or unmodified radiation.

$$I_{sc}=I_{coh}+I_{incoh},$$

where

$$I_{coh}=I_0[e^4(1+\cos^2\theta)F^2/m^2c^42R^2], \qquad (1)$$

in which F is the atomic form factor[8, 9, 10, 11] which expresses the electron density in the atom, and

$$I_{incoh}=I_0[e^4(1+\cos^2\theta)/2m^2c^4R^2]\{(z-\sum_1^z E_r^2)/(1-\gamma(1-\cos\theta))^3\} \qquad (2)$$

as given by Compton,[12] where E_r is the structure factor of the electron in its proper shell in the normal atom as given by Pauling and Sherman[10] and $\gamma=h\nu/mc^2$ or by

$$I_{incoh}=I_0(e^4(1+\cos^2\theta)/2m^2c^4R^2)zG(v) \qquad (3)$$

as given by Heisenberg[13] in which $G(v)$ is a function of the wave-length of the coherent radiation and the atomic number of the scattering substance.

The total scattered radiation for z electrons in an atom, as a function of the scattering angle is given by

$$I_{sc}=I_0[e^4(1+\cos^2\theta)/2R^2m^2c^4]\{F^2+[z-\sum_1^z E_r^2]/(1+\gamma(1-\cos\theta))^3\} \qquad (4)$$

or by

$$I_{sc}=I_0[e^4(1+\cos^2\theta)/2R^2m^2c^4]\{F^2+zG(v)\}, \qquad (5)$$

depending on whether the incoherent radiation is expressed by the Compton or by the Heisenberg relation.

The Eqs. (4) and (5), of course, assume that the scattering substance is in a gaseous state, and that it is monatomic. At first sight one feels that the above relations for the intensity of the scattered radiation may not be applied to explain the results of x-rays scattered from solids such as experimentally measured by Coade, Mertz and Hewlett. However, A. W. Coven[14] and G. E. M. Jauncey and F. Pennell[15] have shown that, in the case of powdered crystals, the intensity of the scattered radiation is very well expressed by the Eq. (4) over a range of scattering angles from 10° to 180°. Below 10° this relation alone does not express the true intensity of the scattered x-rays. In this range of λ there is little error made in assuming that Eq. (4) does represent the scattered radiation since in the calculation of the scattering coefficient the scattered intensity is multiplied by the sine of the scattering angle and the contribution of this range is very small. Jauncey and Pennell[15] also found the electronic structure factor F to be the same in the powdered crystal as in the gas.

Jauncey and Harvey[16] on the other hand have shown in the case of radiation scattered from single crystals, that the scattering angle, at which the intensity of the radiation scattered from the single crystal differs from that scattered from a gas, may be as high as 40°. Therefore, in the case of single crystals, the Eq. (4) does not express the intensity of the scattered radiation to any degree of accuracy. From the description of the scattering substances employed by Coade, Mertz and Hewlett, it is probable that the scattering substances were not

[7] A. H. Compton, Phys. Rev. **35**, 925 (1930).
[8] James and Brindly, Phil. Mag. **12**, 81 (1931).
[9] L. H. Thomas, Proc. Camb. Phil. Soc. **23**, 542 (1927).
[10] Pauling and Sherman, Zeits. f. Krist. **81**, 1 (1932).
[11] D. R. Hartree, Proc. Camb. Phil. Soc. **24**, 89 (1928).
[12] A. H. Compton, Phys. Rev. **21**, 483 (1923).
[13] W. Heisenberg, Phys. Zeits. **32**, 737 (1931).
[14] A. W. Coven, Phys. Rev. **41**, 422 (1932).
[15] G. E. M. Jauncey and F. Pennell, Phys. Rev. **43**, 505 (1933).
[16] G. E. M. Jauncey and G. G. Harvey, Phys. Rev. **38**, 1071 (1931).

single crystals and so far as scattering is concerned they could best be described as powdered crystals.

The mass scattering coefficient, σ/ρ, defined as the fraction scattered per unit mass of a substance per second, is given by the expression,[17]

$$\sigma/\rho=\int_0^\pi I_{ec}2\pi R\sin\theta\cdot Rd\theta/I_0,$$

which leads to

$$\sigma/\rho=(\pi Ne^4/m^2c^4)\int_0^\pi(1+\cos^2\theta)\sin\theta\{F^2+[z-\sum_1^z E_r^2]/(1+\gamma(1-\cos\theta))^3\}d\theta \tag{6}$$

for the case of Compton incoherent scattering, where N is the number of scattering atoms per unit mass, or

$$\sigma/\rho=(\pi Ne^4/m^2c^4)\int_0^\pi(1+\cos^2\theta)\sin\theta\{F^2+zG(v)\}d\theta \tag{7}$$

for the case of Heisenberg incoherent scattering. Eqs. (6) and (7) do not lend themselves to an analytic integration (on account of the method of expression of the structure factor) and it is necessary to resort to graphical methods. The coherent and the incoherent parts of the integrals (6) and (7) were plotted separately in order to determine the amount each contributes to the scattering coefficient. Typical curves are shown in Figs. 1, 2 and 3. In these curves, the areas under the curves are direct measures of the scattering coefficients.

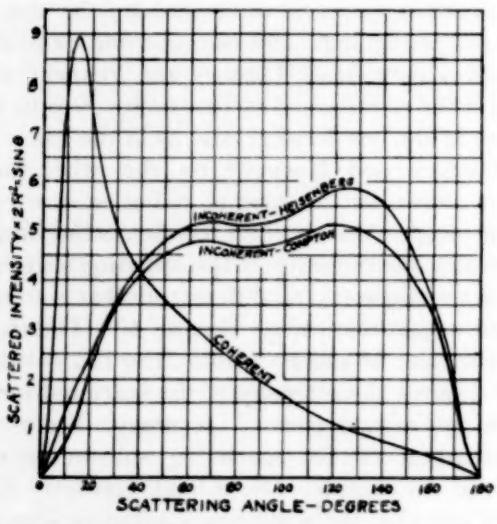

FIG. 1. The separate parts of integrals (6) and (7) *vs.* the scattering angle for carbon at a wave-length of 0.7A. The integral is evaluated in terms of $\pi e^2/m^2c^4$ as a unit.

This calculation of the mass scattering coefficient of course includes only the energy of the incident x-ray beam scattered in the form of radiation. Actually, the measured mass scattering coefficient may also include the energy lost in

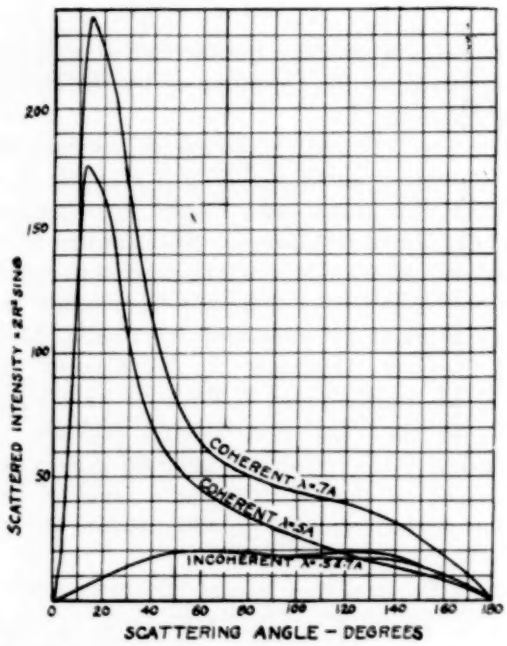

FIG. 2. The separate parts of integral (6) *vs.* the scattering angle for iron at a wave-length of 0.5 and 0.7A. The integral is given in terms of $\pi e^4/m^2c^4$.

[17] A. H. Compton, *X-rays and Electrons*, p. 60, 1927.

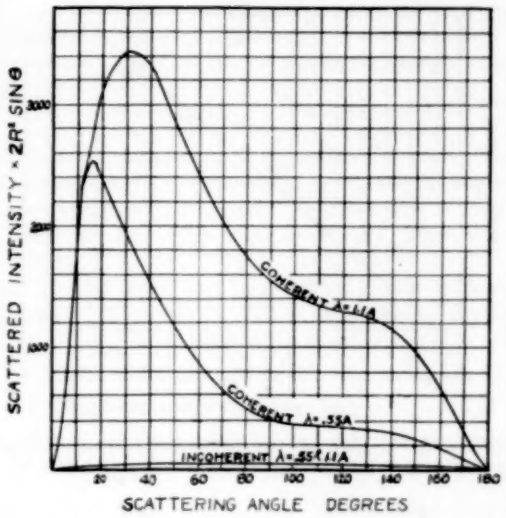

FIG. 3. The separate parts of the integral (6) *vs.* the scattering angle for gold at a wave-length of 0.55 and 1.1A. The integral is given in terms of $\pi e^4/m^2c^4$ as a unit.

the recoil electron. W. R. Harper[18] has shown that the ratio of the energy of the recoil electron to the total energy removed from the incident x-ray beam is about five percent in the case of hydrogen at $\lambda = 0.46$A. Since the present calculations are not accurate to more than three percent there is no serious error in calling these calculated coefficients the total mass scattering coefficients.

RESULTS

The mass scattering coefficients obtained from measurements of the areas under the curves show that, for elements of low atomic number (see Fig. 1), the contribution of the incoherent radiation is comparable with the coherent radiation. For elements of atomic number greater than 50 (see Figs. 2 and 3) the incoherent radiation contributes little to the scattering coefficient and may be neglected for the most part.

It is also obvious from the curves (see Figs. 2 and 3) that the contribution of the coherent radiation to the scattering coefficient increases as the wave-length increases while the part due to the incoherent scattering remains almost constant over the range of wave-lengths investigated. The curves also show as well as the integrated results that the part of the scattering coefficient represented by the Compton relation and that represented by the Heisenberg relation are practically the same.

Table I gives the results of the scattering coefficients in comparison with the experimental values of various observers for the elements, carbon, aluminum, iron, tin and gold, over a wave-length range from $\lambda = 0.42$A to $\lambda = 1.1$A. The agreement between the calculated and observed values is quite good for carbon and aluminum. For iron, tin and gold the agreement is not as good but is probably as good as that expected in the face of the possibility that the solid scattering substance in the experimental work may have consisted of some aggregates of rather large single crystals. It should also be remembered that scattering coefficients are rather difficult to measure experimentally and that disagreements of as much as 30 percent are not uncommon between various observers. The agreement of the calculated value and observed value in the case of carbon at $\lambda = 0.7$A (probably the most accepted value) is quite good.

VARIATION OF THE MASS SCATTERING COEFFICIENT WITH THE WAVE-LENGTH AND ATOMIC NUMBER

When the values of the mass scattering coefficients of the substances carbon, aluminum, iron, tin and gold are plotted against the wave-length (over the range 0.4 to 1.1A, Fig. 4) it is found that a linear relation fits well. Below 0.4A it is probable that the relation would not be linear since for this region the incoherent scattering is the more important and this is not linear as shown by the Dirac expression. Above

TABLE I. *The computed mass scattering coefficients compared with those observed by Coade, Hewlett and Allen.*

Substance	Wave-Length 0.42A	0.5A	0.6A	0.7A	1.0A	1.1A
Carbon				0.21 0.21(4)	0.244 0.28(1)	
Aluminum	0.21 0.16(5)	0.25 0.17(1)		0.35 0.21(1)		0.56 0.39(1)
Iron	0.42 0.28(5)	0.48 0.25(1)	0.59 0.36(1)	0.66 0.45(1)		1.03
Tin	0.86 1.40(5)	0.95 0.40(1)		1.39 0.78(1)		2.27
Gold	1.56	1.81 0.93(1)	1.18 0.60(1)			4.00

[18] W. R. Harper, Proc. Roy. Soc. **A141**, 686 (1933).

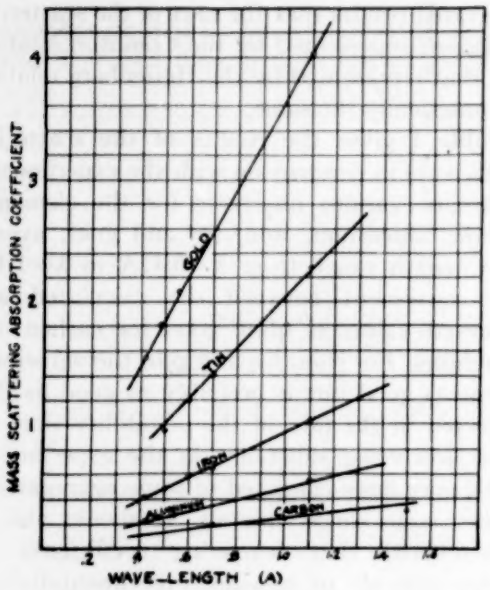

FIG. 4. Relation of the mass scattering coefficient with the wave-length.

1.1A the scattering is mainly coherent and in this range the coherent scattering increases more rapidly than is expressed by the linear relation.

Plotting the logarithms of the scattering coefficients of the various elements against the logarithms of the atomic numbers (Fig. 5) gives a straight line (at $\lambda=1$A) upon which the coefficients of all the elements fall, with the exception of carbon. The slope of this log-log plot is 1.16. It is obvious, then, that over a wave-length range from 0.4A to 1.1A and upward from atomic number 12, the scattering coefficient may be represented as $\sigma/\rho=AZ^{1.16}\lambda$, and A has the value 0.0230 when σ/ρ is the scattering coefficient per unit mass.

COMPARISON OF THE INCOHERENT PART OF THE MASS SCATTERING COEFFICIENT WITH THAT PREDICTED BY THE DIRAC FORMULA

The mass scattering coefficient of the incoherent part of the scattered radiation may be

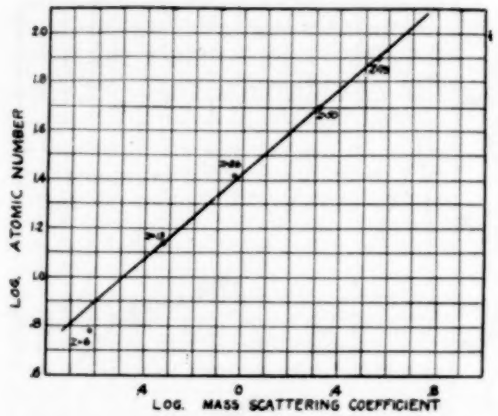

FIG. 5. Log-log plot of the mass scattering coefficient against the atomic number at a wave-length of 1.0A.

obtained by integrating under the incoherent curve only. The integration under the incoherent curve given by the Compton expression for the incoherent scattering for the various elements at a wave-length of 0.5A gives rise to the value of the coefficients in Table II. These values are in terms of the scattering per electron. The average value for the five elements under consideration is 454×10^{-27} against a value of 585×10^{-27} as given by the Dirac[19] expression or 587×10^{-27} as given by the Klein-Nishina[20] expression.

TABLE II. *Incoherent scattering per electron at $\lambda=0.5$A as given by the integrated Compton expression, the Dirac formula and the Klein-Nishina formula.*

	Compton	Dirac	Klein-Nishina
Carbon	545×10^{-27}	585×10^{-27}	587×10^{-27}
Aluminum	510×10^{-27}		
Iron	400×10^{-27}		
Tin	437×10^{-27}		
Gold	380×10^{-27}		
	av. $=454\times10^{-27}$		

[19] P. A. M. Dirac, Proc. Roy. Soc. **A111**, 405 (1926).
[20] O. Klein and Y. Nishina, Zeits. f. Physik **52**, 853 (1929).

The Spectra of Columbium V and Molybdenum VI

M. W. TRAWICK, *Department of Physics, Cornell University*

(Received May 7, 1934)

The Rb I-like spectra of columbium and molybdenum have been excited in a vacuum spark and photographed with a vacuum spectrograph. Identifications of lines corresponding to the transitions $5s\ ^2S-5p\ ^2P$, $5p\ ^2P-5d\ ^2D$, $5p\ ^2P-6s\ ^2S$, $4d\ ^2D-5p\ ^2P$, and $4d\ ^2D-4f\ ^2F$ for Cb V and Mo VI have been facilitated by extrapolation from the corresponding lines in the spectra of the four preceding elements in the Rb I-like isoelectronic sequence. The relative term values $4d\ ^2D$, $5s\ ^2S$, $5p\ ^2P$, $4f\ ^2F$, $5d\ ^2D$, and $6s\ ^2S$ have been determined. Absolute term values have been approximately fixed by extrapolating $\nu^{\frac{1}{2}}$ for the terms of the sequence in such a way as to maintain the validity of the irregular doublet law and they have been compared with those obtained by applying the Rydberg formula to the ^2S and ^2D terms, and with those found by extrapolating values of the quantum defects for the ^2S and ^2P terms.

THE spectra of only the first four elements in the Rb I-like isoelectronic sequence have heretofore been identified. Fowler[1] and Paschen-Götze[2] give the classified lines and terms of Rb I and Sr II. The identifications of the spectra of Y III and Zr IV are due to Gibbs and White,[3] to Bowen and Millikan,[4] and to Kiess and Lang.[5] In this report the sequence has been extended to include the spectra of Cb V and Mo VI.

The spectra of Cb V and Mo VI were excited in the vacuum spark between solid metal electrodes and photographed with a vacuum spectrograph containing a concave grating of 150 cm radius of curvature and ruled with 15,000 lines per inch. The dispersion was about 11.3A per mm. The vacuum spark between aluminum electrodes furnished the standard lines, either those of aluminum itself or those of oxygen and nitrogen brought out in the discharge.

The lowest term in each of these spectra is $4d\ ^2D_{1\frac{1}{2}}$, as was anticipated by an almost linear extrapolation from the square roots of the terms of the preceding members of the sequence.

A fair estimate of the separation of the $5p\ ^2P$ terms was obtained from Sommerfeld's law for regular doublets rising from non-penetrating orbits. The doublet separation is given by the equation,

$$\Delta\nu = R\alpha^2(Z-s)^4/n^3l(l+1).$$

The screening constant s was found by extrapolating from the values of s for the preceding members of the sequence (Fig. 1).

A linear extrapolation of the wave numbers in this sequence for the transition $5s\ ^2S_{\frac{1}{2}}-5p\ ^2P_{\frac{1}{2}}$ (irregular doublet law) gave reliable evidence as to the approximate wave-lengths of the $^2S-^2P$ lines. This information, together with that obtained from the regular doublet law for the ^2P interval made the identification of these two lines quite unambiguous. Further confirmation of the correctness of this interval was obtained from the identification of combinations with other levels. The identification of other lines was facilitated by the linear extrapolation of radiated wave numbers (Fig. 3) and by the use of extrapolations from the Moseley diagram (Fig. 2).

Tables I and II give the experimental data and classifications.

The diagram (Fig. 2) containing the plot of $\nu^{\frac{1}{2}}$ against atomic number was so drawn that the

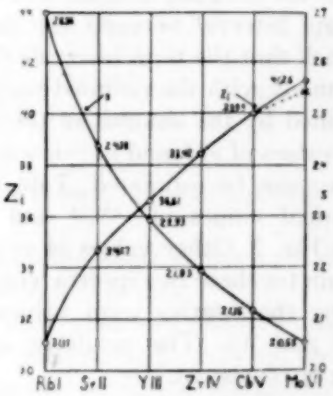

FIG. 1. Z_i and s curves.

[1] Fowler, Report on Series in Line Spectra, pp. 103–105, 131, 132 (1922).
[2] Paschen-Götze, Seriengesetze der Linienspektren, pp. 61–63, 89 (1922).
[3] Gibbs and White, Nat. Ac. Sci. Proc. **12**, 551 (1926).
[4] Bowen and Millikan, Phys. Rev. **28**, 923 (1926).
[5] Kiess and Lang, Bur. Standards J. Research **5**, 305 (1930).

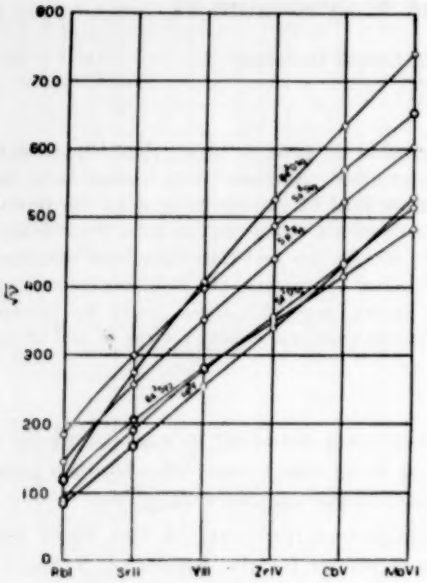

FIG. 2. Moseley diagram.

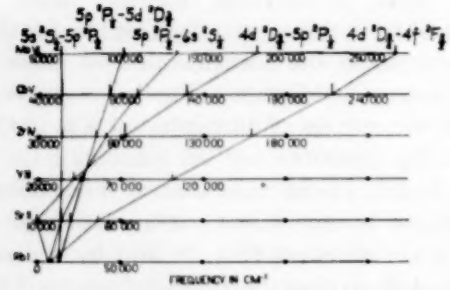

FIG. 3. Linear progression of radiated wave numbers with atomic number.

difference between $(^2S_{\frac{1}{2}})^{\frac{1}{2}}$ and $(^2P_{\frac{1}{2}})^{\frac{1}{2}}$ is nearly constant for the various elements. This is a consequence of the irregular doublet law. Of course, the ordinate interval between the two curves must be such that the term intervals themselves are in harmony with the radiated wave number as determined by the analysis of the spectrum. From the values of $\nu^{\frac{1}{2}}$ found in this way absolute term values can be estimated. Table III gives the numerical values of $(^2S_{\frac{1}{2}})^{\frac{1}{2}}$ and $(^2P_{\frac{1}{2}})^{\frac{1}{2}}$ as plotted in Fig. 2. Other values of $\nu^{\frac{1}{2}}$ plotted in this diagram for these two spectra were obtained by utilizing the relative term values given in Tables V and VI. The resulting curves are satisfactorily consistent.

Another method yielding approximate absolute term values is that of extrapolating a curve

TABLE I. *Classified lines of Cb V.*

Int.	λ(A)	ν(cm⁻¹)	Δν	Classification
10	1877.34	53,266.9	3605.2	$5s\ ^2S_{\frac{1}{2}} - 5p\ ^2P_{\frac{1}{2}}$
10	1758.33	56,872.1		$5s\ ^2S_{\frac{1}{2}} - 5p\ ^2P_{\frac{3}{2}}$
4	1267.60	78,889.2	547.1	$5p\ ^2P_{1\frac{1}{2}} - 5d\ ^2D_{1\frac{1}{2}}$
10	1258.87	79,436.3	3604.8	$5p\ ^2P_{1\frac{1}{2}} - 5d\ ^2D_{2\frac{1}{2}}$
7	1212.21	82,494.0		$5p\ ^2P_{\frac{1}{2}} - 5d\ ^2D_{1\frac{1}{2}}$
5	1044.90	95,702.9	3600.0	$5p\ ^2P_{1\frac{1}{2}} - 6s\ ^2S_{\frac{1}{2}}$
4	1007.02	99,302.9		$5p\ ^2P_{\frac{1}{2}} - 6s\ ^2S_{\frac{1}{2}}$
8	774.02	129,196		$4d\ ^2D_{1\frac{1}{2}} - 5p\ ^2P_{\frac{1}{2}}$
8	763.77	130,929	3604 1871	$4d\ ^2D_{2\frac{1}{2}} - 5p\ ^2P_{1\frac{1}{2}}$
6	753.01	132,800		$4d\ ^2D_{1\frac{1}{2}} - 5p\ ^2P_{1\frac{1}{2}}$
8	468.32	213,529	1733	$4d\ ^2D_{2\frac{1}{2}} - 4f\ ^2F_{3\frac{1}{2}}$
8	464.55	215,262		$4d\ ^2D_{1\frac{1}{2}} - 4f\ ^2F_{2\frac{1}{2}}$

TABLE II. *Classified lines of Mo VI.*

Int.	λ(A)	ν(cm⁻¹)	Δν	Classification
9	1595.45	62,678.2	4925.0	$5s\ ^2S_{\frac{1}{2}} - 5p\ ^2P_{\frac{1}{2}}$
10	1479.22	67,603.2		$5s\ ^2S_{\frac{1}{2}} - 5p\ ^2P_{1\frac{1}{2}}$
4	1047.20	95,492.7	768.2	$5p\ ^2P_{1\frac{1}{2}} - 5d\ ^2D_{1\frac{1}{2}}$
12	1038.65	96,278.9	4927	$5p\ ^2P_{1\frac{1}{2}} - 5d\ ^2D_{2\frac{1}{2}}$
10	995.82	100,420		$5p\ ^2P_{\frac{1}{2}} - 5d\ ^2D_{1\frac{1}{2}}$
6	790.75	126,462	4927	$5p\ ^2P_{1\frac{1}{2}} - 6s\ ^2S_{\frac{1}{2}}$
3	761.10	131,389		$5p\ ^2P_{\frac{1}{2}} - 6s\ ^2S_{\frac{1}{2}}$
15	548.21	182,412		$4d\ ^2D_{1\frac{1}{2}} - 5p\ ^2P_{\frac{1}{2}}$
30	541.24	184,761	4938 2589	$4d\ ^2D_{2\frac{1}{2}} - 5p\ ^2P_{1\frac{1}{2}}$
8	533.76	187,350		$4d\ ^2D_{1\frac{1}{2}} - 5p\ ^2P_{1\frac{1}{2}}$
9	376.98	265,266	2185	$4d\ ^2D_{2\frac{1}{2}} - 4f\ ^2F_{3\frac{1}{2}}$
9	373.90	267,451		$4d\ ^2D_{1\frac{1}{2}} - 4f\ ^2F_{2\frac{1}{2}}$

TABLE III. *Values used in applying the irregular doublet law to the $^2S_{\frac{1}{2}}$ and $^2P_{\frac{1}{2}}$ terms.*

	$(5s\ ^2S_{\frac{1}{2}})^{\frac{1}{2}}$	$(5p\ ^2P_{\frac{1}{2}})^{\frac{1}{2}}$	$(5s\ ^2S_{\frac{1}{2}})^{\frac{1}{2}} - (5p\ ^2P_{\frac{1}{2}})^{\frac{1}{2}}$
Rb I	183.546	145.293	38.253
Sr II	298.249	255.416	42.833
Y III	397.269	351.978	45.291
Zr IV	485.602	438.282	47.320
Cb V	569.64	520.79	48.85
Mo VI	651.5	601.5	50.0

drawn by plotting the values of the quantum defect $(n-n^*)$ for the ^2S and ^2P terms of the sequence against atomic numbers.

The absolute term values of the $5d\ ^2D_{1\frac{1}{2}}$ levels for both spectra found by applying the Rydberg formula to relative term values for both S and D terms are somewhat larger than those obtained from the irregular doublet law, Fig. 2.

The absolute term values for the lowest D levels found by different methods are shown in Table IV. The numbers in the parentheses are the values obtained after correcting the $5s\ ^2S_{\frac{1}{2}}$ terms as obtained from the Rydberg formula by an amount consistent with that found necessary for the other elements of the sequence in which absolute term values can be computed from a three term formula. The absolute term values obtained from the extrapolation of $\nu^{\frac{1}{2}}$ are considered the most reliable. This opinion is well supported by a result obtained from the Landé doublet formula for penetrating orbits,

$$\Delta\nu = R\alpha^2 z^2 Z_i^2/n^{*3}l(l+1).$$

Using the observed $\Delta\nu$'s for the ^2P interval and the n^*'s computed from the preferred $^2P_{\frac{1}{2}}$ values, one obtains values of Z_i which, when plotted against the atomic numbers, give a smooth curve[6] (Fig. 1). If one regards the smoothness of the Z_i curve as essential, its extrapolation from member to member in the sequence furnishes a fairly sensitive check on the term value. For example, if the value of the $^2P_{\frac{1}{2}}$ term for Mo VI is increased by 5000 cm^{-1}, i.e., by about 1 percent, one obtains the value of Z_i marked by the cross in Fig. 1.

Tables V and VI give the term values of Cb V and Mo VI, respectively, relative to $4d\ ^2D_{1\frac{1}{2}}$, and the absolute term values as evaluated from the irregular doublet law.

TABLE IV. *Absolute term values of $4d\ ^2D_{1\frac{1}{2}}$ obtained by different methods.*

	Rydberg formula		$\nu^{\frac{1}{2}}$ extrapolation	$n-n^*$ extrapolation
	From S terms	From D terms		
Cb V	413,400 (404,900)	433,700	400,000	396,000
Mo VI	562,000 (550,000)	590,000	543,600	515,000

[6] Gibbs and White, Phys. Rev. **33**, 157 (1929). The values of Z_i for Y III and Zr IV have been recomputed from the most recent data.

TABLE V. *Term values for Cb V.*

Term	Relative term values	$\Delta\nu$	Approximate absolute term values
$4d\ ^2D_{1\frac{1}{2}}$	0	1871	400,000
$4d\ ^2D_{2\frac{1}{2}}$	1,871		398,129
$5s\ ^2S_{\frac{1}{2}}$	75,929		324,071
$5p\ ^2P_{\frac{1}{2}}$	129,196	3605	270,804
$5p\ ^2P_{1\frac{1}{2}}$	132,801		267,199
$5d\ ^2D_{1\frac{1}{2}}$	211,690	547	188,310
$5d\ ^2D_{2\frac{1}{2}}$	212,237		187,763
$4f\ ^2F_{2\frac{1}{2}}$	215,262	138	184,738
$4f\ ^2F_{3\frac{1}{2}}$	215,400		184,600
$6s\ ^2S_{\frac{1}{2}}$	228,500		171,500

TABLE VI. *Term values for Mo VI.*

Term	Relative term values	$\Delta\nu$	Approximate absolute term values
$4d\ ^2D_{1\frac{1}{2}}$	0	2589	543,600
$4d\ ^2D_{2\frac{1}{2}}$	2,589		541,011
$5s\ ^2S_{\frac{1}{2}}$	119,739		423,861
$5p\ ^2P_{\frac{1}{2}}$	182,417	4928	361,183
$5p\ ^2P_{1\frac{1}{2}}$	187,345		356,255
$4f\ ^2F_{2\frac{1}{2}}$	267,451	404	276,149
$4f\ ^2F_{3\frac{1}{2}}$	267,855		275,745
$5d\ ^2D_{1\frac{1}{2}}$	282,837	787	260,763
$5d\ ^2D_{2\frac{1}{2}}$	283,624		259,976
$6s\ ^2S_{\frac{1}{2}}$	313,807		229,793

The writer wishes to thank Professor R. C. Gibbs for suggesting the problem and for giving much helpful advice in connection with the work.

Dependence of the Dielectric Coefficient of Air Upon Pressure and Frequency

A. R. Jordan, James W. Broxon and Frank C. Walz, *University of Colorado*

(Received March 6, 1934)

A capacity-resistance bridge has been designed to incorporate into an a.c. method of measurement the most desirable features of a previously described electrometer method of determination of the dielectric coefficients of gases. The bridge, which provides for adequate shielding from the effects of solid insulators, has been employed for the measurement of the dielectric coefficient of air at pressures up to 170 atmospheres (18°C) and frequencies up to 70,000 cycles per second. As in the electrometer measurements, the dielectric coefficient at each frequency employed appeared to increase approximately linearly with pressure. The extreme variation among the measured values of the dielectric coefficient, 1.000589 to 1.000593 at N.T.P., was less than one percent, and is considered to lie within the experimental error.

NOT only the early investigations, but to an even greater extent rather recent researches employing highly refined methods, have led to widely discordant values for the dielectric coefficients of air and other gases. The differences among the values obtained by different workers have often greatly exceeded the presumed experimental errors.

There has been some indication that the lack of agreement might to a certain extent be explained in terms of a dependence of the dielectric coefficient upon the frequency of variation of the electric field to which the gas was subjected. Such an explanation is inadequate, however, and it seems the differences must be due largely to unrecognized experimental inaccuracies.

One such source of error has been considered by Cagniard[1] to consist of lack of stability of some of the relatively modern high-frequency arrangements employed. Other plausible causes of disagreement might be varying degrees of impurity among the gases used, unrecognized or improperly corrected mechanical distortion due to variation of gas pressure, and inaccuracies of calibration of variable condensers. Another likely source of error receiving very little consideration from most workers is due to the solid dielectrics introduced for the purpose of maintaining proper spacing of condenser plates and retaining the gas. These solids frequently constitute the dielectric for a considerable fraction of the gas condenser "capacity." Since it is common practice not to eliminate the effects of these solid dielectrics by shielding, and not to take into account the variations[2] in their dielectric coefficients or power losses with variations in pressure, temperature or frequency, it would appear that this might contribute to the discrepancies noted.

In gaseous ionization measurements, it is an essential and common practice to eliminate practically entirely the effects of electrical properties of solid insulators by the employment of properly designed "guard" systems and null methods of measurement. The simple application of this procedure to the "static" measurement of the dielectric coefficients of gases has been described by one of the writers.[3] A further advantage of this method was the elimination of variable condensers and the difficulties of their calibration as well as their mechanical faults. In fact, no absolute capacity measurement was required, the comparatively simple determination of resistances being substituted.

In the present investigation, it has been the purpose of the writers to incorporate the advantages of this method of measurement into an a.c. method. Although the difficulty of securing non-reactive resistances hindered full adaptation to very high frequencies, frequencies up to 70,000 cycles per second have been satisfactorily employed.

Experimental Arrangement and Procedure

Detailed description of the equipment and procedure adopted in the case of the "static"

[1] Cagniard, Ann. de Physique **9**, 460 (1928).

[2] Curtis, MacPherson and Scott, Phys. Rev. **33**, 1080A (1929); Scott, Phys. Rev. **35**, 1429A (1930).

[3] Broxon, Phys. Rev. **37**, 1338 (1931); Phys. Rev. **38**, 2049 (1931).

measurements has been given in an earlier publication.[3] To adapt the significant features to the a.c. measurements, certain modifications were necessary. Instead of the simple capacity-resistance bridge arrangement[3, 4] heretofore employed, a double bridge was designed.

In Fig. 1 the two principal condensers, C_1 and C_2, are shown schematically in longitudinal section, C_1 not being drawn to scale in all respects. C_2 is the same fixed-capacity, air condenser formerly used; its precise construction and details of its insulation and guard system are shown in Fig. 4 of the paper of reference 4. The high-pressure condenser, C_1, was essentially as illustrated by Fig. 3 of the paper of reference 4, the guard system being precisely that shown there but the capacity being increased to practical equality with C_2 by the introduction of two coaxial brass cylinders as illustrated in Fig. 1. The dimensions of the inner cylinder were: I.D., 12/32 in.; O.D., 13/32 in.; O.L., 12.65 cm. Those of the outer cylinder were: I.D., 17/32 in.; O.D., 9/16 in.; O.L., 13.65 cm. Both cylinders were subjected to the same pressure inside and outside. As modified, the capacity or induction coefficient of the inner electrode relative to the outer (the inner being at the potential of the guard) for C_1 at atmospheric pressure was very nearly equal to that of C_2, about 26.3 cm.[4]

That the induction coefficients of the inner conductors of C_1 and C_2 relative to their outer or high-potential conductors could be regarded as "pure" when the inner or central conductor potential was identical with that of the guard system, was assured by the construction of the guards at the critical regions where they served to separate the solid condenser insulation. Here they protected those parts of the solid insulation in contact with the inner conductors from being subjected to any electric field, and prevented the passage of any lines of force to the central conductors from those portions of the solid insulation which were under the influence of electric fields. Under these conditions the charge on an inner conductor corresponding to a given potential of the outer was quite independent of the electrical condition of the insulation, and no conductance current could flow between the inner and outer conductors, apart from that due to the minute natural ionization of the contained gas. The provision of "pure" or non-reactive variable resistances for R_a and R_b, the other two arms of the primary bridge, an equally important requirement, offered some difficulty. At first 500 ohm units were wound by the Ayrton-Perry method in single layers on Pyrex glass tubes 18 in. long and 1 cm O.D. These were mounted at 3-in. intervals in a shielded box. Although these proved to be rather satisfactory at 1000 cycles per sec., the reactances were too great at higher frequencies. They were finally replaced by Leeds and Northrup a.c. resistances, types 4746 and 4745S, of about 10,000 ohms. These were found to be satisfactory for frequencies up to 70,000 cycles per sec.

In the auxiliary bridge arms, c' and c'' consisted of General Radio precision condensers, types 222 and 224, and c_a and c_b, of General Radio type 247E condensers of low power loss. The capacities employed were of the order of a few hundred mmf. r_1 and r_2 consisted of General Radio decade resistances, type 102K, of the order of 10,000 ohms.

A General Radio low-frequency oscillator provided the e.m.f. impressed upon the network. This was directly connected, and was carefully insulated from the guard system which surrounded it. The null indicator, D, consisted of a General Radio type 514A amplifier feeding into a dynatron circuit and producing a beat note which, after amplification, actuated head phones. The D.P.D.T. switch was a highly insulated Leeds and Northrup switch, No. 3298.

As indicated by the dashed lines in Fig. 1, all leads and instruments in the network were individually and thoroughly shielded.

As a preliminary step in balancing the bridge, the switch was thrown into the position grounding (connecting to the guard) the junction point between R_a and R_b and inserting the detector between ground and the central system of the condensers C_1 and C_2. The impedance arms r_1 and c' and r_2 and c'', constituting a "Wagner ground," were then adjusted until the detector did not register, thus indicating that the central system was at the potential of the guard system. Next, the switch was reversed, grounding the

[4] Broxon, Phys. Rev. **37**, 1320 (1931); see Fig. 2.

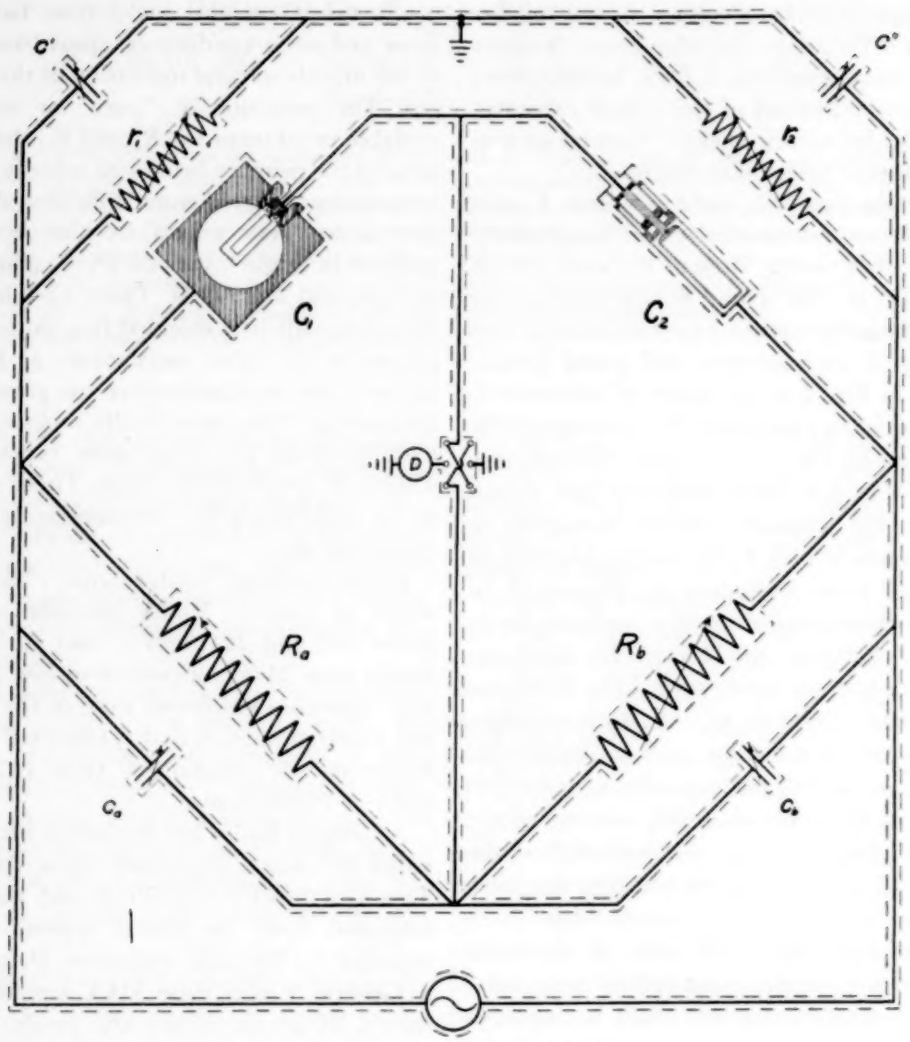

FIG. 1. Wiring diagram.

central system and inserting the detector between ground and the junction point between R_a and R_b. Then R_a and R_b and c_a and c_b were adjusted until a null indication showed that this junction point was at zero potential relative to the earthed guard system. This procedure was repeated until reversal of the switch with no further adjustment resulted in no response from the detector in either position. All "central" points of the network were then at the potential of the surrounding guard system, and the bridge was balanced. It was found that the final conditions at balance were unaltered if the junction point between R_a and R_b was left insulated instead of being grounded during the preliminary adjustment described above. Because the bridge could be balanced a little more rapidly with this arrangement, the cross-member of the switch which served to ground this junction point when the detector was connected to the C_1C_2 central system was omitted during the measurements.

That C_1 and C_2, the induction coefficients of the central conductors of the corresponding principal condensers relative to their respective outer or high-potential conductors, are to be regarded as pure or conductanceless capacitances at balance has been shown above. It has also

been pointed out that R_a and R_b consisted of practically non-reactive resistances. Another fact to be borne in mind is that the impedance consisting of the $c'r_1$ combination, and that consisting of the $c''r_2$ combination, might be regarded as including the impedances between the guard system and the high-potential conductors of C_1 and C_2, respectively, with which they were connected in parallel. With these considerations, not neglecting conductances of the auxiliary condensers nor reactances of the auxiliary resistances, the Kirchhoff equations for the network yield at balance the relation

$$\frac{C_1}{C_2}=\frac{R_b}{R_a}\left[\frac{1+R_a/r_a-1/\omega^2c_ac_br_ar_b}{1+R_b/r_b-1/\omega^2c_ac_br_ar_b}\right],$$

r_a and r_b being the equivalent series resistances of c_a and c_b, respectively, and ω the angular frequency of the impressed sinusoidal e.m.f. With the particular instruments and range of values used in the present investigation, the quantity in brackets varied from unity only slightly more than 10^{-4} under the most extreme conditions at the highest pressure and the highest frequency employed. Therefore, for the purpose of this investigation, the equation

$$C_1/C_2=R_b/R_a$$

served as a very satisfactory approximation, and was used in the calculation of the a.c. values recorded in Table I. Use of the accurate formula gives a value for K at N.T.P. less than that obtained by use of the approximate formula, only by 75×10^{-6} at 70,000 cycles/sec., less than one digit in the last column retained and little more than 0.1 percent of $(K-1)$. The correction would be less at lower frequencies.

The ratio of the induction coefficient of the condenser containing the gas under examination to that of the fixed condenser being equal to the principal resistance ratio, the dielectric coefficient of the gas at any pressure was given by the quotient of the resistance ratio at that pressure by the resistance ratio corresponding to complete evacuation of the gas chamber. This latter value was obtained by a slight extrapolation of the resistance-ratio *vs.* pressure curve as described in earlier work.[3]

The procedure as to preparation of the gas and measurement of pressure and temperature and of resistance was precisely as before[3, 4], except that a more accurate bridge was used for the determination of the d.c. resistances in the present investigation.

Observations

Resistance ratios were determined at about thirteen-atmosphere intervals between atmospheric pressure and 170 atmospheres, for several frequencies extending to 70,000 cycles per sec. The electrometer arrangement[3] was then substituted for the a.c., and the resistance ratios determined by the "static" method with the new capacity arrangement in C_1, for pressures up to about 150 atmospheres. Assuming that after reduction of pressures to a common temperature of 18°C the dielectric coefficient and hence the resistance ratio was a linear function of the pressure, the slope and intercept of the ratio-pressure line upon the resistance ratio axis was determined for each of the frequencies by the method of least squares. The ratio of the slope to the intercept yielded the value of $(K-1)$ for the air at one atmosphere pressure and the average experimental temperature of 18°C. Assuming that at a given pressure $(K-1)$ is inversely proportional to the absolute temperature, the values given in Table I were found for the dielectric coefficient of air at N.T.P. and the designated frequencies.

Some of the data are represented diagrammatically in Fig. 2. In this the open circles represent the 1000 cycle values, and the lower line is the corresponding line determined by least squares. The solid circles represent the 70,000 cycle values, but the upper line is that determined by least squares for the zero fre-

TABLE I. *Dielectric coefficient of air at N.T.P. and various frequencies.*

Frequency cycles/sec.	*K at* N.T.P.	*Frequency* cycles/sec.	*K at* N.T.P.
0	1.000592*	30,000	1.000591
	1.000593		
1,000	1.000589	50,000	1.000591
16,000	1.000589	70,000	1.000591

* This value was determined in an earlier investigation.[3]

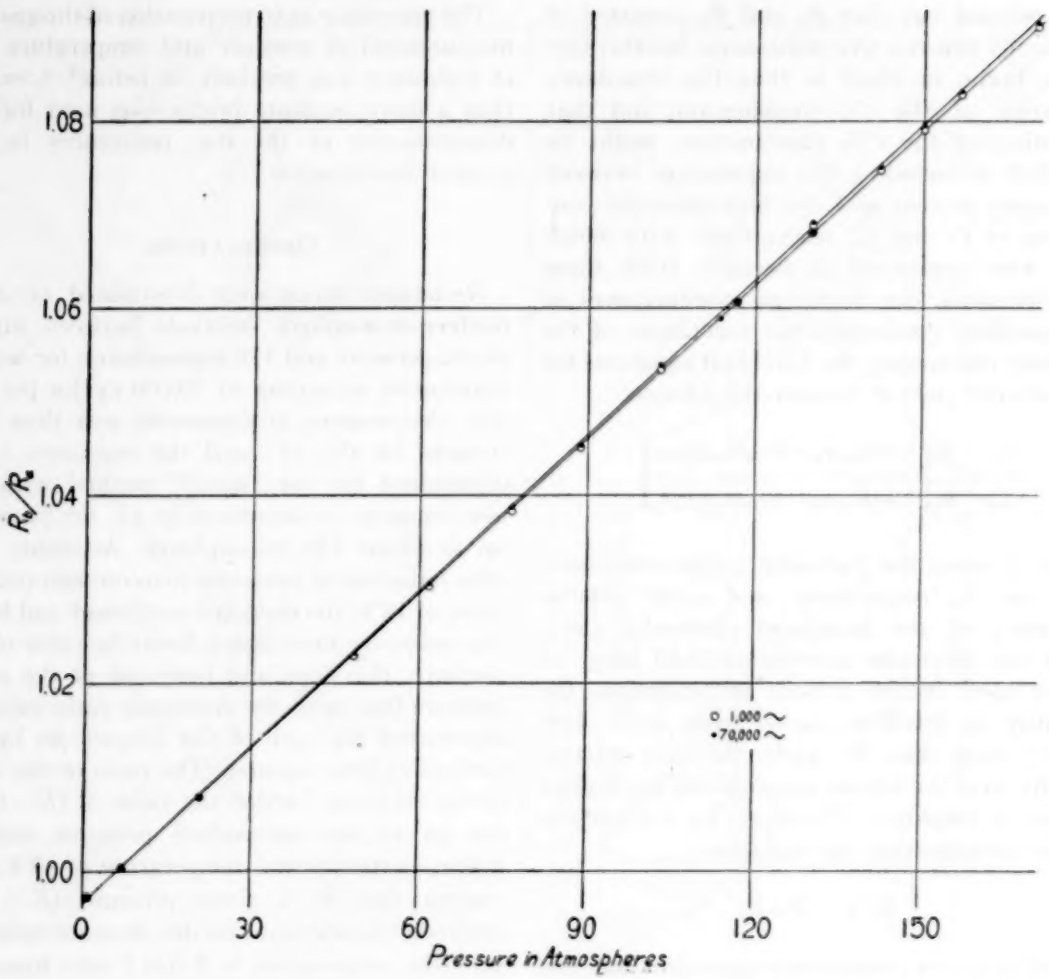

FIG. 2. Variation of resistance-ratio with pressure.

quency values, there being the greatest divergence between this and the 1000 cycle line.

The value formerly[3] obtained from observations by the electrometer method over a pressure range extending to 170 atmospheres was 1.000592. This value was obtained by graphical means. A redetermination from the original data by the least squares method has yielded precisely the same value as did the graphical method for each of the two individual sets of observations on which the graphical determination was based.

DISCUSSION

That an approximately linear relation exists between K and P over the pressure range of the investigation is indicated by Fig. 2, and by Fig. 1 of the first paper of reference 3. In the earlier work it was concluded without detailed statistical analysis that a linear relation between K and P was rather better satisfied by the observations than was the Clausius-Mossotti relation. As a further test, each of the two old sets of data, and the new sets for the frequencies of zero, 1000 and 70,000 cycles per sec. have been investigated in some detail. Employing values of the air density, d, obtained from data by Witkowski[5] and Amagat[6] at 16°C, the only data available, values of $(K-1)/P$, $(K-1)/d$, and $(K-1)/d(K+2)$ were calculated for each

[5] Witkowski, Phil. Mag. **41**, 288 (1896).

[6] Amagat, Ann. Chim. Phys. (6) **29**, 68 (1893). Taken from Physikalisch-Chemische Tabellen, Vol. I (1923) Landolt-Börnstein, p. 108; values given at 15.7°C.

pressure at which observations were made, for each of these five sets of data. Omitting values corresponding to pressures below 25 atmospheres because of considerable fluctuations in that region, the standard deviation from the mean was calculated for each of the three functions for each set. For each set of data, the fractional deviation for $(K-1)/d$ was greater than that for either of the other functions. For all but the new zero-frequency set, the fractional standard deviation was somewhat less for $(K-1)/P$ than for the Clausius-Mossotti function, but in this one instance the relation was reversed. The fact that the pressure range was less in this case may be of some significance. However, the differences among the deviations were of the order of magnitude of the "probable error" of the $(K-1)/P$ values calculated on the basis of the deviations of the individuals from their average, between 0.3 and 0.4 percent. It is considered, therefore, that the data do not make possible a definite conclusion as to which of the three functions, if any, may be regarded as actually constant over the range of pressures investigated. It is perhaps worth noting that for one of the old sets of data, the constancy not only of the above three functions but also of two others, the Mossotti function, $(K-1)/Kd$, and the Macdonald[7] function, $(K-1)/K^{\frac{1}{2}}d$, were investigated. The constancy of the latter of these was comparable with those of the above three functions, but the fractional deviation of $(K-1)/Kd$ was considerably greater and it displayed a tendency to decrease regularly with increasing pressure.

Various errors in the determinations of pressure, temperature and resistance have been considered before,[3] with the conclusion that the error in $(K-1)$ is probably of the order of 1 percent. Similar considerations would pertain to the present investigation. d.c. resistances could be measured somewhat more accurately, but at 50,000 cycles the principal resistances may have had phase angles amounting to as much as 1.5 degrees according to the manufacturer. This lack of "purity" of the resistances may have accounted for some of the variation of K with frequency with the a.c. arrangement. In any case, however, the extreme variation among all the values obtained was only about 0.7 percent of $(K-1)$. The investigation is considered to indicate, therefore, that the dielectric coefficient of air does not vary with frequency in the range investigated. It is interesting to note that Forró[8] found the dielectric coefficient of air to vary over about the same range as herein given, with variation of frequency at very much higher values. Using a beat frequency method of measurement, Forró found K to increase from 1.000586 at about 6×10^5, to 1.000593 at about 4.3×10^6 cycles per sec.

It is considered that mechanical distortion of the gas chamber resulting from variations in pressure did not produce errors amounting to nearly as much as 1 percent of $(K-1)$. It appears that compression of the material of the cylinder walls without alteration of shape might have introduced an error of about 0.1 percent. Because of the symmetry, not much shape distortion would be expected, but one might anticipate an error due to motion of the central conductor along its axis because of lack of rigidity of the ebonite insulation. Certain considerations lead to the conclusion that appreciable errors were not introduced on this account, however. In the first place, as has been pointed out before,[3] the two former independent sets of observations by the electrometer method yielded precisely the same value for K, indicating that any strains in the insulation must have been of an elastic nature. Then, too, with the two vastly different arrangements of condenser plates in the former and the present investigation (a thin 10-inch rod inside the 1-foot spherical cavity in the one case, and the two cylinders in the present case) errors depending upon deformation of the insulation should have been quite different. Nevertheless, the electrometer measurements in the two cases led to values differing by less than 0.2 percent of $(K-1)$. Even in a third case[9] where the plates consisted of a 0.168 in. diameter tube of 0.011 in. wall thickness inserted into a 3.7 in. diameter sphere of 0.006 in. average thickness within the pressure chamber, the value of K obtained by the electrometer method

[7] Macdonald, Proc. Roy. Soc. **A113**, 237 (1926).

[8] Forró, Zeits. f. Physik **51**, 374 (1928).

[9] Broxon, Phys. Rev. **42**, 321 (1932).

(1.000587 for 1 atm. at 0°C) differed from the others by just about 1 percent. In this case considerable deformation of the thin sphere was to be expected since its wall thickness was far from uniform.

There may have been some effect due to CO_2, pump oil vapor, and water vapor content of the air. Careful work by Watson[10] and his associates indicates that in the present investigation the air probably was not thoroughly dried.

Variation of the temperature over a range of a few degrees in the neighborhood of 18°C during part of the work may have had some influence upon the measurements. In this connection, it is considered that arrangements for more accurate determination of temperature and of pressure must be provided before the accuracy of the method can be improved materially.

Probably the arrangement herein described is not as sensitive as some others in the detection of minute variations of K. However, the accuracy of determination of the *absolute value* of the dielectric coefficient probably compares very favorably with others in view of the elimination of electrical effects of solid insulators and errors of calibration of condensers, whether fixed or variable.

The writers wish to acknowledge the assistance of Mr. R. V. Cartwright in the construction of the detector system.

[10] Watson, Rao and Ramaswamy, Proc. Roy. Soc. **A132**, 569 (1931); **A143**, 558 (1934).

LETTERS TO THE EDITOR

Prompt publication of brief reports of important discoveries in physics may be secured by addressing them to this department. Closing dates for this department are, for the first issue of the month, the twentieth of the preceding month; for the second issue, the fifth of the month. The Board of Editors does not hold itself responsible for the opinions expressed by the correspondents.

Fluorescence X-Ray Yields from K Shells of Atoms

In a recent article Berkey[1] reports measurements on the yield of fluorescence x-rays from the K shells of 13 elements. The interesting point of this work lies in a maximum value for the fluorescence yield from molybdenum—the yield rapidly decreasing as the atomic number increases.

That the fluorescence yield does not actually go to zero for the heavy elements is known, although no actual measurements have been made beyond xenon (54); this measurement being made by Auger.[2]

The value given by Berkey for the fluorescence yield w_K from the K shell of tellurium (52) is 0.59; Martin[3] gives 0.75 for w_K from iodine (53), while Auger gives 0.71 for w_K from xenon (54).

It seems that an error is present in Berkey's values of the fluorescence yield due to his neglect of the scattering of the x-rays by the argon which was used in the ionization chamber. The argon used was commercial grade and contained 14 percent by volume of nitrogen and for this latter gas the scattering correction is large at short wave-lengths. The wave-length λ' of the incident radiation from the $BaSO_4$ was (0.378A), while the wave-length λ'' from the various fluorescing bodies will depend on the atomic number of the element.

Eq. (2) in Berkey's paper gives R the ratio of the energy spent in producing ionization to the absorbed energy as

$$R=1-\frac{\delta-1}{\delta}\times e^{-\mu''s}\times\left(w_K\times\frac{\tau}{\mu}\times\frac{\lambda}{\lambda''}\right)_{\text{Argon}}-\frac{\sigma}{\mu}\times e^{-\mu's}.$$

The second term in this equation can be neglected as w_K for argon is small (0.07) and any argon K radiation excited has such a long wave-length that it will be absorbed in the gas before reaching the walls of the ionization chamber.

The third term however cannot be neglected, as for the short wave-lengths 0.378A, for example, the term amounts to approximately 0.12. What applied to argon applies still more to the nitrogen present. Values for the scattering coefficients for argon and nitrogen were kindly supplied by Dr. E. O. Wollan, of this laboratory from unpublished data.

For the resultant σ/μ, 0.86 of σ/μ for argon was added to 0.14 of σ/μ for nitrogen.

Table I gives the values of the various corrections as well as the recalculated values of w_K.

TABLE I.

Element	λ''	Argon 0.86 σ/μ	Nitrogen 0.14 σ/μ	R''	R'/R''	w_K (Berkey)	w_K Recalculated
27 Co	1.77	0.008	0.007	0.985	0.77	0.38	0.29
29 Cu	1.51	.012	.008	.98	.77	.43	.33
33 As	1.16	.015	.014	.97	.78	.53	.42
38 Sr	0.859	.026	.026	.95	.80	.72	.58
42 Mo	.696	.035	.042	.92	.82	.79	.65
47 Ag	.549	.053	.070	.88	.87	.72	.62
50 Sn	.482	.067	.098	.84	.90	.66	.60
52 Te	.443	.076	.118	.80	.94	.59	.56
56 Ba	.378	.10	.140	$R'=0.76$			

These values for w_K are now somewhat low compared to other authors, Auger,[2] Martin[3] and Compton.[4] This difference may be due in part to the use of relatively short wave-length x-rays $\lambda'=0.378$ incident on all the fluorescing bodies. The energy in the incident beam is determined directly by the ionization chamber measurement and it is assumed that a fraction $(\delta-1)/\delta$ (where $\delta=K$ absorption jump) is absorbed photoelectrically in the K shell.

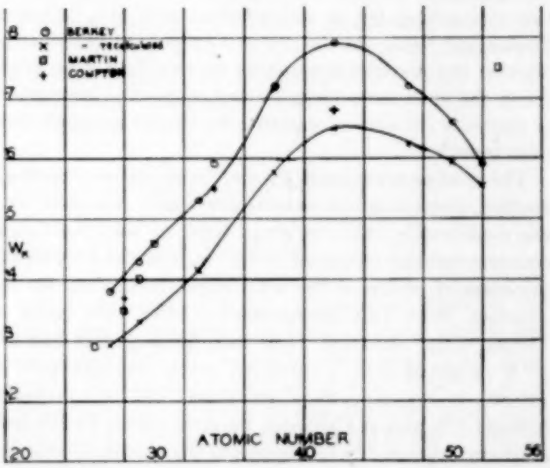

FIG. 1. Fluorescence yield as function of atomic number.

[1] D. K. Berkey, Phys. Rev. **45**, 437 (1934).
[2] Auger, Ann. de Physique **6**, 183 (1926).
[3] Martin, Proc. Roy. Soc. **A115**, 420 (1927).
[4] Compton, Phil. Mag. **8**, 961 (1924).

This is true only if the shape of the absorption wave-length curve is the same on the short wave-length side of the K absorption limit as it is on the long wave-length side.

For low atomic number fluorescing bodies, e.g., copper, a fraction of the incident beam λ' will be scattered rather than absorbed photoelectrically, i.e., in the equation $\mu=\tau+\sigma$ the σ is not negligible. This presumably causes the ionization current measurement i'' of the fluorescence beam λ'' to be too low. This would cause the values of w_K to be too small, which may account for the recomputed measurements of w_K lying below the values given by other authors.

Also if the incident beam λ' is not of uniform intensity along its cross section or if fluorescence radiation from the diaphragm is present it may be that by reducing the area of the beam such that the ratio of areas $S'/S''=0.003305$ that the intensity of the beam is not cut down in the same ratio.

Though the corrections proposed do not remove the maximum value of w_K for molybdenum, they do make the decrease of w_K with atomic number smaller than previously.

R. J. STEPHENSON

Ryerson Physical Laboratory,
University of Chicago,
April 24, 1934.

Comments on Letter of A. J. Stephenson

The recalculation of the writer's results on fluorescence x-ray yields by Dr. Stephenson is, I believe, of importance, and properly done. It does not seem right, however, to place too much emphasis on the values reported by Martin[1] for selenium, bromine and iodine. These were not experimentally determined by Martin himself, as were his other values, but were calculated by him from the work of Barkla[2] and Beatty,[3] done some years previously. The possible source of error mentioned by Dr. Stephenson as arising from the absorption-curve not being the same on both sides of the absorption-limit would have very little effect on the elements nearer to barium, but might easily affect those much lighter. If this is so, then the work of Locher[4] on argon, neon and oxygen may be seriously affected. The value of the ratio $S'/S''=0.003305$ was not taken from measurements of the diaphragm apertures, but was found by employing several diaphragms of intermediate sizes and measuring the ratios of ionization-currents using them. Incidentally, the value was within two percent of that obtained by taking the ratio of the areas.

DONALD K. BERKEY

Canajoharie, New York,
May 19, 1934.

[1] L. H. Martin, Proc. Roy. Soc. **A115**, 420 (1927).
[2] Barkla and Philpot, Phil. Mag. **25**, 849 (1923).
[3] Beatty, Proc. Roy. Soc., **A85**, 329 (1911).
[4] Locher, Phys. Rev. **40**, 484 (1932).

Penetrating Power of Asymmetric Component of Cosmic Radiation

A study of the asymmetric component of cosmic radiation was undertaken in collaboration with Drs. Millikan, Bowen and Neher for the primary purpose of determining whether the particles responsible for this East-West effect are in the main secondaries formed within the atmosphere or electrons (+ and −) entering the earth's magnetic field from outside.

The studies were made by the "coincidence counting" method, employing instruments previously described[1] with the modification that the stand built to hold the Geiger counters was also equipped to hold lead blocks with a total thickness of 30 cm in the solid angle determined by the counters. With this arrangement studies were made at Mexico City, elevation 7250 feet, geomagnetic latitude 29°N reckoned from a corrected north magnetic pole at 78° 30′; at Arequipa, Peru, elevation 7750 feet, magnetic latitude 3°S, and at Cailloma, Peru, elevation 14,350 feet, magnetic latitude 2°S. Observations were made by rotating the counter arrangement about a vertical axis at intervals of 90 minutes, alternately east and west of the magnetic meridian. Alternate days the apparatus was operated with and without lead in front of the counters. The ratio of the counting rates, West/East, with and without lead is given in Table I.

TABLE I. *Counting rates, with and without lead, West/East.*

Geomag. lat.	Elev. ft.	Zenith angle	W/E, no lead	W/E, 30 cm Pb
29° N	7,250	45°	1.091±0.014	1.060±0.016
3° S	7,750	15	1.06 ± .02	1.00 ± .03
		30	1.095± .02	1.02 ± .03
		45	1.138± .014	1.09 ± .016
		60	1.120± .02	1.05 ± .03
2° S	14,350	50	1.16 ± .03	1.09 ± .03

The counting rates observed without lead are in good agreement with those reported by Johnson[2] in the same latitudes. It is evident from the data that the introduction of lead produces a marked decrease in the "west excess."

In order to determine the amount of this decrease as a function of the thickness of lead, a run was made with various thicknesses. These results are presented in Table II. The observations were made at Mexico City, zenith angle 45°, and represent about 12,000 coincidences.

[1] S. A. Korff, Phys. Rev. **44**, 515 (1933).
[2] T. H. Johnson, Phys. Rev. **43**, 834 (1933); Alvarez, Phys. Rev. **43**, 835 (1933).

TABLE II. *Reduction of west excess by lead.*

Cm Pb	West/East	Probable error
0	1.091	±0.0145
2	1.075	0.021
10	1.065	0.021
20	1.065	0.021
30	1.060	0.017

Consider now the interpretation of this effect. Suppose N_1 rays of whatever nature, capable of exciting the counters enter from the east; and N_1+N_2 enter from the west, where N_2 is the "west excess." The East-West experiment determines the ratio $(N_1+N_2)/N_1$ which is found at Mexico to be about 1.09; or, N_2/N_1 is 0.09. If the zenith angle is not changed, and lead is inserted in front of the counters, the number of counts recorded in unit time with the counters pointing east will be N_3, and west, N_3+N_4. The observations show that at Mexico N_4/N_3 is 0.06. A ratio of the rates gives $N_4N_1/N_2N_3=2/3$. In order to evaluate experimentally N_1/N_3, the counting rates were determined with and without lead in front of the counters, other conditions being kept unchanged. The ratio thus obtained for N_3/N_1 was 0.6 ± 0.04. The value of N_4/N_2 is therefore experimentally determined as 0.41. We see, therefore, that less than half the particles which produce the west excess have energies sufficient to enable them to penetrate 30 cm Pb.

From the data of Anderson[3] on penetrating power, we find that particles of electronic charge and mass require about 10^9 volts to penetrate 30 cm lead. This estimate is almost certainly not in error by fifty percent; but even larger departures will not invalidate the conclusion that in the equatorial latitudes a large fraction of the particles which produce the west excess are of far too low energy to have ever been able to come from outside into our atmosphere through the blocking effect of the earth's magnetic field. The observations in Peru strengthen this conclusion, for in Peru it requires energies of above about 8×10^9 volts to penetrate the earth's field.

It appears, therefore, that the counting tubes are excited predominantly by secondaries produced within the earth's atmosphere. The distribution of energies of the secondaries as shown by the ratio of N_4/N_2 as 0.4 is, moreover, in good agreement with the measures of Anderson, who finds in cloud chambers that more than half the secondaries are of energies below 10^9 volts. It should be borne in mind, however, that these secondaries will follow the general direction of the incoming primaries, ejection as observed in cloud chambers taking place mainly in the forward direction. This direction will not be materially altered by the earth's field, owing to the short range of the secondaries, and is consequently independent of the sign of the charge of these particles.

A series of electroscope observations to study the penetrating power through various metals, and the transition effect; the total intensity at various altitudes; and the latitude effect was also made, which will be reported in detail later. The latitude run shows an increase of 6 ± 1 percent in the total intensity of the radiation at sealevel as measured in an unshielded electroscope on the trip from Panama to Los Angeles; and no change within the limits of error (±1 percent) from Peru to Panama.

The author wishes to take this opportunity to thank the Peruvian Minister of Marine and Aviation, and Commandantes Gilardi, Bellatin and Escanlante, whose cooperation made possible the electroscope observations at the highest altitudes; Mr. F. F. Hixson of the Central Railway of Peru, who put the facilities of the railway at the author's disposal; Dr. R. Monges Lopez for assistance in Mexico; Dr. Vinelli and Mr. Roden of the Cailloma mines, thanks to whom the observations at Cailloma were obtained; and to Mr. L. S. Blaisdell, Dr. G. A. Wagner and Mr. T. L. Blackwood for various assistance to the expedition. Thanks are also due to Captains Nielsen and Anderson on whose ships the latitude runs were made. The expedition was made possible by a grant from the Carnegie Corporation of New York, to be administered by the Carnegie Institution of Washington to Professor R. A. Millikan who along with Drs. Bowen and Neher collaborated in the planning and equipping of the expedition and in the analyses and interpretation of the results.

S. A. KORFF

California Institute of Technology,
Pasadena, California,
May 26, 1934.

[3] C. D. Anderson, Phys. Rev. **44**, 406 (1933).

Some Remarkable Multiple Sunset Flashes in Southern California

In a letter in *Nature*[1] I have described successive green flashes occurring at the same sunset in connection with clouds and the ocean. When the sun sets over a hill with a curved outline in the path of the rays several successive flashes may also be seen. Thus I have seen first a flash at the northern edge of the image, then at the southern edge, and then at or near the middle. The color in a single flash often appears at the sharp end or ends of the image first, and advances inward.

Green and blue flashes of a far more interesting character often occur when the sun sets over the ocean, or a low lying cloud, with its image greatly distorted on account of the inhomogeneity of the atmosphere. Thus on one occasion the image (over the ocean) became almost perfectly rectangular and remained of appreciably the same width as the height gradually diminished. Finally a green flash appeared at the northern end; then two other green flashes, one at the southern end and one in the middle, all disappearing together.

Much more remarkable flashes appear when atmospheric stratification causes, as it often does, the sun's image to be distorted in such a way that the sides are more or less serrated like those of a Japanese lantern or an accordion

[1] Barnett, Nature, March 22, 1930.

bellows. When the serrations are sufficiently marked, one layer after another in succession, beginning with the uppermost, separates itself from the lower part of the image, becomes narrower horizontally and much thinner vertically, turns green or blue, often at least at the pointed extremities first, and disappears. In the last two or three years I have repeatedly witnessed this phenomenon, obtaining all the way from two to six green and blue flashes. In the one case in which six colored flashes were certainly observed, the serrations were quite deep, the sun's disk was not very red, and all or nearly all the flashes were distinctly *blue*. The last layer at disappearance became whitish, as the upper edge of the image often does when the sun sets red. When the serrations are not deep and the layers are thin, the layers may shrink horizontally without becoming distinctly separated from the lower image, the pointed and colored ends moving inward slowly until the layer disappears.

In one very interesting case the sunset over the ocean red and oval (as usual becoming flatter beneath), but at first without noticeable serrations. As the sunset progressed the image became sharply divided by a horizontal line, ending in somewhat deep and sharp depressions. Below the line the image was distinctly and uniformly yellowish green, above the line uniformly reddish, or reddish yellow, the redder portion having an area perhaps three-quarters that of the whole image. As the sunset progressed further, the color again became homogeneous and red and the depressions disappeared, while the image took on the form of a rectangle capped by an isosceles triangle with somewhat rounded top. The top of the triangle now came off, turned blue, and disappeared. Then in between the point at which this disappearance occurred and the flattening disk another blue flash appeared, where nothing had been visible before. The image then became more and more flattened, and thinner vertically, without changing appreciably in horizontal width, and disappeared red (as the image often does).

Most of these observations were made with one inch achromatic binoculars magnifying about six diameters.

S. J. BARNETT

University of California at Los Angeles and
California Institute of Technology,
May 31, 1934.

The Magnetic Moment of the Neutron

Our application[1] of the g-formula to the spin and orbit of a neutron in the nucleus is only partially correct, although the result (neutron $= -0.6$ magneton) is not affected. But the coordination of l and j in the tables is to be changed. The correct theory together with important generalizations is given meantime independently by I. Tamm and S. Altschuler.[2] They find the value -0.5 similar to ours. We do not agree with the analysis of H. Schueler[3] who gives the neutron -1.65 magnetons.

ALFRED LANDÉ
D. R. INGLIS

Ohio State University,
June 7, 1934.

[1] Inglis and Landé, Phys. Rev. **45**, 842 (1934).
[2] Tamm and Altschuler, Comptes Rendus de l'Acad. des Sciences de l'USSR **1**, 458 (1934).
[3] Schueler, Zeits. f. Physik **88**, 323 (1934).

Remarks on Super-Novae and Cosmic Rays

We have recently called attention to a remarkable type of giant novae.[1] As the subject of super-novae is probably very unfamiliar we give here a few more details which are not contained in our original articles.

1. Distribution of super-novae

In our calculations we made use of the assumption that on the average one super-nova appears in each galaxy every thousand years. This estimate is based on the occurrence of super-novae in the following galaxies,

Our own galaxy	in 1572
Andromeda	1885
Messier 101	1907

These three systems are located within a sphere of radius 12×10^5 light years.

In the Virgo cluster, which contains about 500 nebulae, six super-novae were found on plates taken during the last thirty years. As a curiosity we mention that in N.G.C. 4321, which is a member of Virgo, two super-novae have appeared in 1901 and 1914, respectively.

In the same interval of 30 years six additional super-novae were found in isolated nebulae.

We wish to emphasize that all of these finds are chance finds since a systematic search for super-novae has been organized only recently.

From the estimate of one super-nova per galaxy per thousand years it follows that 10^7 super-novae appear per year in the 10^{10} nebulae which are contained in a sphere of 2×10^9 years radius (critical distance derived from the red shift of nebulae). If cosmic rays come from super-novae their intensity in points far away from any individual super-nova will be essentially independent of time.

2. Comparison with the lifetime of stars

The lifetime of stars is supposed to be of the order of at least 10^{12} years. A nebula contains about 10^9 stars. These estimates, combined with the frequency of occurrence of one super-nova per galaxy per 10^3 years suggest that the super-nova process might occur to every star once in its lifetime, marking perhaps the cessation of its existence as an ordinary star. We realize that this suggestion is highly speculative in view of the possibility that the frequency of occurrence of super-novae may depend on time and in view

[1] W. Baade and F. Zwicky, Proc. Nat. Acad. Sci. May, 1934.

of our complete ignorance with respect to the evolution of the universe.

3. *Ions in super-novae*

If super-novae are giant analogues to ordinary novae we may expect that ionized gas shells are expelled from them at great speeds. If this assumption is correct, part of the cosmic rays should consist of protons and heavier ions. Direct tests by cloud chamber experiments at high altitudes are desirable in order to test this conclusion. Also the problem suggests itself to investigate how much energy corpuscular particles lose on their long journey through space. On the picture of an expanding universe this loss has been computed by R. C. Tolman.

4. *Fluctuations of cosmic rays*

In our original papers we have calculated the change in intensity of cosmic rays caused by flare-ups of super-novae in nearby galaxies. The estimates given are perhaps too optimistic in view of the fact that the velocities of different particles are different. If various particles are ejected simultaneously at the time $t=0$ from a galaxy which is 10^8 L.Y. away the times t of arrival on the earth are

$t_1 = 10^8$ years + 410 seconds for 10^{11} volt electrons.
$t_2 =$ " + 47.6 days " 10^9 " "
$t_3 =$ " + 44 years " 10^{11} " protons.

These time lags $t_i - t$ would tend to smear out the change of intensity caused by the flare-up of individual super-novae. Dr. R. M. Langer in one of our seminars was the first to call attention to the straggling of simultaneously ejected particles.

5. *The super-nova process*

We have tentatively suggested that the super-nova process represents the transition of an ordinary star into a neutron star. If neutrons are produced on the surface of an ordinary star they will "rain" down towards the center if we assume that the light pressure on neutrons is practically zero. This view explains the speed of the star's transformation into a neutron star. We are fully aware that our suggestion carries with it grave implications regarding the ordinary views about the constitution of stars and therefore will require further careful studies.

W. BAADE
F. ZWICKY

Mt. Wilson Observatory and
California Institute of Technology, Pasadena.
May 28, 1934.

$t = 10^8$ years for light if its velocity does not depend on the frequency.

Doubly-Excited States in Helium

The authors have been interested in the calculation of energy levels in doubly-excited helium with the purpose of verifying the identifications of far ultraviolet helium lines suggested by Kruger[1] and by Compton and Boyce,[2] and Rosenthal's[3] theory of the corona spectrum. Variational calculations of the states $(2s)(2p)^1P$ and $(2s)(2p)^3P$ (with the use of two-parameter trial functions as accurately orthogonal as possible to the functions of all the lower states) places $(2s)(2p)^1P$ at 296,118 cm^{-1} above $(1s)^+$ (the limit of single ionization) and $(2s)(2p)^3P$ at 274,526 cm^{-1} above this limit. We have found that the combinations $(1s)(2s)^3S-(2s)(2p)^3P$ and $(1s)(2p)^1P-(2s)(2p)^1P$ correspond with good accuracy to the lines 320.39A and 309.04A, respectively. The first transition gives a calculated wave-length 319.51A, agreeing with the experimental value to 3 parts in a thousand. The second gives 309.32A, agreeing with the experimental value to one part in a thousand.

The first transition is a perfectly good permitted transition and would be expected to appear prominently in the far ultraviolet spectrum. The error has the correct sign; that is, a more accurate calculation of the level, $(2s)(2p)^3P$ would place it slightly lower, thus increasing the corresponding wave-length and improving the agreement. We thus agree with Compton and Boyce, who suggested that this line is $(1s)(2s)-(2s)(2p)$ without specifying singlet or triplet and with Kruger only in the fact that we make it a triplet. (Kruger has $(1s)(2p)^3P-(2p)^2\,{}^3P$ for the 320 line.)

The assignment of $(1s)(2p)^1P-(2s)(2p)^1P$ for the 309 line we suggest tentatively simply because of the very good numerical agreement and are perfectly aware of the objections to it. In the first place the error has the wrong sign for a variational method which uses a trial function orthogonal to the lower state wave functions. Such a method should place the level higher than the true level. If this assignment is correct, our calculated level is lower than the correct level. This fact, however, is not serious, because one can never be sure of the orthogonality and may thus overshoot the mark. In the second place the transition violates the Laporte rule and would thus have to be attributed to quadrupole radiation or to electric field-perturbed dipole radiation. Compton and Boyce state that their light source was field-free and Kruger does not find the line.

A rough calculation of $(2s)^2\,{}^1S$ places this level at about 275,000 cm^{-1} above $(1s)^+$. $(1s)(2s)^1S-(2s)^2\,{}^1S$ thus becomes about 307,000 cm^{-1}. Kruger gives 279,715 cm^{-1} for the 357 line, which he attributes to $(1s)(2s)^1S-(2s)^2\,{}^1S$. Our calculation thus casts doubt upon this assignment.

Rosenthal[3] has suggested that the corona lines are due to jumps between levels of doubly-excited helium, corresponding to lines of the ordinary helium spectrum with the inner electron a $2s$ rather than a $1s$ electron. He selects the corona lines 5303.12, 3986.88 and 3600.97 as forming a series and attributes them to the transitions $(2s)(2p)^3P-(2s)(nd)^3D$, with $n=3$, 4, 5, respectively. Using a Hicks formula, he computes the series limit, obtaining for $(2s)(2p)^3P$ a figure which corresponds to 296,904 cm^{-1}

[1] P. G. Kruger, Phys. Rev. **36**, 855 (1930).
[2] K. T. Compton and J. C. Boyce, J. Frank. Inst. **205**, 497 (1928).
[3] A. H. Rosenthal, Zeits. f. Astrophysik. **1**, 115 (1930).

above $(1s)^+$. This disagrees violently with our value 274,526 cm^{-1} for $(2s)(2p)^3P$, but agrees rather well with our value 296,118 for $(2s)(2p)^1P$, suggesting that the assignments may be correct if one makes them singlets rather than triplets. To test this point, we have calculated (without variation) $(2s)(3d)^1D$ and $(2s)(3d)^3D$ (by integrating the exact energy operator over a properly symmetrized hydrogenic wave function with the $2s$ electron moving in the unshielded field of the nucleus and the $3d$ electron in the field of a charge $(Z-1)e$). We place $(2s)(3d)^1D$ at 309,428 cm^{-1} above $(1s)^+$ and $(2s)(3d)^3D$ at 308,018 cm^{-1} above $(1s)^+$, thus obtaining $(2s)(2p)^3P-(2s)(3d)^3D$ equal to 33,492 cm^{-1} as against the experimental value 18,852 cm^{-1} for the corona line 5303 supposed to be due to this transition. Also $(2s)(2p)^1P-(2s)(3d)^1D$ comes out 13,310 cm^{-1}, disagreeing almost as violently. The disagreement is so bad that it is quite clear that a more accurate calculation of these levels would not lead to a check. This series assignment of Rosenthal seems thus to be definitely untenable.

Most of the computations involved in this work were done by one of us (F. G. F.) and will appear later as a separate paper, with further work on the same general problem.

F. G. Fender
J. P. Vinti

Randal Morgan Laboratory of Physics,
University of Pennsylvania,
June 4, 1934.

Disintegration of H^2 and the Stellar Abundance of H^2 and H^3

The nuclear disintegration processes

$$H^2+H^2 \rightarrow H^3+H^1 \quad (1)$$

and

$$H^2+H^2 \rightarrow He^3+n^1 \quad (2)$$

are characterized by high efficiency even for low projectile energies. (The efficiency of (1) is about 10^{-6} at 0.1 m.e.v.)[1] Therefore, appreciable disintegration of H^2 should occur at the temperatures assigned to stellar interiors and during the time usually given for the age of the stars. This implies that reactions (1) and (2) will influence the stellar abundance of the nuclear particles concerned. Among the expected results are the following:

(a) Reactions (1) and (2) will tend to reduce the stellar abundance ratio $H^2 : H^1$. Now it is known that the $H^2 : H^1$ ratio is abnormally low in stellar atmospheres. Though $H^2 : H^1 = 1 : 5000$ on the earth, the value for the stars is estimated as $H^2 : H^1 < 1 : 600{,}000$ and $H^2 : H^1 < 1 : 100{,}000$ by Menzel[2] and by Unsold[3] from their unsuccessful attempts to find H^2 by means of the isotope effect in stellar line spectra.

The discrepancy between the stellar and the terrestrial abundance ratio $H^2 : H^1$ may be accounted for, solely on the basis of reactions (1) and (2) if we assume that

(1) At the time of its formation the earth obtained representative amounts of the H^2 and H^1 then present in the star.

(2) These reactions (1) and (2) have been proceeding in the star for at least 3×10^9 years.

(3) The temperature and density of some inner layer of the star are sufficiently high to yield an overall efficiency of about 10^{-14} for (1) and (2). (The temperature and density required are not unreasonably high.)

(4) There is transfer of material from such a layer to the stellar surface.

(5) There are no nuclear processes which replenish the star's supply of H^2 as rapidly as it is reduced by reactions (1) and (2). (No processes which yield H^2, let alone efficiently, are known as yet.)

This explanation does not require that the terrestrial $H^2 : H^1$ ratio change appreciably with time. It also fits the current astronomical belief that the age of the sun is not much greater than that of the earth.

Reactions (1) and (2) have been emphasized though there are several other known disintegrations with capture of deutons which would help to lower the stellar $H^2 : H^1$ ratio. However, an examination of the excitation curves for these reactions[4] indicate that they play only a minor rôle in stellar interiors.

The difference between the $H^2 : H^1$ ratio on the earth and on the stars may also be ascribed, as Menzel has pointed out, to the differential escape of H^2 and H^1 from the earth. This would result in a higher terrestrial $H^2 : H^1$ ratio. However, Russell and Menzel[5] have shown that it is probable that a very large proportion of gases as heavy as N_2 has escaped from the earth, and in this case it is hard to see how any great relative concentration of H^2 relative to H^1 could occur. Quite apart from this difficulty, Menzel's explanation forces one to assume, in the light of the occurrence of reactions (1) and (2), that either the H^2 supply is recreated in the star or the escape of H^1 from the earth affects the abundance ratio to a greater extent than the disintegration of H^2 in the stars.

(b) Reaction (1) will tend to increase the stellar abundance ratio $H^3 : H^2$. This suggests that H^3 may be more abundant than H^2 in the stars despite an approximate ratio $H^3 : H^2 = 1 : 200{,}000$ on the earth. One immediately thinks of a search for H^3 in stellar spectra. This is likely to be rendered difficult by the interference of relatively intense and broad neighboring lines, since the maximum abundance of $H^3 : H^1$ to be expected from reaction (1) is about 1 : 20,000. Thus if one takes the most favorable examples, the Hα and Hβ lines in the solar spectrum, the calculated isotope shift gives $H^3\alpha = 6560.428$ and $H^3\beta = 4859.575$. These lines will probably be masked, especially in the absorption (Fraunhofer) spectrum, by the telluric H_2O vapor

[1] Oliphant, Harteck and Rutherford, Proc. Roy. Soc. **A144**, 692 (1934).
[2] Menzel, Publ. Astr. Soc. of the Pacific **44**, 41 (1932).
[3] Unsold, Naturwiss. **20**, 936 (1932).
[4] Cockroft and Walton, Proc. Roy. Soc. **A144**, 704 (1934).
[5] Russell and Menzel, Proc. Nat. Acad. Sci. **19**, 997 (1933).

line at 6560.570 (Rowland intensity =1) and by the Fe line at 4859.749 (Rowland intensity =4), respectively. Search of the solar emission (flash) spectrum offers more hope.

This discussion involves assumptions similar to those in (a). In addition, it implies that H^3 will not appreciably disintegrate in stellar interiors during the age of the earth. That H^3 is stable is indicated by its mass defect and by its recent discovery in natural sources.[6, 7] However, experiments on the disintegration of H^3 by low energy particles are needed to help decide whether H^3 is more stable than H^2 inside a star. Ignorance of the stability of He^5 even under terrestrial conditions renders similar discussion for this nucleus less profitable at present.

I wish to record my indebtedness to Professor Henry Norris Russell for a helpful discussion of this subject.

H. H. GOLDSMITH

Columbia University,
New York, New York,
June 9, 1934.

[6] Lozier, Smith and Bleakney, Phys. Rev. **45**, 655 (1934).
[7] Tuve, Hafstad and Dahl, Phys. Rev. **45**, 840 (1934).

Information Concerning Crystal Structure from Data on Magnetic Susceptibilities

Beevers and Lipson[1] have recently published their results on the crystal structure of the pentahydrate copper sulphate. It seems worth while to call attention to the general agreement between their experimental results and the conclusions which the author published[2] after an analysis of the magnetic susceptibility data for this salt.

The author has shown that the temperature variation of the principal magnetic susceptibilities of the hexahydrate double sulphates of copper is adequately explained on the assumption that the metal ion is located in a crystalline field of predominantly cubic symmetry. By analogy with the known crystal structure of other hexahydrate sulphates, it seemed reasonable to ascribe to the water molecules of these copper salts an octahedral arrangement which would provide the crystalline field of desired symmetry. The data which were available on the magnetic susceptibility of the pentahydrate copper sulphate[3] seemed to require a similar potential field for the copper ion in this salt and consequently a similar arrangement of the crystal groups. Although there are only five water molecules per copper atom in $CuSO_4 : 5H_2O$, the author suggested[2] that the octahedral structure, and the crystalline field of predominantly cubic symmetry, might be obtained by the sharing of two water groups between the two copper atoms of the unit crystal cell.

Beevers and Lipson actually find[1] that each copper atom is surrounded by an octahedron consisting of four water groups and two oxygen molecules. Thus the crystalline field should have predominantly cubic symmetry as was assumed. The departure from cubic symmetry is due to the effect of the other atoms or groups in the unit cell and to the fact that the field of an oxygen atom is different from that of a water dipole. The asymmetry of the crystalline field is secured in the calculations by superposing a smaller field of rhombic symmetry.

The important result of this investigation is that it is often possible to obtain some information about the crystal structure of salts from an analysis of the data on the principal susceptibilities. The information thus obtained should be valuable in the case of crystals of low symmetry where the x-ray analysis is difficult and the results possibly ambiguous. However, an accurate analysis requires precise data on the principal susceptibilities over a large range of temperatures extending as low as possible. Such data are at the present time very meager, and for many salts are entirely lacking.

O. M. JORDAHL

Knox College,
Galesburg, Illinois,
June 9, 1934.

[1] C. A. Beevers and H. Lipson, Nature **133**, 215 (1934).
[2] O. M. Jordahl, Phys. Rev. **45**, 87 (1934).
[3] W. J. de Haas and C. J. Gorter, Leiden Comm. 210d (1930).

OH^+ Bands

We have undertaken the analysis of the two bands found by Rodebush and Wahl[1] in the spectrum excited by an electrodeless discharge in pure water vapor. They have been photographed in the first and second orders of a 30,000 line/inch, 21 foot grating in some 20 hours, which was sufficient to bring out several of the fainter, "satellite" branches. We have also found two new bands, which are the (0,1) and (1,1) bands of the system of which those reported by Rodebush and Wahl are the (1,0) and (0,0) bands.

There are nine strong branches in each band, three R's, three Q's, and three P's. These have been checked by the four-band combination relations and by the PR combinations and the Λ type doubling determined. There are also some satellite branches. It is evident that the upper state is an inverted $^3\Pi$ with coupling intermediate between Hund's cases a and b and that the lower state is $^3\Sigma$. The similarity in this respect, and in many details, to the spectra of NH and PH, together with the fact that the bands are obtained in the electrodeless discharge through very pure water, is sufficient to establish that they are emitted by OH^+. Superficially, however, these bands are not very similar to those of NH, since the latter are headless while those of OH^+ are sharply degraded to the red.

A detailed report on this spectrum will be published later.

F. W. LOOMIS
W. H. BRANDT

The University of Illinois,
June 11, 1934.

[1] Rodebush and Wahl, J. Chem. Phys. **1**, 696 (1933).

On the Scattering of the Th C″ γ-Rays

The absorption of Th C″ γ-rays in matter may be satisfactorily accounted for by the Compton scattering, the photo-effect, and the production of electron positron pairs, for the theoretical formulae[1] for these three effects give an absorption which agrees with experiment within experimental precision and the accuracy of the formulae. For the scattered radiation observed we have no such satisfactory understanding, for the experimental findings[2] here not only fail to agree with theoretical expectation, but disagree radically with each other. The radiation to be expected theoretically is quite complex, and we believe that the discrepant results of various observers must be in part ascribed to an inadequate recognition of this complexity. There are in fact four known sources for this scattered radiation:

(1) The Compton scattered radiation, which must in some cases be corrected for multiple scattering, and, particularly for large angle scattering, for the reabsorption of the radiation in the scatterer.

(2) The annihilation radiation of the positrons, which should consist almost wholly[3] of an isotropic radiation of energy of 500 kilovolts, and with an intensity corresponding to 2 quanta per positron. According to theory[1] there should be 0.25 positron formed for every Compton recoil electron in lead; and this prediction is roughly confirmed[4] by observations on the number of positrons ejected from thick plates. Independent evidence[5] indicates that the annihilation radiation has the hardness and isotropy to be expected from theory, and that the number of quanta per positron is roughly two, and can hardly be less than 1.5 or greater than 2.5. The intensity of this annihilation radiation per atom of scatterer should increase with Z^2.

(3) A coherent radiation[6], highly anisotropic, scattered by the electron positron cloud about nuclei. If the cross section for scattering per atom be expanded in powers of αZ, the first non-vanishing terms are of the order $(\alpha Z)^4 e^4/m^2c^4$. This corresponds to an intensity for the scattered radiation of the order of one percent (in lead) of that of the annihilation radiation, and of this only a small part will be scattered through 90° or more. Unless existing theory be inapplicable to the calculation of this effect, the scattering can hardly be of importance.

(4) A continuous X-radiation, emitted by the secondary electrons (and positrons), and with greatest intensity by the Compton recoil electrons. This radiation is itself complex:

The high frequency limit of the spectrum is at 2.35×10^6 volts. The intensity of the radiation near this limit (which comes from Compton recoil electrons sent directly forward, and which have suffered no great energy loss and have been little deflected by the nuclei of the scatterer) is proportional to Z^2, and is markedly anisotropic[7] (1/2 the radiation of about 1.5×10^6 volts lies within 15°). The intensity of the spectrum will increase rapidly with decreasing frequency. The probability that the fastest Compton recoil electron will emit a quantum of energy greater than 10^6 volts is about 5 percent; that it will emit a quantum harder than 5×10^5 volts about 10 percent. The softer components of this radiation will tend to be nearly isotropic, at least for heavy elements; for not only will the less energetic Compton electrons be ejected at larger angles, but all electrons will be scattered by their elastic impacts with the nuclei of the scatterer. The radiation observed at large angles will come chiefly from electrons which have suffered at least two nuclear impacts, and its intensity will thus increase more rapidly than Z^2 (roughly Z^3).

From (4), and perhaps from (3), we may expect to find a small amount of radiation nearly as hard as the primary γ-ray, strongly anisotropic, increasing in intensity with Z^2, and whose total intensity for radiation harder than 1.5×10^6 volts can hardly be greater than 10 percent of that of the annihilation radiation. Experimentally the existence of such hard radiation from heavy scatterers seems definitely established. Bothe and Horn[2] are able to fit their absorption curve for scattering at 114° in lead by assuming a hard component 10 percent as intense as the annihilation radiation. Because of the anisotropy of the hard components, this value seems rather too high to fit with expectation. On the other hand it must be remembered that in their analysis this component has to represent all radiation harder than 5×10^5 volts.

Quite different are the results of Gray and Tarrant[2], who observe at large scattering angles (135°), and analyze the radiation by a cylindrical absorber immediately surrounding the ionization chamber. They find no radiation harder than 10^6 volts, and can reproduce their absorption curves by assuming, in addition to radiation of about 5×10^5 volts, a component of 10^6 volts, roughly isotropic, increasing in intensity with $Z^{3.3}$; and with an intensity relative to the soft component of about 15 percent in lead. This corresponds qualitatively to what we should expect from the continuous x-ray spectrum. For at these angles the harder parts of this spectrum will be very weak, and the arrangement used is not suitable for detecting a very weak hard component in the presence of large intensities of soft radiation. And radiation of roughly the frequency, absolute intensity, Z-dependence, and isotropy of that observed is to be expected from the x-ray spectrum.

For the softer components of the scattered radiation, where we should expect to find the annihilation radiation of the positrons, there is also an apparent disagreement between observers. Thus Gray and Tarrant find twice as

[1] H. Hall, Phys. Rev. **45**, 620 (1934). J. R. Oppenheimer and M. S. Plesset, Phys. Rev. **44**, 53 (1933). W. Heitler and F. Sauter, Nature **132**, 892 (1933).

[2] L. H. Gray and G. T. P. Tarrant, Proc. Roy. Soc. **A143**, 681 (1934). W. Bothe and W. Horn, Zeits. f. Physik **88**, 683 (1934). Full references are given in these papers.

[3] E. Fermi and G. Uhlenbeck, Phys. Rev. **44**, 510 (1933).

[4] J. Chadwick, P. M. S. Blackett and G. P. S. Occhialini, Proc. Roy. Soc. **A144**, 235 (1934).

[5] J. Thibaud, Phys. Rev. **35**, 781 (1934). H. R. Crane and C. C. Lauritsen, Phys. Rev. **45**, 430 (1934).

[6] M. Delbrueck, Zeits. f. Physik **84**, 144 (1934).

[7] For quantitative theoretical results on the radiation from such electrons we are indebted to Dr. Carlson and Dr. Phillips, who have investigated the problem in detail.

much radiation as is to be expected, and Bothe and Horn, in making an explicit comparison with expectations, claim to find less than a fifth. This claim appears to be based, however, on the assumption that the Compton scattered radiation at 114° from 2.5 mm of lead has an intensity equal to that from an equivalent thickness of aluminum, whereas the reabsorption in the lead is several times that in aluminum. This leads Bothe and Horn seriously to overestimate the anisotropy of the 5×10^5 volt radiation and to underestimate the isotropic component of this radiation. In fact Bothe and Horn themselves give evidence, based on absorption and reabsorption curves, that the radiation scattered at this angle from lead has a component of energy 5×10^5 volts and of intensity about 47.5 percent of the total intensity. This value for the intensity of the annihilation radiation is 8 times as large as that used by Bothe and Horn, completely resolves the discrepancy which they report, and is in rough agreement with what we should expect. On the other hand, Gray and Tarrant's values inevitably include the softer parts of the continuous x-ray spectrum and will thus give somewhat too high an intensity for the 5×10^5 volt component.

Because of the complications here discussed, which arise essentially from the superposition of a continuous x-ray spectrum upon the partially reabsorbed Compton and annihilation radiations, we believe that the experimental results on the scattered radiation afford no clear evidence for the existence of further sources of absorption of the Th C'' γ-rays. From the absorption measurements themselves we can conclude that such sources can contribute only very little to the total absorption.

C. C. LAURITSEN
J. R. OPPENHEIMER

California Institute of Technology,
Pasadena,
June 12, 1934.

The Production and Identification of Helium of Mass Three

In the May 1 issue of the *Physical Review* we reported experiments which we believed indicate the production of hydrogen of mass three (T) from hydrogen of mass two (D) in quantities great enough to detect, with a mass-spectrograph. The work of Oliphant, Harteck and Rutherford[1] indicates that collisions of deuterium nuclei may produce a T nucleus and a proton or an He^3 nucleus and a neutron. They have not, however, observed the He^3 directly.

Using the same discharge tube and approximately the same conditions that we use for the production of T we have looked for He^3 in the treated gas. To determine its presence with the mass-spectrograph a different procedure is necessary from that used for T. First the sample of gas that has been run in the discharge tube is allowed to stand over night on copper oxide at 300°C with an appendix at liquid air temperature to remove the hydrogen in the form of water. In the meantime the mass-spectrograph is baked out to reduce the amount of mass three (H D) residual gas as much as possible. Though the "peak" due to this ion from the residual gas in the spectrograph can be reduced to an intensity corresponding to a partial pressure of the order of 10^{-10} mm it still gives a current comparable in magnitude to that obtainable in our sample to be analyzed. Therefore in spite of purifying the sample and baking out the mass-spectrograph it is necessary to distinguish between a "peak" at mass three due to pure H D and one due to a mixture of H D and He^3. This can be done by studying the intensity of the mass three ion "peak" as a function of the energy of the electrons producing the ions.

Such a study is represented by curves (a) and (b) in Fig. 1. They are tracings of photographic records showing the variation of the galvanometer deflection measuring the ion current as the electron voltage is varied. Curve (a) was taken on the residual H D peak in the spectrograph. Curve (b) was on a sample that had been treated five hours in the canal-ray discharge at about 80 kv and 10 m.a. The difference in shape of the two curves is obvious and

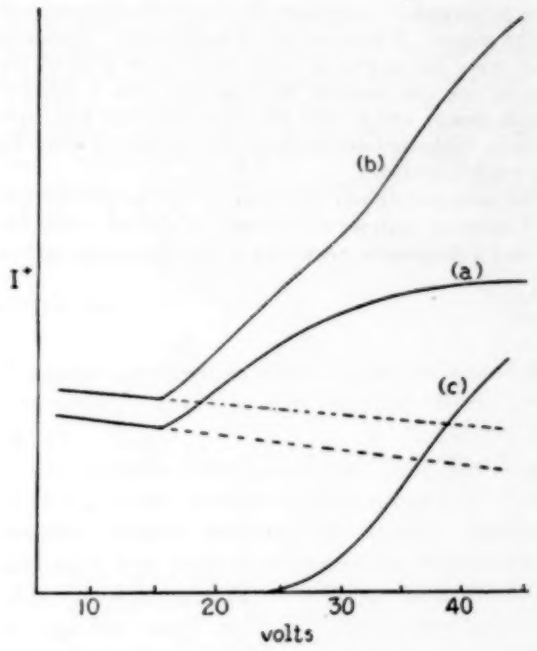

FIG. 1. Ions of mass 3 as a function of electron energy. (a) Residual hydrogen, (b) treated sample, (c) difference after fitting and correcting for electron current and zero drift.

furthermore a definite departure can be seen at about twenty-six volts. This is interpreted as caused by the ionization of He^3 atoms which should take place first at 24.5 volts. If the ordinates of (a) and (b) are adjusted so that the lower parts coincide and a small correction made for the variation in electron current a difference curve (c)

[1] Oliphant, Harteck and Rutherford, Proc. Roy. Soc. **A144**, 692 (1934).

can be obtained. This should represent the effect of He^3 in the treated sample and it is seen to cut the axis at the helium ionization potential within the limits of error. We have ten curves of this sort representing five analyses of three different samples.

Naturally we wish to know not only that He^3 is produced but to estimate the amount. From a knowledge of the ion current, the electron current, the ionization efficiency of helium, etc., we conclude that the partial pressure of He^3 in the mass-spectrograph is of the order of 10^{-10} mm. By a rough knowledge of the characteristics of the gas leak it is possible to estimate the corresponding partial pressure in the original sample. The conclusion is that there is about one part of He^3 to a hundred thousand of deuterium in a sample that has been run five hours. We are not yet in a position to say what this corresponds to in terms of yield per collision of deuton with deuton except that it is certainly very large.

There has been some question as to the stability of He^3 and T. To test this a point counter of very small volume was attached to the canal-ray apparatus. A sample of deuterium was run through the discharge for an hour and then compressed to a pressure of about half an atmosphere in the counter. It gave no sign of radioactivity. Assuming that every disintegrating atom would have affected the counter one can conclude that the life of the T and He^3 atoms present was at least 10^8 years. This test was made twice by Professor Ladenburg and Mr. Samson to whom we are much indebted.

We were particularly interested in this radioactive test as a series of analyses on a sample of treated deuterium showed a progressive weakening of the relative strength of the mass five peak in the course of two or three days. We do not yet know the cause of this effect. No such effect was found for He^3. At least analyses taken $\frac{1}{2}$, $2\frac{1}{2}$ and $3\frac{1}{2}$ days after a sample was run showed only such a reduction in ion current as was adequately explained by the shrinkage of the sample in the course of the analyses.

It has been suggested that He^4 might be produced by the combination of two deutons. The mass four peak in the analysis of our helium samples was a good deal smaller than the mass three. It was probably all D_2 but it was too small for ionization potential measurements on it. We have therefore no evidence for the production of He^4 and can say that its probability of production is at least five times less than for He^3.

We have made attempts with this mass-spectrograph to find He^2 and He^5 in ordinary helium without success. Preliminary results indicate that He^2 is present to less than 1 in 10^5 and He^5 to less than 1 in 10^6.

We are indebted to the Department of Chemistry for supplying us with deuterium. The gas samples were prepared by Harnwell and Smyth and the analyses were carried out by Bleakney, Lozier and Smith.

WALKER BLEAKNEY*
G. P. HARNWELL
W. WALLACE LOZIER
PHILIP T. SMITH†
H. D. SMYTH

Palmer Physical Laboratory,
Princeton, New Jersey,
June 18, 1934.

* In alphabetical order.
† National Research Fellow.